LOCAL CALIBRATION OF MECHANISTIC EMPIRICAL PAVEMENT DESIGN GUIDE FOR NORTH EASTERN UNITED STATES

by

SHARIQ A. MOMIN

Presented to the Faculty of the Graduate School of

The University of Texas at Arlington in Partial Fulfillment

of the Requirements

for the Degree of

MASTER OF SCIENCE IN CIVIL ENGINEERING

THE UNIVERSITY OF TEXAS AT ARLINGTON

AUGUST 2011

ACKNOWLEDGEMENTS

I would like to sincerely thank my supervising professor, Dr. Stefan A. Romanoschi, for his constant guidance and unconditional support throughout the period of this research and my study. Without his support, help, and encouragement, this study would not have been possible for me.

I would like to extend my thanks to other members of my committee, Dr. Siamak Ardekani and Dr. James Williams, for their valuable time to review my thesis and their valuable inputs. I would also like to thank the Department of Civil Engineering at the University of Texas at Arlington for their valuable assistance during the course of my graduate studies.

I would like to thank the New York State Department of Transportation for sponsoring this research. I would also like to thank my colleague Tito Nyamuhokya for his support and help and all my friends at the University of Texas at Arlington. Also, I would like to thank Jessica Rennells (climatologist, NRCC) who provided me with the climatic data.

I would like to express my special thanks to Mr. and Mrs. Naranbhai and Kashyap Patel for their very kind support and help. I thank all my friends back in India for their constant support, and encouragement.

I would like to thank Shreepad Maldikar, Vijaykumar Savanth, and the rest of the members of apartment 102.

Lastly I would like to express my deepest gratitude and appreciation to my Mother, Father and my uncle (Iqbal Momin) and to all my family members who supported me unconditionally and encouraged me to achieve my goals.

June 29, 2011

ABSTRACT

LOCAL CALIBRATION OF MECHANISTIC EMPIRICAL PAVEMENT DESIGN GUIDE

FOR NORTH EASTERN UNITED STATES

Shariq A. Momin, M.S

The University of Texas at Arlington, 2011

Supervising Professor: Dr. Stefan Romanoschi

The Mechanistic-Empirical Pavement Design Guide (MEPDG) developed under the National Cooperative Highway Research Program (NCHRP) 1-37A project is based on mechanistic-empirical analysis of the pavement structure to predict the performance of the pavement under different sets of conditions (traffic, structure and environment). MEPDG takes into account the advanced modeling concepts and pavement performance models in performing the analysis and design of pavement. The mechanistic part of the design concept relies on the application of engineering mechanics to calculate stresses, strains and deformations in the pavement structure induced by the vehicle loads. The empirical part of the concept is based on laboratory developed performance models that are calibrated with the observed distresses in the in-service pavements with known structural properties, traffic loadings, and performances. These models in the MEPDG were calibrated using a national database of pavement performance data (Long Term Pavement Performance, LTPP) and will provide design solution

for pavements with a national average performance. In order to improve the performance prediction of the models and the efficiency of the design for a given state, it is necessary to calibrate it to local conditions by taking into consideration locally available materials, traffic information and the environmental conditions.

The objective of this study was to calibrate the MEPDG flexible pavement performance models to local conditions of Northeastern region of United States. To achieve this, seventeen pavement sections were selected for the calibration process and the relevant data (structural, traffic, climatic and pavement performance) was obtained from the LTPP database. MEPDG software (*Version 1.1*) simulation runs were made using the nationally calibrated coefficients and the MEPDG predicted distresses were compared with the LTPP measured distresses (rutting, alligator and longitudinal cracking, thermal cracking and IRI). The predicted distresses showed fair agreement with the measured distresses but still significant differences were found.

The difference between the measured and the predicted distresses were minimized through recalibration of the MEPDG distress models. For the permanent deformation models of each layer, a simple linear regression with no intercept was performed and a new set of model coefficients (β_{r1}, β_{GB}, *and* β_{SG}) for asphalt concrete, granular base and subgrade layer models were calculated. The calibration of alligator (bottom-up fatigue cracking) and longitudinal (top-down fatigue cracking) was done by deriving the appropriate model coefficients (C_1, C_2, and C_4) since the fatigue damage is given in MEDPG software output. Thermal cracking model was not calibrated since the measured transverse cracking data in the LTPP database did not increase with time, as expected to increase with time. The calibration of IRI model was done by computing the model coefficients (C_1, C_2, C_3, and C_4) based on other distresses (rutting, total fatigue cracking, and transverse cracking) by performing a simple linear regression.

TABLE OF CONTENTS

ACKNOWLEDGEMENTS iii

ABSTRACT iv

LIST OF FIGURES viii

LIST OF TABLES x

Chapter Page

1. INTRODUCTION 1

1.1 Introduction 1

1.2 Research Objective 3

2. BACKGROUND 4

2.1 MEPDG Framework 4

2.1.1 Hierarchical Design Approach 4

2.1.2 Performance Models – Flexible Pavements 7

2.2 Design Models for Flexible Pavement Design 10

2.2.1 Fatigue Cracking 11

2.2.2 Thermal Cracking 16

2.2.3 Rutting 17

2.3 Long Term Pavement Performance (LTPP) 24

2.3.1 Long Term Pavement Performance Database (LTPP) 27

2.4 MEPDG Calibration Efforts for Local Conditions 38

2.4.1 Ohio MEPDG Calibration Study 38

2.4.2 Minnesota MEPDG Calibration Study 44
2.4.3 Washington State MEPDG Calibration Study 48
2.4.4 Utah MEPDG Calibration Study 50
2.4.5 North Carolina MEPDG Calibration Study 53
3. DATA ASSEMBLY 57
3.1 Selection of LTPP sections 57
3.2 Extraction of Traffic Data 58
3.3 Structural Data 63
3.4 Climatic File Generation 64
3.5 LTPP Pavement Performance Data 66
4. DEVELOPMENT OF CALIBRATION FACTORS 67
4.1 Introduction 67
4.2 Permanent Deformation Model 67
4.3 Bottom-Up Fatigue Cracking Model 73
4.4 Top – Down Fatigue Cracking Model 75
4.5 Transverse Cracking Calibration 77
4.6 Smoothness Prediction Model (International Roughness Index) 78
5. CONCLUSION AND RECOMMENDATIONS 85
APPENDIX A
A. LONG TERM PAVEMENT PERFORMANCE (LTPP) TRAFFIC DATA 89
B. LONG TERM PAVEMENT PERFORMANCE (LTPP) STRUCTURAL DATA 105
C. LONG TERM PAVEMENT PERFORMANCE DISTRESS SUMMARY 124
REFERENCES 131
BIOGRAPHICAL INFORMATION 135

LIST OF FIGURES

Figure Page

2.1: Rutting 7

2.2: Alligator Cracking 8

2.3: Transverse cracking 9

2.4: Longitudinal Cracking 10

2.5: Rut progression for increasing load repetitions 18

2.6: Schematic diagram of the sub layers 21

2.7: FHWA Vehicle Classification Chart [*Google Images*] 37

2.8: Plot of measured v/s predicted total rutting 41

2.9: Measured v/s Predicted HMA total rutting 43

2.10: Measured and predicted rutting over the pavement age (section 1) 44

2.11: Measured and predicted rutting over the pavement age (section 2) 45

2.12: Predicted rutting using modified equation (section 1) 47

2.13: Predicted rutting using modified equation (section 2) 47

2.14: Measured v/s predicted total rutting 51

4.1: Measured v/s predicted AC rutting (National Calibration) 69

4.2: Measured v/s predicted AC rutting (Local Calibration) 69

4.3: Measured v/s predicted base rutting (National Calibration) 70

4.4: Measured v/s predicted base rutting (Local Calibration) 70

4.5: Measured v/s predicted subgrade rutting (National Calibration) 71

4.6: Measured v/s predicted subgrade rutting (Local Calibration) 71

4.7: Measured v/s predicted total rutting (National Calibration) 72
4.8: Measured v/s predicted total rutting (Local Calibration) 72
4.9: Measured v/s predicted alligator cracking (National Calibration) 74
4.10: Measured v/s predicted alligator cracking (Local Calibration) 74
4.11: Measured v/s predicted longitudinal cracking (National Calibration) 76
4.12: Measured v/s predicted longitudinal cracking (Local Calibration) 76
4.13: Measured v/s predicted thermal cracking (National Calibration) 77
4.14: Measured v/s Predicted thermal cracking 78
4.15: Measured v/s predicted IRI (National Calibration) 80
4.16: Measured v/s predicted IRI (Local Calibration) 81

LIST OF TABLES

Table Page

2.1: Levels of input 5

2.2: Fine Aggregate Angularity Index 23

2.3: Coarse Aggregate Angularity Index 23

2.4: List of General Pavement Studies 26

2.5: List of Specific Pavement Studies 27

2.6: Summary of Model Accuracy 39

2.7: Statistical comparison of measured and predicted total rutting data 42

2.8: Statistical comparison of measured and recalibrated rutting model predicted rutting data 43

2.9: Final calibration factors 49

2.10: AASHTO 2008 (estimated number of projects required for the validation and local calibration) 51

2.11: Statistical comparison of measured v/s predicted rutting 52

2.12: Locally calibrated coefficients 53

2.13: Calibration results summary (statistics) of permanent deformation prediction 54

2.14: Validation results statistics summary 55

2.15: Validation Result 55

2.16: Final set of calibration factors (Rutting Model) 55

2.17: Summary of local calibration factors 56

3.1: List of Total LTPP sections for the study-All GPS Sections 58

3.2: FHWA Vehicle Classification System 59

3.3: Exponential Growth Rate for LTPP selected sections [*22*] 62

4.1: Local Calibration Coefficients for the Permanent Deformation Models 68

4.2: Local Calibration Coefficients for Flexible Pavement Performance Models 84

CHAPTER 1

INTRODUCTION

1.1 Introduction

In 1960 to 1993, versions of American Association of State Highway and Transportation Officials (AASHTO) Pavement Design Guide, the design of flexible pavements were based on the empirical regression equations developed at American Association of State Highway Officials (AASHO) Road Test in the late 1950 in Ottawa, Illinois. The 1993 AASHTO Design Guide has served well in the recent years as the primary design method, but it contains too many limitations to be continued as the nation's primary design method. The main limitation is that the models were developed from a test that was carried out in one geographic location, traffic loadings, soil type and construction methods and not for a range of conditions. Design of pavement outside the original test range and condition requires extrapolation. The original AASHO Road Test was conducted for a period of two years under the same traffic loading, climatic zone and material type in the pavement structure.

Due to these limitations in the current design procedure, the National Cooperative Highway Research Program (NCHRP) initiated two research projects aiming to improve pavement design. The two research projects were 1-37A and 1-40 with their end results being the mechanistic-empirical pavement design guide (MEPDG) and its software [*1*]. The new design guide, named MEPDG is based on the mechanistic-empirical principle that takes into account advanced modeling concepts and pavement performance models in performing the analysis and design of pavements. The mechanistic part of the MEPDG relies on the application

of engineering mechanics to calculate stresses, strains and deflections generated in the pavement structure by the repeated vehicle loads. The empirical part is based on performance models that are calibrated from observed distresses in the actual pavements [*2*, *3*, *4*]. These models require user defined inputs for the following: materials, traffic, environment and pavement structure. There are three levels of design in MEPDG based on input data used. The MEPDG uses a hierarchical design approach; the level of design is selected depending on the design accuracy and reliability of the project in consideration. The general framework of the MEPDG can be briefly described in two steps:

- Step 1: Development of input values (strength and stiffness, drainage, frost heave, and thaw weakening). The traffic in MEPDG is considered in terms of Axle Load Spectra (single, tandem, and tridem and quad axles). For new pavements, the foundation analysis consists of strength and stiffness determination and, where appropriate, an evaluation of volume change, frost heave, thaws weakening, and drainage concerns. The Integrated Climatic Model is used to generate climatic inputs for pavement response and foundation analysis [*5*].
- Step 2: Structural/performance analysis. A structural model that uses the input data prepared in step 1 is used to estimate the pavement responses based on type of pavement structure or rehabilitation alternative. The structural model in flexible pavement design is a multi-layer elastic program JULEA [*5*] for linear elastic analysis. The pavement responses computed using the structural model is then used to estimate the pavement performance.

The pavement performances are measured in terms of distresses that evolve over time. Major distresses in flexible pavements are: rutting, load associated cracking, temperature

associated cracking, and roughness of the longitudinal profile. The performance models in the MEPDG are used to estimate these distresses in flexible pavements.

The performance models in the MEPDG are calibrated using a national database which contains pavement performance data from all over the country. For use of MEPDG at the local and regional level, the performance models need to be calibrated to local conditions to provide better accuracy in prediction and reduce the error between the measured and predicted distresses. The calibration of the performance models using local materials, traffic and environment will produce realistic predictions of distresses. The calibration of the performance model is done by reducing the standard error between the measured and predicted distresses using the calibration coefficients of the model. The model calibration coefficients are empirical factors which need to be calibrated before they are used in the design and analysis of new and rehabilitated pavement structure. Due to the long term benefits achieved by implementing the MEPDG, the efforts involved in model calibration for local and regional conditions need to be encouraged [*6*].

1.2 Research Objective

The primary objective of this study is to calibrate the Mechanistic Empirical Pavement Design Guide to local conditions of the Northeastern United States. The study consisted of:

1. Literature review of other state's efforts for local calibration of MEPDG and comparison of results with this study
2. A summary of design practices followed by the MEPDG
3. Extraction and collection of data
4. Development input data for the MEPDG along with implementation guidelines
5. Calibration of performance models in the MEPDG for local conditions

CHAPTER 2

BACKGROUND

2.1 MEPDG Framework

2.1.1 Hierarchical Design Approach

The MEPDG offers a hierarchical design approach. The hierarchy provides the designer the flexibility in selecting the input variables according to the functional class of the highway or reliability of the design. The hierarchical approach is used for the input parameters like: traffic, materials, and environment. The hierarchical nature of the design guide provides flexibility to designers for obtaining design inputs based on the project and available resources. Since the input data requirement is not easy to meet, the flexibility of the hierarchical nature helps designers to choose from the default data and related site specific data based on the need of the project and scope of the design. This feature of the new design guide makes it unique and feasible for the designers to design the pavement structure according to the desired specifications of the project. The analysis procedure and the pavement response models are all the same at all levels of designs. The MEPDG offers three levels of inputs as shown in Table 2-1 and the general features of each level are:

Level 1: Level 1 is the top order of input and with the highest reliability. This level is usually used for design of heaviest traffic corridors, safety problems, or early failure problems. This level requires the data of a site specific (traffic-axle load spectra) nature and/or from laboratory testing (dynamic modulus of asphalt concrete).

Level 2: This level has less accuracy than the Level 1 in terms of data collection and/or testing. This level is usually used for routine design. The inputs are usually user selected from an agency database or would be empirically estimated. Examples of these inputs would be

dynamic modulus estimated from binder, aggregate, and mix properties. The site specific traffic volume and classification data can be used along with the agency based axle load spectra.

Level 3: This level is the lowest level in precision and requires a minimal amount of site specific and/or testing data. This level of design is usually used for low volume roads and where there are no major consequences of early failure. Input examples for this level would be default dynamic modulus for given mix and default axle load spectra for a given functional class of the highway.

Table 2.1: Levels of input

Level	Level of accuracy	General input source
Level 1	Highest	Site specific data
Level 2	Intermediate	Agency database
Level 3	Minimal	Default or user defined

In MEPDG, hierarchy levels exist for the traffic input data and are based on the amount of traffic data available for the design process. The traffic input requirements for MEPDG are:

1. Traffic Volume – Base year information
    - Two-way annual average daily truck traffic (AADTT)
    - Number of lanes in the design direction
    - Percent trucks in design direction
    - Percent truck in design lane
    - Vehicle operational speed (mph)
2. Traffic Volume Adjustment Factors
    - Monthly Adjustment Factors (MAF)
    - Vehicle Class Distribution (VCD)
    - Hourly Truck Distribution Factors (HTDF)

- Traffic Growth Factors (No growth/Linear/Compound)

3. Axle Load Distribution Factors (ALDF)

- Single, Tandem, Tridem, and Quad axles

4. General Traffic Inputs

- Mean wheel location (inches from the lane marking)
- Traffic wander standard deviation (in.)
- Design lane width (ft.)
- Number of axles per truck
- Axle configuration
- Tire pressure
- Wheel spacing
- Axle spacing
- Average axle width

In MEPDG, all flexible pavement materials are classified in one of the following categories:

A. Hot Mix Asphalt–Dense Graded (HMA)

B. Open graded asphalt treated materials

C. Cold Mix Asphalt (CMA)

D. Cementitious Stabilized Materials (CSM)

E. Non-stabilized granular base/subbase

F. Subgrade soils

G. Bedrock

2.1.2 Performance Models – Flexible Pavements

Permanent Deformation Model

This model predicts the permanent deformation in each layer/sublayer for the entire analysis period. The average vertical resilient strain is computed for each analysis for the entire design life of the pavement with a linear elastic program for each axle load configuration. Rutting distress is measured in absolute terms and not based on an incremental approach (Miner's Law). The models contained in the MEPDG needs to be locally calibrated for its use. The national calibration of the model was based on permanent deformation data collected from 88 pavement sections in 28 states. The models are empirical in nature. The effect of temperature and moisture content is included in the computation of permanent deformation through their effect on resilient modulus for granular layers and dynamic modulus for asphalt concrete. Figure 2-1 represents typical rutting (permanent deformation) on the surface of the flexible pavement

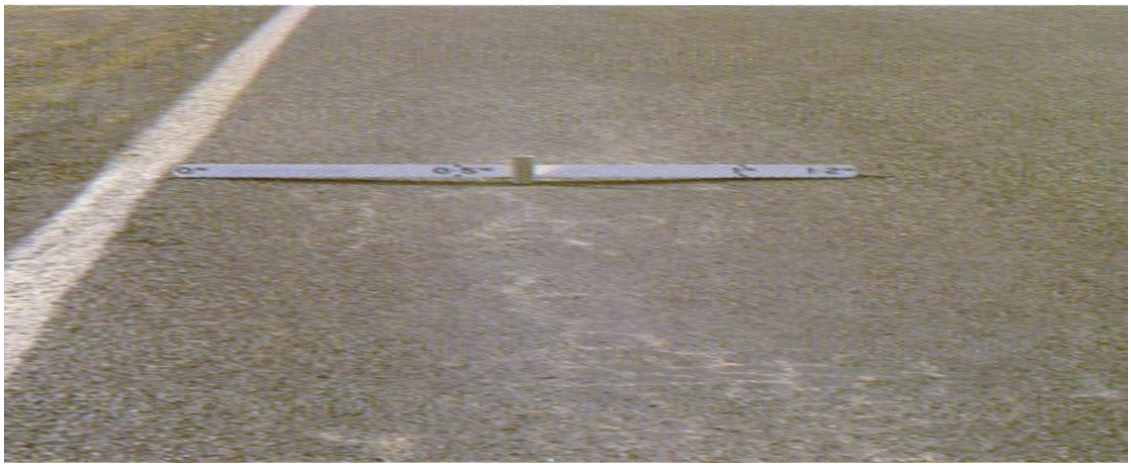

Figure 2.1: Rutting

Load Associated Cracking Models

Load associated cracking is one of the major types of flexible pavement distresses. These distresses occur in the pavement due to repeated vehicle loading that develop tensile

stresses in the bound layers. The fatigue crack initiates at the point where tensile stresses and strains are highest. The location of these crack initiation points depend on factors such as structural configuration, axle configuration, and stiffness of the layers. The crack propagates through the entire layer as the effect of repeated loading. These cracks reduce the overall performance of the pavement because of infiltration of water through the cracks. These cracks begin at the bottom of the asphalt layer and then propagate upward. These cracks are termed as bottom-up fatigue cracking. The MEPDG considers the bottom-up fatigue cracking as alligator cracking. In addition to alligator cracking, top-down cracking is also taken in to consideration in MEPDG and referred to as top-down longitudinal cracking. The top-down longitudinal cracking occurs in the wheel path.

Bottom-up fatigue or Alligator cracking

It is caused by repeated applications of tensile strain due to wheel loading which initiates the propagation of cracks from the bottom of the HMA layer. The pattern of the alligator cracks is represented by a series of cracks on the surface of the HMA layer under repeated loading is shown in Figure 2-2. In thin pavements the tensile strain is highest at the bottom of

Figure 2.2: Alligator Cracking

the HMA layer, from where the initiations of the cracks start and progress upwards in one or more longitudinal cracks. The LTPP database provides the cracking data based on the severity level (low, medium, and high) of the cracking.

Transverse or Thermal cracking

In new flexible pavements, transverse cracks are caused by low temperatures which prevent the friction at the bottom of the HMA surface; therefore they are also called thermal cracking as presented in Figure 2-3. When the tensile stress at the bottom of the HMA surface exceeds its tensile strength, cracks initiate at the surface of the pavement. It may also be caused due to daily temperature cycles, cold weather, and moisture in the pavement. Transverse cracking in the LTPP database is recorded on the basis of severity level (low, medium, and high) of the cracking.

Figure 2.3: Transverse cracking

Surface-down fatigue or longitudinal cracking

These types of cracks are generally parallel to the pavement centerline as shown in Figure 2-4. Longitudinal crack may be a load or non-load associated crack depending on the location of the crack within the travel lane. It may also be due to reflection of the cracks from the

underlying layer. The longitudinal cracking in the LTPP database is reported in terms of low, moderate, and high severity cracking.

Figure 2.4: Longitudinal Cracking

The Asphalt Institute Model is used to predict the number of repetitions to fatigue cracking. The MEPDG adopted Miner's law to estimate fatigue damage. The fatigue cracking model in the MEPDG was calibrated based on the data from 88 LTPP sections in 28 states. The bottom-up cracking is measured as a percentage of total lane area, whereas, top-down longitudinal cracking is measured in linear feet per mile of the pavement.

2.2 Design Models for Flexible Pavement Design

The MEPDG is based on mechanistic calculation of the pavement response under wheel loads and the empirical prediction of the damage accumulated over the design life of the pavement. The performance models are based on pavement structural data and take into account traffic and environmental loadings to give a more reliable result for the design of the pavements.

2.2.1 Fatigue Cracking

Fatigue cracking is a major distress in asphalt pavements, along with rutting and thermal cracking. Load induced fatigue cracking is caused by repeated heavy loading on the pavement structure which produces tensile stresses in the layers, fracture of the bound materials and reduces the structural capacity of the pavement. This ultimately results in the development of cracks which propagate through the entire asphalt layer which later allow water to infiltrate in to the bottom layers which causes weakening of the subsequent layers and of the entire pavement structure.

In the MEPDG, the performance prediction of the fatigue cracking in flexible pavements is based on the cumulative damage concept which uses Miner's law [7]. The damage is calculated as the ratio of cumulative predicted wheel load repetitions to the allowable number of wheel load repetitions. The equation to calculate the total fatigue damage is:

$$D = \sum_{i=1}^{T} \frac{n_i}{N_i} \tag{2-1}$$

Where,

D = damage

T = total number of periods

n_i = actual traffic for period i

N_i = allowable failure repetitions under conditions prevailing in period i

The fatigue cracking model in the MEPDG is a function of the tensile strain developed at the bottom of the asphalt layer and the stiffness of the asphalt layer [7]. The equation for calculating the number of load repetitions to fatigue of asphalt concrete is:

$$N_f = \beta_{f1} k_1 (\varepsilon_t)^{-\beta_{f2} k_2} (E)^{-\beta_{f3} k_3} \tag{2-2}$$

Where,

N_f = number of repetitions to fatigue cracking

ε_t = tensile strain at critical location

E = stiffness of the material (psi)

$\beta_{f1,}$ $\beta_{f2,}$ β_{f3} = adjustment factors for local calibration

$\beta_{f1,}$ $\beta_{f2,}$ β_{f3} = 1.0 in national calibration

k_1, k_2, k_3 = material constants, where k_1 is obtained using Equation (2-3)

$$k_1 = 0.004325 * 10^{4.84\left(\frac{V_b}{V_a+V_b}-0.69\right)} \quad (2\text{-}3)$$

V_a = air voids (%)

V_b = effective binder content (%)

k_2 = 3.291

k_3 = 0.854

The fatigue damage transfer function for longitudinal (top-down) and alligator cracking (bottom-up) is given by the equations:

$$F.C_{Top\text{-}down} = \left(\frac{1000}{1+e^{C_1-C_2*\log D}}\right)*(10.56) \quad (2\text{-}4)$$

$$F.C_{Bottom-up} = \left(\frac{6000}{1+e^{C_1*C'_1+C_2*C'_2*\log_{10}(D*100)}}\right)*\left(\frac{1}{60}\right) \quad (2\text{-}5)$$

$F.C_{Top\text{-}down}$ = fatigue cracking (ft/mile)

$F.C_{Bottom\text{-}up}$ = fatigue cracking (% of total lane area)

$C'_1 = -2*C'_2$

$C'_2 = -2.40874-39.748*(1+h_{ac})^{-2.85609}$ (2-6)

h_{ac} = asphalt layer thickness (inches)

D = damage in percentage

C_1, C_2= regression coefficients (7.0, 3.5) for top-down cracking

C_1, C_2= regression coefficients (1.0, 1.0) for bottom-up cracking

The value 6000 in the above equation is the total area of the lane (Lane width = 12 feet and length of the LTPP test section = 500 feet, 12 * 500 = 6000 sq.ft.). The multiplication value of (1/60) is a conversion value to obtain alligator cracking in percentage of lane area and not in square feet. The default values of regression coefficients were used for this study [8].

2.2.1.1 MEPDG Fatigue Cracking Model

The recently developed MEPDG program under NCHRP 1-37A uses the revised MS-1 model alligator fatigue cracking model [9]. The MEPDG uses three sub models for determination of total fatigue and are given as follows:

- The number of load repetitions fatigue model

$$N_f = 0.00432 * \beta_{f1} * C * k_1 \left(\frac{1}{\varepsilon_t}\right)^{3.9492} \left(\frac{1}{E}\right)^{1.281} \quad (2\text{-}7)$$

N_f = number of load repetitions to cause fatigue cracking

ε_t = tensile strain at the critical location

E = stiffness of the material

$\beta_{f1} = \beta_{f1} * k_1$

β_{f1} = numeric value (adjustment factor for local calibration)

k_1 = function of AC layer thickness using Equation (2-9)

C = correction factors

$$C = 10^{4.84\left(\frac{V_b}{V_b + V_a} - 0.69\right)} \quad (2\text{-}8)$$

$$k_1 = \frac{1}{0.000398 + \frac{0.003602}{1 + e^{11.02 - 3.49 * h_{ac}}}} \quad (2\text{-}9)$$

V_a = air voids (%)

V_b = effective binder content (%)

h_{ac} = asphalt layer thickness (inches)

2.2.1.2 Modeling for fatigue cracking cement stabilized materials (CSMs)

Stabilization of the base, subbase and subgrade layers to enhance the structural capacity of the pavement is a very common technique today. Stabilization of soils increases the stiffness of the layers and provides a strong support to the surface layer. It improves the load carrying capacity and modifies the structural responses of the pavement under traffic loading conditions. Cementitious bases improve the fatigue behavior of asphalt surface layers and subgrade rutting [*10*]. The modeling of CSMs needs more emphasis because of its semi rigid nature. It should be done in the same way for flexible and rigid pavements. Since, the performance gain generated by the use of stabilized layer is not well assessed in the MEPDG; there is an ongoing NCHRP project to study in detail the characterization of modeling of CSMs in MEPDG.

Several distress models that MEPDG currently uses for modeling of CSMs are fatigue cracking, damage accumulation, and reflection of fatigue cracks from stabilized layers. The MEPDG does not address some important distress models, such as transverse cracking and block cracking, which greatly affect the performance of stabilized pavement systems and ultimately the service life of semi rigid pavement structures [*10*].

In the fatigue cracking model for CSMs, the allowable number of load applications to material failure is done using an incremental damage approach; the allowable number of load applications is calculated using equation (2-10).

$$N_{f-CTB} = 10^{\left[\frac{k_{c1}\beta_{c1}\left(\frac{\sigma_t}{M_R}\right)}{k_{c2}\beta_{c2}}\right]} \quad (2\text{-}10)$$

$N_{f\text{-}CTB}$ = allowable number of axle load applications

σ_t = tensile stress at the bottom of the cement treated base (CTB) layer, psi

M_R = 28-day modulus of rupture for CTB layer, psi

In this model, the fatigue cracking is measured depending on the distressed area (sq.ft.).

$$FC_{CTB} = C_1 + \frac{C_2}{1 + e^{(C_3 - C_4 Log(DI_{CTB}))}} \quad (2\text{-}11)$$

FC_{CTB} = area of fatigue cracking, sq.ft.

DI_{CTB} = damage index for the CTB layer

k_{c1}, k_{c2} = global calibration factors

β_{c1}, β_{c2} = local calibration constants

C_1, C_2, C_3, C_4 = transfer function regression constants; C_1=1.0, C_2=1.0, C_3=0, and C_4=1,000.

The degradation of the CTB layer over the time due to loading is also modeled in the fatigue cracking model. Since the damage index increases over time, the elastic modulus of the stabilized layer decreases. Therefore it is justified to incorporate the degradation of the CTB layer in to the model. The equation for the degradation of the CTB layer stiffness is:

$$E_{CTB}^{D(t)} = E_{CTB}^{Min} + \left(\frac{E_{CTB}^{Max} - E_{CTB}^{Min}}{1 + e^{(-4+14)DI_{CTB}}} \right) \quad (2\text{-}12)$$

$E_{CTB}^{D(t)}$ = equivalent damage elastic modulus at time t for the CTB layer, psi

E_{CTB}^{Min} = equivalent elastic modulus for total destruction of the CTB layer, psi

E_{CTB}^{Max} = 28-day elastic modulus of the intact CTB layer at zero damage, psi

DI_{CTB} = damage index for the CTB layer

One of the major issues with the stiffness model is the inadequate implementation into the MEPDG software [*10*]. Several runs of MEPDG for the analysis of semi rigid pavements designed for 20 years and over 160 million flexible Equivalent Single Axle Loads (ESALs) predicted no degradation of the stabilized layer. Also, the MEPDG does not have a model to account for shrinkage and transverse cracks in the CSM layer. The CSMs are prone to

shrinkage due to loss of moisture and also due to thermal changes which results in development of tensile stresses that can exceed the tensile strength and cause transverse cracking in the layers. Therefore it is very important to take into consideration the distress prediction model for transverse cracking phenomenon for CSMs in MEPDG.

2.2.2 Thermal Cracking

Thermal cracking is associated with the contraction of the material due to temperature drop. This phenomenon affects the change in volume of the materials. Because of the contraction and restrained condition, development of stresses occur which ultimately results in cracking. In low temperatures, the asphalt concrete behaves as an elastic material and the thermal stresses that develop due to contraction are not dissipated. These stresses which are not relieved due to restrained boundary condition can cause cracking in the pavement. The temperature at which failure occurs is referred to as the fracture temperature [*11*].

The mechanism of thermal cracking occurs due to temperature drop at the pavement surface in cold winter nights. The tensile stresses which develop in the asphalt concrete layers become equal to or greater than the tensile strength of the layers causing the initiation of a transverse crack at pavement surface. In time, this initial crack propagates to the bottom of the pavement layers when additional thermal cycles occur.

Thermal cracking calculations are done on the basis of change in crack depth due to cooling cycles [*11*] and are given by:

$$\Delta C = A(\Delta K)^n \quad (2\text{-}13)$$

ΔC = change in crack depth due to cooling cycles

ΔK = change in stress intensity factor due to a cooling cycle

A, n = fracture parameters for the HMA mixtures using Equations (2-14) and (2-15).

$$A = 10 k_t \beta_t (4.389 - 2.52 Log(E_{HMA} \sigma_m n)) \quad (2\text{-}14)$$

$$n = 0.8\left[1 + \frac{1}{m}\right] \quad (2\text{-}15)$$

Where,

k_t = coefficient determined through global calibration for each input level

(Level 1 = 5.0, Level 2 = 1.5, and Level 3 = 3.0)

E_{HMA} = HMA indirect tensile modulus, psi

σ_m= mixture tensile strength, psi

m = the m-value derived from the indirect tensile creep compliance curve measured in the laboratory

β_t = local or mixture calibration factor

Thermal cracking is given by the equation:

$$TC = \beta_{t1} N\left[\frac{1}{\sigma_d} Log\left(\frac{C_d}{H_{HMA}}\right)\right] \quad (2\text{-}16)$$

Where,

TC = observed amount of thermal cracking, ft/mi

β_{t1} = regression coefficient determined through global calibration (β_{t1} = 400)

N = standard normal distribution evaluated at [z]

σ_d = standard deviation of the log of the depth of cracks in the pavement (0.769)in.

C_d = crack depth, in.

H_{HMA} = thickness of the HMA layer, in.

2.2.3 Rutting

Rutting is an important distress in HMA pavements. It appears as a longitudinal depression in the wheel path of the HMA pavement, caused by consolidation of the pavement layers due to repeated load applications. Rutting is of major concern for at least two reasons: 1) The rut traps water in the depression area if the surface is impervious and if the depth is more than 0.2 in., seepage of water in the pavement structures causes formation of ice in the wheel

path during winter time; 2) As the rut depth increases due increased loading application, steering of the vehicle becomes difficult, leading to safety concerns [*9*]. Many factors influence rutting such as binder type, binder content, mix type, temperature, initial compacted density etc.

The phenomenon of rutting in flexible pavement is characterized in three stages (primary, secondary, and tertiary) [*12*]. In the initial primary stage, deformation of the HMA layer accumulates very rapidly and tends to decrease, reaching a constant value in the secondary stage. The development of stresses and strains within the pavement structure during the secondary stage is quite rapid and tends to increase at a slow rate due to the densification of the materials and shear distortion. Lastly the accumulated permanent deformation tends to increase in the pavement layers leaving behind a depression along the wheel path. The flow point is the point where magnitude of rut depth is greater than what would be typically tolerated in actual practice. A typical field rut progression curve shown in Figure 2-5.

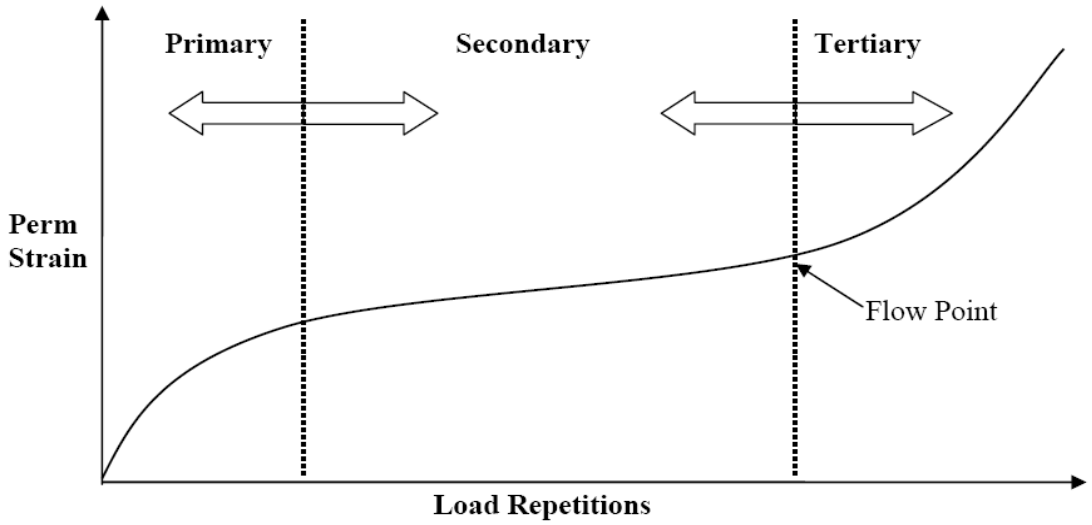

Figure 2.5: Rut progression for increasing load repetitions

2.2.3.1 MEPDG Model (2004)

The model depends on the laboratory test data for permanent strain. Test data from Leahy's model and other test results were used in developing the model [*12*]. The developed

model was calibrated with the help of seven sections of Minnesota Road Research Study (Mn/ROAD) trench rutting data. The calibrated form of the model used in the design guide is given by:

$$\frac{\varepsilon_p}{\varepsilon_r} = k_z \beta_{r1} 10^{-3.1552} T^{1.734*\beta_{r2}} N^{0.39937*\beta_{r3}} \quad (2\text{-}17)$$

ε_p = accumulated permanent strain at N repetitions of load (in/in)

ε_r = resilient strain of the asphalt material as a function of mix properties, temperature, and time rate of loading (in/in)

T = mix temperature, ^oF

N = number of load repetitions

$k_z = (C_1+C_2*D)*0.328196^D$ = function of total asphalt layer thickness and depth to computational point

$C_1 = -0.1039(H_{HMA})^2+2.4868H_{HMA}-17.342$

$C_2 = 0.0172(H_{HMA})^2-1.7331H_{HMA}+27.428$

D = depth below the surface (in)

H_{HMA} = total HMA thickness (in)

β_{r1}, β_{r2}, β_{r3} = calibration factors for the asphalt mixtures in the rut model; for national calibration these constants were set to 1.0

The vertical resilient strain at any given depth of the pavement cross section along a vertical axis in the X-Y plane can be defined by the equation (2-18) [*13*].

$$\varepsilon_{rz} = \frac{1}{E^*}(\sigma_z - \mu\sigma_x - \mu\sigma_y) \quad (2\text{-}18)$$

Where,

ε_{rz} = vertical resilient strain

E^* = dynamic modulus, a function of mix properties, temperature, and time of load.

μ = poisson's ratio

$\sigma_x, \sigma_y, \sigma_z$ = normal stresses in rectangular coordinate system

The incremental rut depth for each layer as shown in Figure 2-6 is estimated using Equation (2-19).

$$\Delta R_{di} = \varepsilon_{pi} * \Delta h_i \quad (2\text{-}19)$$

Where,

ΔR_{di} = incremental rut depth at each layer through AC layer

ε_{pi} = plastic strain at sub layer i

Δh_i = height of sub layer i.

The Figure 2-6 shows the division of each layer into smaller sublayers to account for the changes in temperature and frequency in the asphalt layer, as well as, the changes in the moisture content in the unbound base, subbase and subgrade layers.

The first 1-inch of the asphalt layer is subdivided into two 0.5 inch sublayers. Then the asphalt layer is further subdivided into 1-inch sublayers to a depth of 4 inches. If the thickness of the asphalt layer is greater than 4 inches then a sublayer is added with a maximum thickness of 4 inches, which allows for a total asphalt thickness of 8 inches. The remaining thickness of the asphalt layer is taken as one final AC sublayer [*14*]. All the layers of pavement structure are divided as shown in the Figure 2-6. The chemically stabilized layers are not subdivided into sublayers. Also it is important to recognize that no sublayering is conducted for any layer material greater than 8 feet from the surface. The maximum number of layers that can be input in the MEPDG is 10.

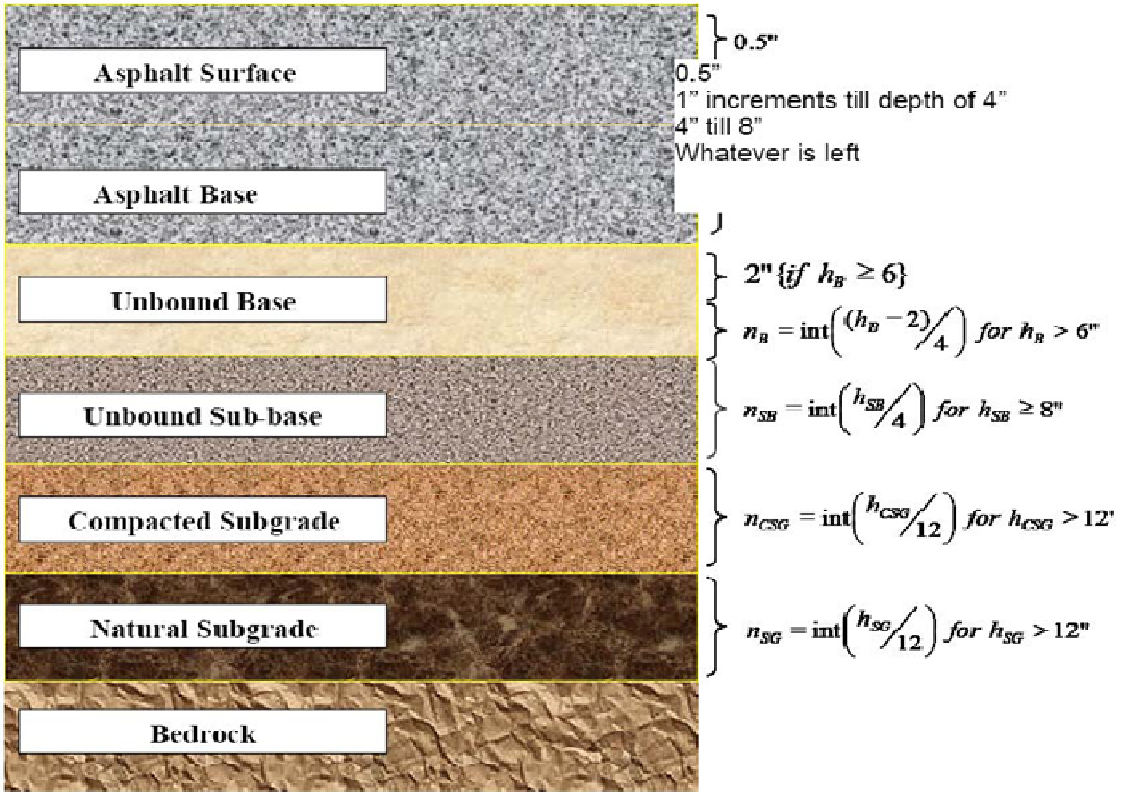

Figure 2.6: Schematic diagram of the sub layers

The total rut depth is obtained by simply summing all the rut depth values of each layer and is given by the equation (2-20).

$$\Delta R_d = \sum_{i=1}^{n} \Delta R_{di} \qquad (2\text{-}20)$$

Where,

ΔR_{di} = incremental rut depth at each layer through AC layer

n= number of sub layers.

The disadvantage of the model is that it was developed from unconfined repeated load tests and no confining pressure was taken into consideration which should be present. One of the major short coming of the model is the increased rutting with the increase in asphalt concrete

thickness which do not conform to the field observations. Therefore the model was revised in NCHRP project 1-40 and a better model was proposed.

2.2.3.2 NCHRP 1-40 Rutting Model

It has the same format as the MEPDG model with a slight enhancement to adjust permanent deformation constants based on HMA volumetric properties [9]. The form of the model is given by:

$$\frac{\varepsilon_p}{\varepsilon_r} = k_z * \beta_{r1}(10^{k_{r1}} T^{k_{r2}*\beta_{r2}} N^{k_{r3}*\beta_{r3}}) \quad (2\text{-}21)$$

The final calibrated model along with the coefficients is:

$$\frac{\varepsilon_p}{\varepsilon_r} = k_z * (10^{-3.35412} T^{1.5606} N^{0.479244}) \quad (2\text{-}22)$$

β_{r1} = 1.0 (for global calibration; the constant was set as 1.0)

β_{r2} = 1.0 (for global calibration; the constant was set as 1.0)

β_{r3} = 1.0 (for global calibration; the constant was set as 1.0)

k_z = depth adjustment function and is given by Equation (2-23)

$$k_z = (C_1 + C_2 * depth) * 0.328196^{depth} \quad (2\text{-}23)$$

$$C_1 = -0.1039 h_{ac}^2 + 2.4868 h_{ac} - 17.342 \quad (2\text{-}24)$$

$$C_2 = 0.0172 h_{ac}^2 - 1.7331 h_{ac} + 27.428 \quad (2\text{-}25)$$

k_{r1}, k_{r2}, k_{r3} = material properties in Equation (2-21) is obtained using Equations (2-26, 2-27, 2-28)

$$k_{r1} = \log[1.5093 * 10^{-3} * K_{r1} * V_a^{0.5213} * V_{beff}^{1.0057}] - 3.4488 \quad (2\text{-}26)$$

K_{r1} = intercept coefficient

V_{beff} = effective asphalt content in volume (%)

$$k_{r2} = 1.5606 \left(\frac{V_a}{V_{a(design)}} \right)^{0.25} \left(\frac{P_b}{P_{b(opt)}} \right)^{1.25} F_{index} C_{index} \quad (2\text{-}27)$$

V_a= air voids

$V_{a(design)}$ = design air voids

P_b = asphalt content by weight

$P_{b(opt)}$ = design asphalt content by weight

F_{index} = fine aggregate angularity index using Table 2-2

Table 2.2: Fine Aggregate Angularity Index

	Fine Aggregate Angularity	
Gradation – External to restricted zone	< 45	> 45
Dense grading – External to restricted zone	1.00	0.9
Dense grading – Through restricted zone	1.05	1.00

C_{index} = coarse aggregate angularity index using Table 2-3

Table 2.3: Coarse Aggregate Angularity Index

	Percent Crushed material with two faces				
Type of Gradation	0	25	50	75	100
Well Graded	1.1	1.05	1.0	1.0	0.9
Gap Graded	1.2	1.1	1.05	1.0	0.9

$$k_{r3} = 0.4791 * K_{r3} * \frac{P_b}{P_{b(opt)}} \quad (2\text{-}28)$$

Where,

K_{r3} = slope coefficient

Fine grade mixes with Gradation Index (GI) GI< 20 K_{r3} =0.4;

Coarse graded mixes with 20<GI<40 K_{r3} = 0.7;

With GI > 40 K_{r3} = 0.8.

GI = Gradation Index $=\sum_{i=3/8}^{\#\,50} |\mathrm{P_i} - \mathrm{P_i}\,(0.45)|$

2.2.3.3 Unbound Granular Layer MEPDG Model:

Prediction of rutting in unbound layers (unbound granular and subgrade materials) in the pavement structure is done with the final calibrated model [*3*]:

$$\partial_a(N) = k_1 * \beta_1 \left(\frac{\varepsilon_o}{\varepsilon_r}\right) e^{-\left(\frac{\rho}{N}\right)^{\beta}} \varepsilon_v h \quad (2\text{-}29)$$

Where,

∂_a = permanent deformation for the layer/sublayer (in)

N = number of traffic repetitions

$\varepsilon_o, \beta, \rho$ = material properties

ε_r = resilient strain imposed in laboratory test to obtain the above material properties $\varepsilon_o, \beta, \rho$ (in/in)

ε_v = average vertical resilient strain in layer/sublayer as obtained from the primary response model (in/in)

h = thickness of the layer/sublayer (in)

β_1 = calibration factor for unbound granular base and/or subgrade material (β_1=1 in national calibration)

The model in Equation (2-29) is used for both granular base and subgrade permanent deformation prediction. The calibration coefficient used in the national calibration of the model is 1.0.

β_{1GB} = 1.0 (for global calibration; the constant was set as 1.0)

β_{1SG} = 1.0 (for global calibration; the constant was set as 1.0)

k_1 = 2.03 for granular base layer (national calibration)

k_1 = 1.35 for fine soil layer (national calibration)

2.3 Long Term Pavement Performance (LTPP)

The Transportation Research Board (TRB), under the sponsorship of Federal Highway Administration (FHWA) and with the cooperation of American Association of State Highway and Transportation Officials (AASHTO), undertook a research study of the deterioration of the

nation's highway and bridge infrastructure system. During the early 1980's, the study conducted under the program named Strategic Highway Research Program (SHRP) focused on research and development activities in the highway transportation sector. In 1984, TRB published a special report TRB 202 of the study as *America's Highways, Accelerating the Search for Innovation,* in which six strategic research areas were recommended, LTPP being one of them [*15*]. The LTPP program is a comprehensive program for collecting pavement information and technical knowledge of the pavements currently available in order to develop models that will better explain pavement performance. The LTPP was developed as a long term national effort to study the behavior of pavements and to establish a database containing information regarding the pavement performance parameters. LTPP is also a publicly available database and database tools for pavement.

The in service pavement sections in LTPP database are classified as General Pavement Studies (GPS) and Specific Pavement Studies (SPS). There are nearly 800 GPS in service pavement section across the United States and Canada. The main difference between the GPS and SPS test sections is that GPS test sections are existing pavements while SPS are constructed projects which contain multiple test sections with differing experimental treatment factors. SPSs are intensive studies of specific variables involving new construction, rehabilitation and maintenance activities.

The GPS test sections are the pavement structures which had been built 15 years prior to the start of the LTPP program. A detailed research level measurement is not available for the early years of these pavement structures. The SPS test sections which were later rehabilitated were then re-classified as GPS experiment section.

The SPS program is a long term study of constructed, maintained, or rehabilitated pavement test sections wherein they consist of special design features, rehabilitation techniques and maintenance activities. The SPS serve as a detailed and complete base of data

to extend and refine the results obtained from the GPS. Essentially multiple test sections are constructed at a given SPS site to investigate the newly constructed, rehabilitated pavement structures subjected to maintenance treatments. Table 2-4 shows the list of GPS experiments and Table 2-5 list the SPS experiments conducted in the LTPP program. In this study we will be only dealing with new flexible pavements and so the test sections involved are GPS-1 and -2 and SPS-1.

Table 2.4: List of General Pavement Studies

List of GPS Experiments	
Experiment	Experiment Title
GPS-1	Asphalt Concrete (AC) Pavement on Granular Base
GPS-2	AC Pavement on Bound Base
GPS-3	Jointed Plain Concrete Pavement (JPCP)
GPS-4	Jointed Reinforced Concrete Pavement (JRCP)
GPS-5	Continuously Reinforced Concrete Pavement (CRCP)
GPS-6A	Existing AC Overlay of AC Pavement (existing at the start of the program)
GPS-6B	AC Overlay Using Conventional Asphalt of AC Pavement–No Milling
GPS-6C	AC Overlay Using Modified Asphalt of AC Pavement–No Milling
GPS-6D	AC Overlay on Previously Overlaid AC Pavement Using Conventional Asphalt
GPS-6S	AC Overlay of Milled AC Pavement Using Conventional or Modified Asphalt
GPS-7A	Existing AC Overlay on PCC Pavement
GPS-7B	AC Overlay Using Conventional Asphalt on PCC Pavement
GPS-7C	AC Overlay Using Modified Asphalt on PCC Pavement
GPS-7D	AC Overlay on Previously Overlaid PCC Pavement Using Conventional Asphalt
GPS-7F	AC Overlay Using Conventional or Modified Asphalt on Fractured PCC Pavement
GPS-7R	Concrete Pavement Restoration Treatments With No Overlay on PCC Pavement With Previous AC Overlay
GPS-7S	Second AC Overlay Which Includes Milling or Geotextile Application
GPS-9	Unbonded PCC Overlay on PCC Pavement

Table 2.5: List of Specific Pavement Studies

Category	Experiment	Title
Pavement Structural Factors	SPS-1	Strategic Study of Structural Factors for Flexible Pavements
	SPS-2	Strategic Study of Structural Factors for Rigid Pavements
Pavement Maintenance	SPS-3	Preventive Maintenance Effectiveness of Flexible Pavements
	SPS-4	Preventive Maintenance Effectiveness of Rigid Pavements
Pavement Rehabilitation	SPS-5	Rehabilitation of AC Pavements
	SPS-6	Rehabilitation of Jointed Portland Cement Concrete (JPCC) Pavements
	SPS-7	Bonded PCC Overlays of Concrete Pavements
Environmental Effects	SPS-8	Study of Environmental Effects in the Absence of Heavy Loads
Asphalt Aggregate Mixture Specifications	SPS-9P	Validation and Refinements of Superpave Asphalt Specifications and Mix Design Process
	SPS-9A	Superpave Asphalt Binder Study

The layout pattern of each GPS and SPS test section consists of a monitoring portion before and after the test sections. The monitoring portion is used for maintenance work and for material sampling. Multiple test sections were built at SPS sites; therefore the maintenance control zone is extended to cover for groups of test sections.

2.3.1 Long Term Pavement Performance Database (LTPP)

The LTPP database is designed to store data collected by the LTPP program for easy use in a Microsoft Access 2000 database. The LTPP data is collected on a regional basis and uploaded by the respective regions on a 6 month cycle. There are four regional contractors who collect the data and upload it periodically to the database.

The LTPP database contains separate, but related, tables of data in which data is stored in a simple row/column format. Rows contain records and columns are referred to as fields. The data are identified in the database according to the SHRP_ID and STATE_CODE, which are unique and represents the test sections and projects. STATE_CODE is a two digit

code used to identify the state or province where the test section is located. These codes are, in part, based on Federal Information Processing Standards (FIPS) codes. SHRP_ID is a four character identifier for the test section. The descriptions of all tables are given in *"Long Term Pavement performance Information Management System: Pavement Performance Database User Reference Guide."*[15] In the GPS, the SHRP_ID does not have any significance except representing a unique section when combined with the STATE_CODE. For SPS sites, the second character represents the experiment number; the third and fourth character represents the section of the project. The first character is typically "0" for such projects constructed in a given state or province, "A" for the second such project and so on. When SPS test sections end with "00," it means it is a project level identifier and does not represent actual test section.

If an SPS test section changes due to rehabilitation work, it will be referred to as a GPS rehabilitation experiment and its SHRP_ID will stay the same. The EXPERIMENT_NO is an important field to identify the type of test section. It is a code used to differentiate between the GPS and SPS test sections. The CONSTRUCTION_NO is used to identify if there is any change made to the test section in terms of rehabilitation work or maintenance activities. It also helps to identify the sections which are changed from SPS to GPS because of rehabilitation work on that section. The CONSTRUCTION_NO is 1 when the section is first introduced in the LTPP and it is incremented by 1 for each subsequent maintenance work. For example, 09-1803-1 (STATE_CODE – SHRP_ID – CONSTRUCTION_NO) represents a GPS experiment with construction number 1 in the state of Connecticut that had no maintenance since it entered the LTPP program.

The LTPP database uses the Structured Query Language (SQL) as its standard language. The SQL can be used to combine data, create new tables and draw queries for specific objectives. Several Quality Control (QC) checks are performed before uploading the data in to the database to insure the validity of the data and completeness of the information.

The LTPP database is divided into four modules containing different sets of tables. In total fourteen modules are in the primary data set of the LTPP database as follows.

Administration (ADM) Module (Latitude and Longitude): It contains the information about the structure of the database, tables, and very important table LTPPDD, which contain information about each field in each table. It also contains the table CODES, describing all the codes which are used in the database. The experiment section table represents the master table for the experiment sections used for the study and a detailed description about the regions.

1. Automated Weather Station (AWS) Module: This module contains information about the climatic parameter from the weather station installed on some of the SPS projects. It contains the data for daily temperature, humidity and precipitation from automated weather stations installed closest to the SPS projects.
2. Climate (CLM) Module: This module contains data for climate collected from an offsite weather station. These offsite weather station data are used to obtain virtual weather stations for LTPP sites by interpolating between the offsite weather stations. This information is used for the input file required by the MEPDG for climate. Older climatic data can be obtained from this table with the use of STATE_CODE and SHRP_ID for specific sites.
3. Dynamic Load Response (DLR) Module: This module contains load response data from the instrument collected at SPS sites located in North Carolina and Ohio. DLR is used to measure the pavement response under controlled loading conditions. Deflection and strain measurements are recorded by strain gauges. North Carolina conducted the test on a plain cement concrete (PCC) test section, while Ohio conducted the same test on asphalt concrete (AC) and PCC test sections.

4. Ground Penetrating Radar (GPR) Module: This module consists of information about the layer thicknesses of SPS projects.
5. Inventory (INV) Module: The INV module contains information on all GPS and SPS test sections. It also contains information about the pavement structure that was in service 15 years prior to be considered as an LTPP test section. All GPS and SPS maintenance and rehabilitation test sections are included. The stored SPS section information is before the application of experimental treatments given to the test sections. It includes information like pavement type, layer thicknesses, and types, material properties, composition, previous construction activities, and other background information. The information in this module comes from the agency records and not directly from test site or actual measurements. Therefore the information may not represent specific conditions found on the actual site or project.
    - INV_LAYER (Layer Thickness): This table contains layer information from highway agency records. The LAYER_NO column refers to the layer structure and it may differ from the actual layer structure found at the test site. The table contains information about the mean thickness of each layer, material type in each layer, and general layer type designation used to identify the inventory data requirements.
    - INV_GRADATION (Gradation Data): This table contains data on the gradation of coarse, fine and combined aggregates for PCC, AC, base, and subgrade layer. The LAYER_NO links to the INV_LAYER which indicates the type of layers. The table contains detailed information on sieve analysis for each layer of the pavement structure.
    - INV_PMA_ORIGINAL_MIX (Binder Content): This table contains information regarding field and laboratory compacted mix properties of plant mixed asphalt

(PMA) bound layers: maximum specific gravity, bulk specific gravity, voids in mineral aggregate, mean asphalt content, mean percentage of air void content, and effective asphalt content. It also contains the results of Marshall and Hveem stability tests.

- INV_PMA_ASPHALT (Binder Gradation): This table contains data on asphalt cement used in PMA-bound layers: binder grade of asphalt, specific gravity, viscosity at different temperatures, penetration number of asphalt and ductility.
- INV_BASE (Base Layer): This inventory table consists of information about the properties of the unbound base layer: plasticity indices, classification of the soil, density of the soil, moisture content, and mean compressive strength.
- INV_SUBGRADE (Soil Type): This table contains information on properties of the subgrade from the highway agency records: properties such as plasticity indices, soil classification, soil strength, moisture content, density measurements of the soil, and frost susceptibility classification. It also contains the unique sequential numbering of the pavement layers

6. Maintenance (MNT) Module: This module contains information on the maintenance activities performed on the pavement test sections. This module includes the LTPP section information after their inclusion as test sections. Several activities related to maintenance are recorded in this module: the application of seal coats, patching work, milling and grooving. In maintenance activity there is no change in the pavement structure and therefore there is no change in the maintenance layer table. The maintenance and rehabilitation modules are very similar. As such it is planned to merge the tables into a single module in the near future.
7. Mechanistic-Empirical Pavement Design Guide (MEPDG) module: This module contains formatted input for the M-E design guide for new and rehabilitated pavement

structure developed under NCHRP 1-37A. At this time it only contains traffic data developed from the traffic module of the LTPP traffic database.

8. Monitoring (MON) Module: This is the largest module containing information on the pavement performance data. It contains performance data: deflection measured by falling weight deflectometer (FWD), distresses (manual and photographic), friction measurements, and profile of the pavement by automated profiler or manual by dipstick measurements, transverse profile (rut measurements) and drainage data.

    - MON_RUT_DEPTH (Rutting): The rutting data is extracted from the MS Access database using the SHRP IDs and state code and is filtered into MS Excel file format. The rutting data contained in the database is divided into right and left rutting wheel path data measurements. The rutting data is measured in inches.
    - MON_DIS_PADIAS42_AC (Cracking): The cracking in the asphalt concrete consist of three major types and they are bottom up fatigue or alligator cracking, transverse or thermal cracking, and surface-down fatigue or longitudinal cracking. The cracking data is extracted from the database using the state code and SHRP IDs in to MS Excel file format for use in MEPDG.

      Alligator cracking is calculated as a percentage of area cracked out of the total available lane area. The calculation of alligator cracking is as follows:

        - Alligator cracking value extracted from the database = 0.14 sq.m.
        - Convert the value from sq.m. to sq.ft. and then divide the alligator cracking value by 6000 sq.ft. (total lane area of LTPP sections = 12 * 500 ft) to obtain in percentage.

- The transverse cracking is calculated in percentage area cracked of the total lane area. It is measured in feet/mile. The calculation of the transverse cracking is as follows:
- Transverse cracking value extracted from the LTPP database = summation of low, medium, and high severity cracking (in m, as reported in database).
- The summation of cracking value is converted to feet and then it is multiplied by 10.56 to convert the value from feet per 500 feet to feet per mile.
- Since the LTPP test sections are 500 feet long and the output from the MEPDG is in feet per mile; the values of transverse cracking need to be changed to feet per mile.

Longitudinal cracking is also calculated in percentage area cracked of the total lane area. It is measured in feet/mile. The calculation of the longitudinal cracking is as follows:

- Longitudinal cracking data extracted from the database = summation of low, medium, and high severity cracking values.
- The summation of cracking value is converted to feet and then it is multiplied by 10.56 to convert the value from longitudinal feet per 500 feet to longitudinal feet per mile.
- Since the LTPP test sections are 500 feet long and the output from the MEPDG is in feet per mile; the values of longitudinal cracking need to be changed to feet per mile.

- MON_PROFILE_MASTER (International Roughness Index, IRI): IRI is used to define the longitudinal characteristics of the travelled wheel track and

constitutes standardized roughness measurements. It is a scale for roughness based on the simulated response of the generic motor vehicle to the roughness in a single wheel path of the road surface. The roughness based on condition of the road surface is given by: good < 95 and acceptable < 170 inches/mile. The roughness of the pavement surface can be deteriorated due to rutting, cracking, and also due to extreme temperatures. The primary data set module of the LTPP database contains the monitoring sub module, in which the profile master table contains the roughness data; related measuring device, computed profile, ride parameters and the IRI values which are divided in to right and left wheel path of the pavement. The data is extracted from the LTPP database based on relevant state code and SHRP IDs into MS Excel file format for further usage.

9. Rehabilitation (RHB) Module: This module contains information regarding rehabilitation activities performed on the pavement section. Any change; alteration to the pavement structure; made to the pavement after it is constructed is recorded in this module. The tables included in this module contain information on overlay construction, shoulder replacement and joint repair; resurfacing, reconstruction and addition of lanes are also included in rehabilitation. During rehabilitation activities the structure of the pavement is altered and therefore information on changes in layer information are also recorded.
10. Seasonal Monitoring Program (SMP) Module: This module contains data regarding air temperature, precipitation, and moisture content. Sixty three sites were selected from the GPS and SPS and studied for air temperature, precipitation, moisture changes and distresses, deflection and longitudinal profile. Devices used for the measurement are:
    - Time-Domain Reflectometry: Subsurface moisture changes.
    - Thermistor Probes: Subsurface temperature changes.
    - Electrical Resistivity: Frost/thaw depth.

- Piezometer: Groundwater table determination.
- Air Temperature Probes: Ambient temperature.
- Tipping-Bucket Rain Gauge: Precipitation.
- SMP_WATERTAB_DEPTH_MAN (Water Table): This table contains information regarding the depth of water table from the pavement surface. Peizometric well is used for the observation of the water table depth. A null in the water table depth column indicates that there is no water found in the peizometric well.

11. Specific Pavement Studies (SPS) Module: This module contains information about the construction and location of all the SPS projects. This module includes information on new construction and rehabilitated SPS projects. There are tables for layer thicknesses and materials included in this module.
12. Traffic (TRF) Module: This module contains estimates of annual traffic volumes and loads and traffic characteristics of the LTPP test section lane. The traffic monitoring measurements are recorded by highway agencies and given to the LTPP. Traffic volumes and loads prior to 1990 are referred to as “Historical Data” and the data recorded from the installed monitoring equipments are called “Monitoring Data.” The traffic data is collected by the participating highway agencies onsite. They submit the data to the LTPP without modification to reflect the expected values. The raw traffic data is stored in a different traffic database (Central Traffic Database, CTDB) and submitted to LTPP for quality control. Then after the assurance given by the submitting agency, the data is stored in the pavement performance database. The LTPP adopted the Federal traffic data monitoring format which is hourly and per-vehicle by vehicle classification, traffic volume and truck axle weights.

All the traffic data are stored in Traffic Data Module of the LTPP database. The data from the database is extracted using the specific state code and a unique SHRP IDs assigned by the

LTPP program. The extracted data is filtered using the state code and SHRP IDs in to MS Excel file format.

- TRF_MEPDG_AADTT_LTPP_LN: This table contains information regarding Annual Average Daily Truck Traffic (AADTT) according to specific state and SHRP IDs.
- TRF_MEPDG_AX_DIST_ANL (Axle Load Distribution Factor, ALDF): This table consist of normalized axle distribution by month, truck class and axle group. The ALDF represents the percentages of different axles by load ranges, single, tandem, tridem, and quadrem, for different vehicle class (classes 4 – 13). The load ranges for different weight bins are single (3 – 41 kips), tandem (6 – 82 kips), tridem (12 – 102 kips), and quad (12 – 102 kips). There are 39 load ranges for single and tandem axle group, and 31 load ranges for tridem and quad axle group. The data is extracted using the state code and SHRP IDs in to MS Excel file format.
- TRF_MEPDG_VEH_CLASS_DIST (Vehicle Class Distribution): This table contains the percentages of trucks by vehicle class within the AADTT (TRF_MEPDG_AADTT_LTPP_LN). Several different techniques are available to collect the data for vehicle class distribution and they are Weigh in Motion (WIM), Automatic Vehicle Classifier (AVC), and Automatic Traffic Recorder (ATR). The sum of all the percentages of trucks for all the vehicle classes should be 100 percent. The classification is based on FHWA vehicle classification system shown in Figure 2-7.

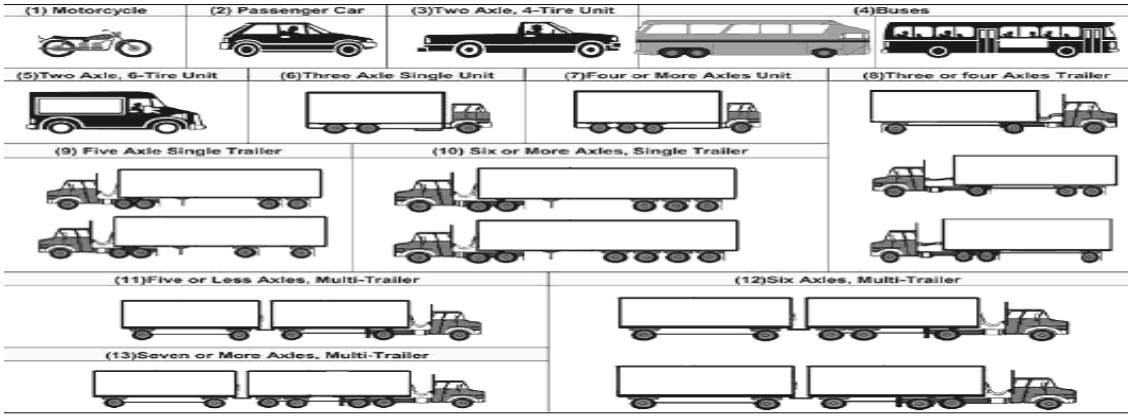

Figure 2.7: FHWA Vehicle Classification Chart [*Google Images*]

- TRF_MEPDG_MONTH_ADJ_FACTR (Monthly Adjustment Factor, MAF): Monthly adjustment factors define the monthly variation in truck traffic through the entire year. The adjustment factor represents a portion of truck traffic for specific vehicle class and month. The MAF for a specific month and vehicle class is equal to average daily truck traffic for that vehicle class and month divided by total truck traffic for that class for entire year. The monthly adjustment factors are extracted from the database using the state code and SHRP IDs in to MS Excel file format.
- TRF_MEPDG_AX_PER_TRUCK (Number of Axles per Truck): It is the annual average number of axles for each truck class and axle type for each year. The average number of axles per truck is estimated with the weigh in motion data.

13. Test (TST) Module: This module contains field and laboratory testing data on HMA and thermal expansion of PCC materials. Several field tests, material sampling and laboratory tests are performed on LTPP test sections to provide a detail description of the variation of material properties and pavement structure. Resilient Modulus and associated characteristics of Hot Mix Asphalt (HMA) materials and coefficient of thermal expansion of PCC materials are also conducted as part of material testing works. A

detailed list of test, protocols and test name are specified for each and every material in the pavement structure.

All the relative data are extracted from the LTPP database for the local calibration of the M-E Pavement Design Guide. The LTPP DataPave program provides access to database through a user based format. The DataPave is an online product of the LTPP that provides a static release of data from a majority of tables in a user-interactive format. [*15*, *16*]

2.4 MEPDG Calibration Efforts for Local Conditions

2.4.1 Ohio MEPDG Calibration Study

The calibration and validation of the MEPDG for the state of Ohio was done by collecting the relevant input data for the MEPDG followed by the development of time series data. The calibration of the model was done by statistical analysis of the data to check for the adequacy of the predicted results or was done by using a non-statistical approach when the measured distresses/IRI were mostly zero or close to zero. Therefore computation of statistics such as determination of R^2 value and the standard error of estimate (SEE) to check for the adequacy of the model was either not possible or meaningless. So a simple comparison of the measured and predicted distresses/IRI was made by categorizing the results into groups. In this comparison technique, the goal was to determine how often the measured and predicted results remain in the same group and this also gives the amount of bias in the data [*17*].

The standard error of estimate (SSE) was used to determine the model accuracy. A summary of the model accuracy is given in Table 2-6.

Table 2.6: Summary of Model Accuracy

Pavement Type	Performance Model	Model Statistics		
		Coefficient of Determination, R^2	Standard Error of Estimate, SEE	Number of Data Points, N
New HMA	Alligator Cracking	0.275	5.01%	405
	Transverse Cracking	Level 1 = 0.344	-	-
		Level 2 = 0.218		
		Level 3 = 0.057		
	Rutting	0.58	0.107 in	334
	IRI	0.56	18.9 in/mile	1926

Determination of Bias

The bias gives the amount of over or under prediction of distresses. The bias was determined by performing a simple linear regression using the measured and predicted values of the distresses and performing a statistical hypothesis with a 5% significance level to validate the results. The two hypotheses performed are: one for the determination of the intercept of the model and one for the determination of the slope. Also a paired t-test is performed to check for the similarity of the population.

The sequence of hypothesis performed was:

1. First hypothesis (5% significance level), determining the model intercept

   $H_{0:}$ model intercept =0

   H_A: model intercept ≠0

2. Second hypothesis, determining the model has a slope of 1.0

   H_0: model slope = 1.0.

   H_A: model slope ≠ 1.0

3. A paired t-test to determine the measured and predicted distress/IRI represents the same population

   H_0: mean measured distress/IRI = mean predicted distress/IRI.

H_A: mean measured distress/IRI ≠ mean predicted distress/IRI.

The hypotheses were performed sequentially as mentioned above. No further testing of the hypotheses is done if the null hypothesis is rejected. The models that passed successfully all three test were termed as unbiased. The results of both statistical and non-statistical analysis were employed to measure the overall accuracy of the MEPDG models. If the models were not satisfactory for Ohio conditions, the models were recalibrated.

Validation

If a model produced biased results and a poor correlation coefficient, it was recalibrated. The model may produce biased results because of the small data set (13 sections) and all the test locations are drawn from the same site (Delaware) and it didn't represent the diverse conditions, and site factors of the Ohio region. A more rigorous and large data set is required for the accurate model prediction.

Recalibration

In the process of recalibration of the model, the coefficients of HMA, base, and subgrade were modified to match the local conditions. Total of 17 LTPP sections (SPS-1 and SPS-9 type) were used for the recalibration process. A statistical comparison of measured and predicted distresses were performed to determine the accuracy and precision of the model shown in Table 2-7. Figure 2-8 shows the measured v/s predicted total rutting before recalibration.

- The trend in HMA, base, and subgrade layer were analyzed and it followed the traditional trend of increasing HMA thickness with decreased predicted rutting.

- Predicted HMA rutting was high as compared to predicted total rutting with the fact that most of the SPS-1 and SPS-9 sections were relatively thick. It indicated that the rutting accumulated in the unbound layers and subgrade needed to be adjusted. Therefore, unbound base/subgrade calibration coefficients were modified (β_{s1} and β_{s2})

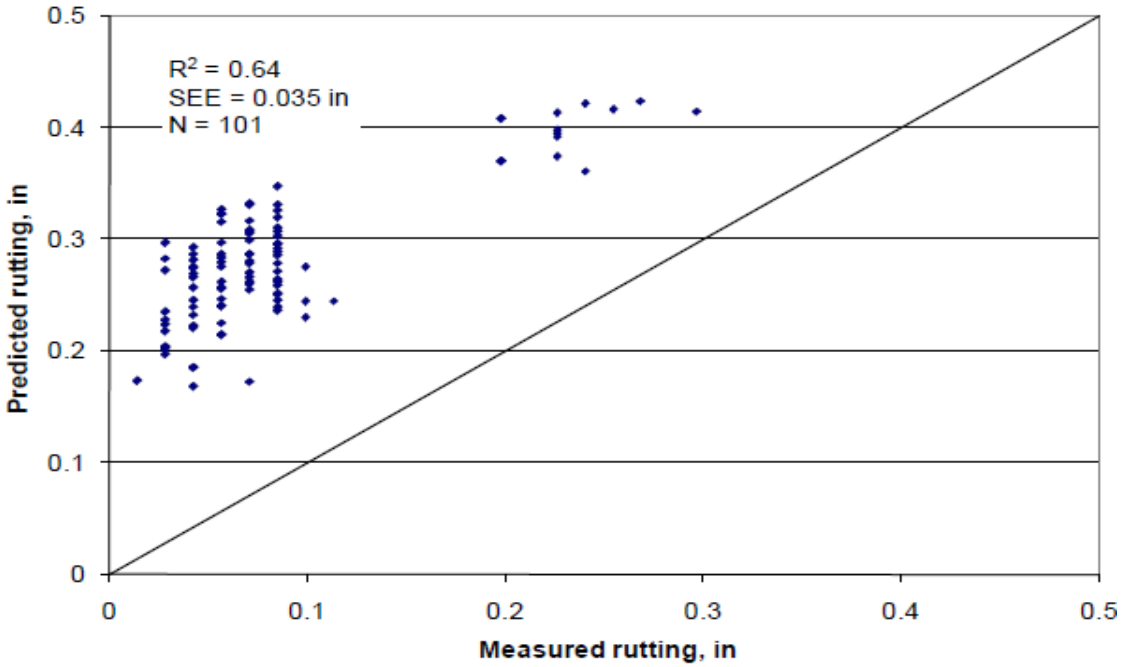

Figure 2.8: Plot of measured v/s predicted total rutting

- The slope of the rutting vs. age curve does not well match with the MEPDG prediction. It was identified that MEPDG over predicts rutting for lower magnitudes of measured rutting and under predicts rutting for the higher magnitudes of measured rutting. This requires adjustment to β_{2r} and β_{3r} of the HMA rutting submodel. The adjustment to these coefficients should be based on laboratory investigation of accumulation of permanent deformation with repeated loadings.

Based on the findings, recalibration was limited to modifying the local calibration coefficient β_{1r} of the HMA rutting submodel and β_{s1} and β_{s2} of the base and subgrade rutting submodels.

Table 2.7: Statistical comparison of measured and predicted total rutting data

N = 101							
R^2 = 0.64							
Adj. R^2 = 0.64							
SEE = 0.035 in.							
Hypothesis testing							
Hypothesis	DF	Parameter Estimate	Std. Error	t value	p-value (Pr>|t|)	95 percent confidence limits	
H_o: Intercept = 0	1	0.2178	0.006	36.8	<0.0001	0.21	0.23
H_o: Slope = 1.0	1	1.0228	0.057	13.49	<0.0001	0.65	0.88
H_o: Measured rutting - MEPDG predicted rutting =0	101			-52.7	<0.0001		

The recalibrated model is of the form shown in equation 2-30.

TRUT = 0.51*ACRUT + 0.32*BASERUT + 0.33*SUBGRUT (2-30)

Where,

TRUT = total rutting

ACRUT = rutting in the asphalt layer predicted using NCHRP 1-40 model

BASERUT = rutting in the base layer predicted using NCHRP 1-40 model

SUBGRUT = rutting in the subgrade layer predicted using NCHRP 1-40 model

The new model (2-30) coefficients after the recalibration process are as follows:

β_{r1} = 0.51 (HMA rutting prediction local calibration factor)

β_{B1} =0.32 (Unbound base rutting prediction local calibration factor)

β_{s1} =0.33 (Subgrade rutting prediction local calibration factor)

A statistical comparison of measured and predicted distresses were performed to determine the accuracy and precision of the model shown in Table 2-8. After the recalibration process, the goodness of fit of the recalibrated model was adequate; the revised model is still deficient because of the presence of bias in the predictions shown in Figure 2-9. A more

detailed and comprehensive information regarding the HMA mixtures of Ohio pavement materials and a larger data set is required for the calibration process of the models.

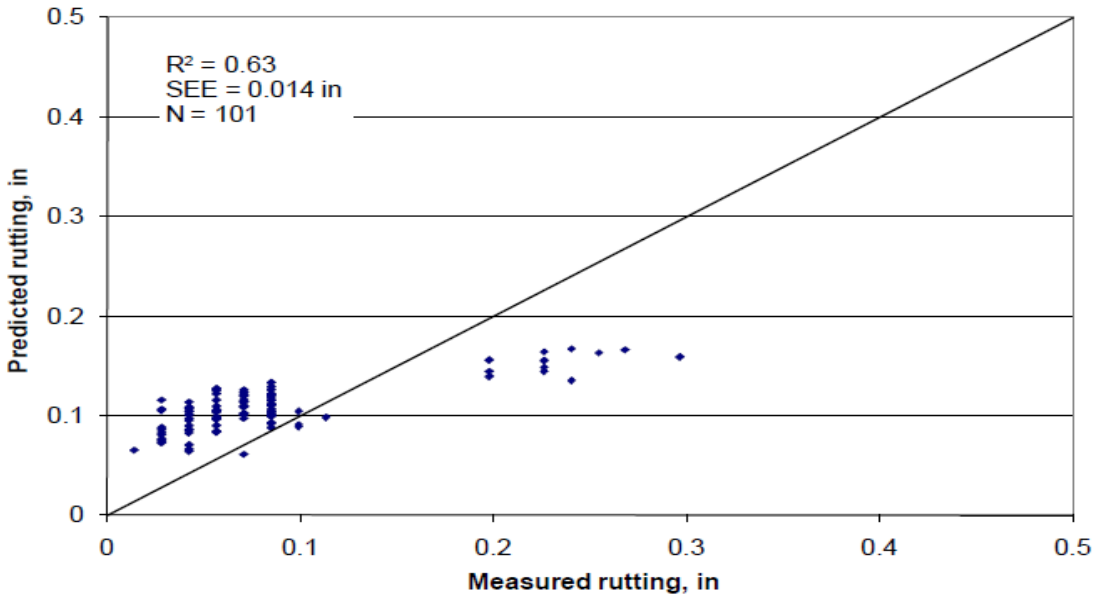

Figure 2.9: Measured v/s Predicted HMA total rutting

Table 2.8: Statistical comparison of measured and recalibrated rutting model predicted rutting data

N = 101							
R^2 = 0.63							
Adj. R^2 = 0.63							
SEE = 0.014 in.							
Hypothesis testing							
Hypothesis	DF	Parameter Estimate	Std. Error	t value	p-value (Pr>|t|)	95 percent confidence limits	
H_o: Intercept = 0	1	0.083	0.002	34.4	<0.0001	0.078	0.087
H_o: Slope = 1.0	1	0.952	0.049	19.4	0.3395	0.855	1.05
H_o: Measured rutting - MEPDG predicted rutting =0	101			-52.7	<0.0001		

2.4.2 Minnesota MEPDG Calibration Study

The calibration and verification of the MEPDG for the state of Minnesota was done using the data collected at the MnROAD project. The mainline section of the MnROAD was used for the measurement of rutting distress and comparing it with the MEPDG predicted value. The MnROAD test sections were used for the actual measurement of rutting data located on Interstate Highway 94 with 31 test sections of similar environmental and traffic conditions. The rutting performance was also simulated using the MEPDG software to compare the predicted rutting with the actual rutting measurement from the MnROAD test sections. Actual traffic input data was used for MEPDG run as it was available from the test sections. The MEPDG predicts the total rutting due to HMA layer, base, and subgrade layer. [*18*]

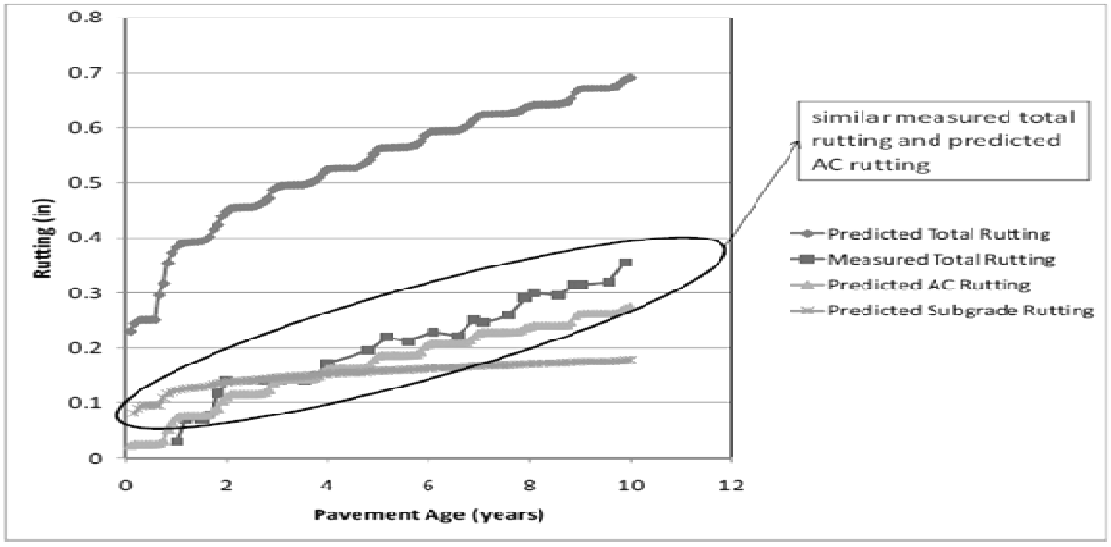

Figure 2.10: Measured and predicted rutting over the pavement age (section 1)

Rutting Total = rutting AC + rutting base + rutting subgrade (2-31)

The predicted total rutting for all the test sections was significantly higher than the measured total rutting. The comparison revealed the complexity of the issue because in some sections, the predicted AC rutting was similar to the measured total rutting while in some sections the predicted AC rutting was lower than the measured total rutting. Figure 2-10 and 2-

11 represents the examples of measured and predicted HMA, base and subgrade layer rutting for section 1 and 2.

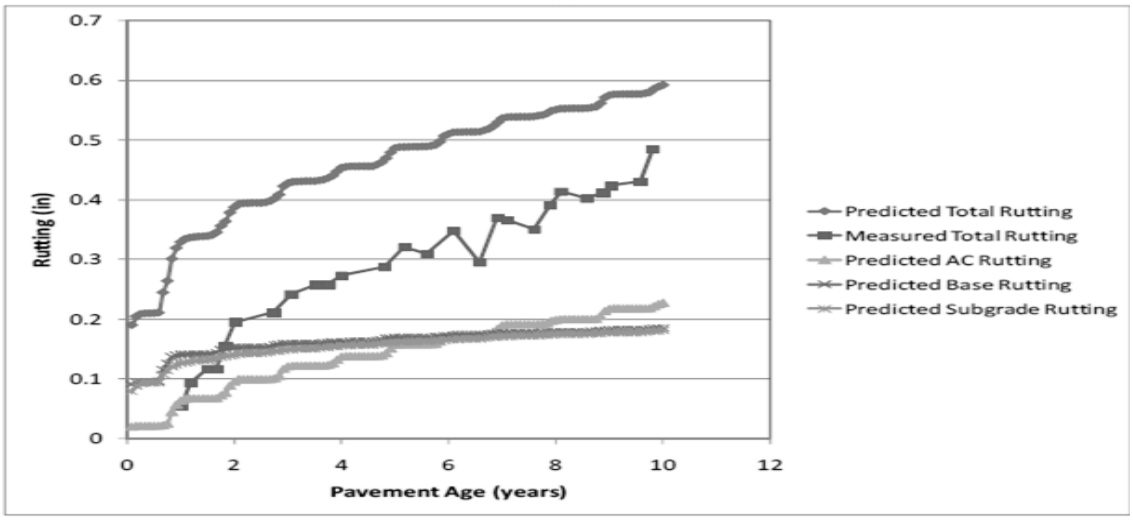

Figure 2.11: Measured and predicted rutting over the pavement age (section 2)

From Figure 2-11, it is clear that HMA rutting is similar to measured total rutting. Since MnROAD studies showed that most of the measured rutting occurred in the HMA layer, the MEPDG rutting model is fairly accurate in predicting rutting in the HMA layer. The MEPDG base and subgrade model overestimates the rutting for the sections where AC rutting is similar to measured rutting. Therefore, the base and subgrade models for these sections should be excluded from rutting prediction.

The above observation about the base and subgrade model does not always hold true. For most sections, use of only the predicted AC rutting would highly under predict the rutting as shown in Figure 2-11. Use of MEPDG total rutting model (Equation 2-31) would cause gross over prediction of rutting. Therefore to avoid under prediction of the rutting model, it is important to incorporate the base and subgrade rutting. Also, to avoid over prediction of rutting especially at early ages, the base and subgrade rutting model needs to be modified.

There are no distinguishable design parameters between the sections 1 and 2 used in the process where 1) AC predictions are similar to measured total rutting and 2) AC predictions are lower than the measured total rutting. Since the section does not differ in design parameters, the performance trends should be same but it is not true. As can be seen from Figures 2-10 and 2-11, sections with very similar design characteristics show different performance trends. Therefore, after further investigating the base and subgrade, it was identified that during the first month of pavement life the rutting is very high in the base and subgrade layers. The subgrade rutting after the first month of life was 0.08 inches. However, after ten year of pavement life, the subgrade rutting was 0.18 inches which is unrealistic. Similar observations were made for base layer and was concluded that the first month of base and subgrade rutting should be excluded from the analysis.

MEPDG simulation runs were made using the nationally calibrated model. The MEPDG manual of practice asserts the need for local calibration of MEPDG. In this study, it was not possible to calibrate the rutting model by using the calibration parameters because of the observations mentioned in the above paragraph. Therefore a modification of the rutting model is proposed in this study.

Total Rutting = Rutting AC + Rutting Base* + Rutting Subgrade* (2-32)

Rutting Base* = Rutting Base – Rutting Base 1

Rutting Subgrade* = Rutting Subgrade – Rutting Subgrade 1

Where,

Total Rutting = predicted surface rutting

Rutting AC = predicted rutting in the asphalt layer

Rutting Base* = modified predicted rutting in the base layer only

Rutting Subgrade* = modified predicted rutting in the subgrade layer only

Rutting Base = predicted rutting in the base layer only using the original MEPDG predictions

Rutting Subgrade = predicted rutting in the subgrade layer only using the original MEPDG predictions

Rutting Base 1 = predicted rutting in the base layer after only one month

Rutting Subgrade 1 = predicted rutting in the subgrade layer after one month

The predicted rutting using equation 2-32 shows the improvement in the prediction values of rutting. The modified rutting prediction equation improves the total rutting for the entire range of pavement age. The modified equation also reduces the discrepancy between measured and predicted total rutting as shown in Figures 2-12 and 2-13.

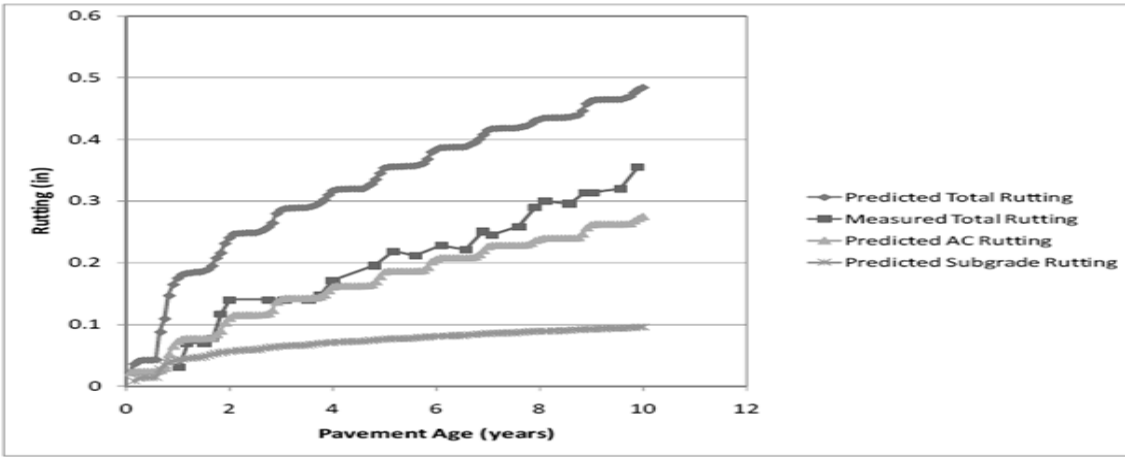

Figure 2.12: Predicted rutting using modified equation (section 1)

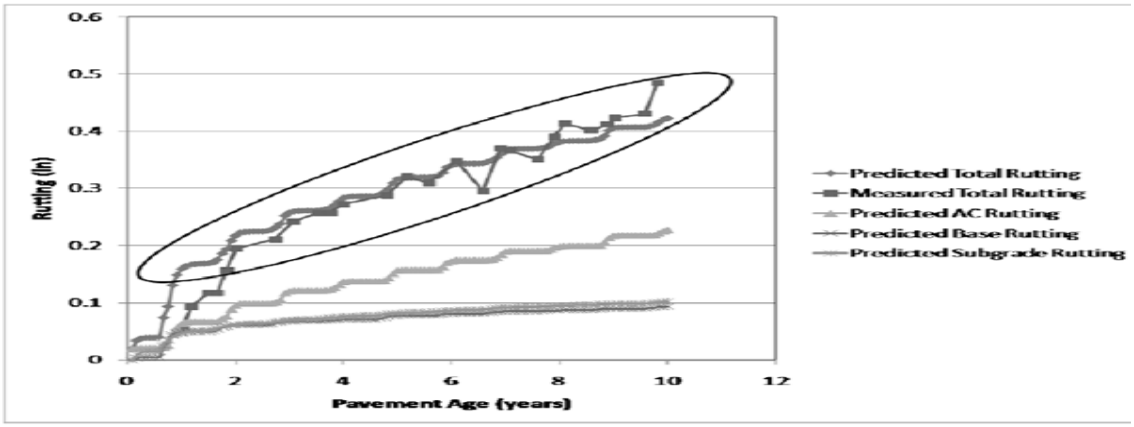

Figure 2.13: Predicted rutting using modified equation (section 2)

After recalibration of the model, rutting predictions were improved and were better than the previous model. A procedure to apply the modified rutting model was developed and recommended for use over nationally calibrated model for conditions similar to MnROAD.

2.4.3 Washington State MEPDG Calibration Study

The Washington State Department of Transportation (WSDOT) undertook the project of local calibration of MEPDG using a combination of processes: split sample approach and jackknife testing approach. The split-sample approach uses half the selected sections for calibration and another half for validation. The jackknife approach withholds each selected section as prediction measurements and other sections for calibration [*19*]. The reason to use the combination of the above both approaches is to provide stable and accurate predictions with limited sample size. The local calibration of MEPDG involves five steps: 1) bench testing, 2) model analysis, 3) calibration, 4) validation, and 5) iteration.

Bench testing involves checking for the MEPDG run time issues, model prediction reasonableness and to identify calibration needs based on the model predictions and WSPMS (Washington State Pavement Management System) data.

In model analysis, the MEPDG default predicted values for the transverse cracking model matched with the trends of the WSPMS data quite well. Therefore the default calibration factors for transverse cracking will be used. The asphalt layer fatigue model needs to be calibrated before longitudinal and alligator cracking models because the estimated fatigue damage act as a major variable for longitudinal and alligator cracking models. Thus, longitudinal and alligator cracking model are highly dependent on fatigue cracking outputs. The cracking and rutting models need to be calibrated before the roughness model as they serve as input for the roughness prediction model. In the four different models, fatigue damage, longitudinal cracking, alligator cracking and rutting model, there are 13 calibration factors to be considered.

In the calibration process, the calibration sections were selected based on their design input parameters and pavement condition data which represents typical WSDOT flexible pavements. Two pavement sections were considered as the calibration sections in eastern and western parts of Washington State. In this group of pavements, design input values and distress condition data from WSPMS were processed.

A set of calibration factors was chosen and the simulation runs were made on each of the two selected calibration sections. From the measured and the predicted values of the results, calibration factors were adjusted in order of high to low elasticity and the process continued until the values converged on an acceptable set of calibration factors. The final calibration factors, Table 2-9, were considered based on least root mean square error (RMSE) between the MEPDG predicted values and WSPMS data over the design life of the pavement.

Table 2.9: Final calibration factors

Calibration Factor	Default	Calibrated
AC Fatigue		
β_{f1}	1	0.96
β_{f2}	1	0.97
β_{f3}	1	1.03
Longitudinal Cracking		
C_1	7	6.42
C_2	3.5	3.596
C_3	0	0
C_4	1000	1000
Alligator Cracking		
C_1	1	1.071
C_2	1	1
C_3	6000	6000
AC Rutting		
β_{r1}	1	1.05
β_{r2}	1	1.109
β_{r3}	1	1.1
Subgrade Rutting β_{s1}	1	

Validation of the model was done by using a broad range of data sets independent of the two calibration sections used previously in the calibration process. The final set of calibration factors was repeated on the validation sections. The data for validation were selected from three sources: from previous study sections, from WSPMS, and sections used in the original calibration of MEPDG.

2.4.4 Utah MEPDG Calibration Study

In local calibration and validation of MEPDG for the state of Utah, several necessary steps were used. [*20*]

1. Select hierarchical input level
2. Experimental factorial and matrix or sampling template: Extracting input data and assembling it in to a matrix form (traffic, climate, material, and structural)
3. Sample size based on Table 2.10
4. Extract and evaluate distress and project data: The distress data was extracted from the LTPP database and from Utah Department of Transportation (UDOT) Pavement Management System (PMS) performance data files for UDOT PMS projects.
5. Assess local bias and standard error of estimate from global calibration factors and eliminate/reduce standard error of estimate and local bias of distress prediction models. Interpretation of results and deciding on adequacy of calibration factors. Model accuracy is checked using limited sensitivity analysis of the locally calibrated models and also the difference between the nationally calibrated and locally calibrated prediction results.

Table 2.10: AASHTO 2008 (estimated number of projects required for the validation and local calibration)

Pavement Type	Performance Indicator	Perf. Indicator Threshold @ 90 percent reliability (σ)	SEE	Minimum number of projects required for validation and local calibration	Minimum number of projects required by each pavement type
New HMA and HMA overlaid HMA	Alligator Cracking	20 percent lane area	5.01%	16	18
	Transverse Cracking	Crack spacing> 100 ft. of 630 ft/mi	150 ft/mile	18	
	Rutting	0.4 in	0.107 in	14	
	IRI	169 in/mile	18.9 in/mi	80	

6. Local calibration: It involves investigating the causes of poor goodness of fit and bias between the MEPDG nationally calibrated model and measured data by modifying the coefficients of HMA, base, and subgrade according to local conditions. The national calibration plot between measured and total rutting is shown in Figure 2-14.

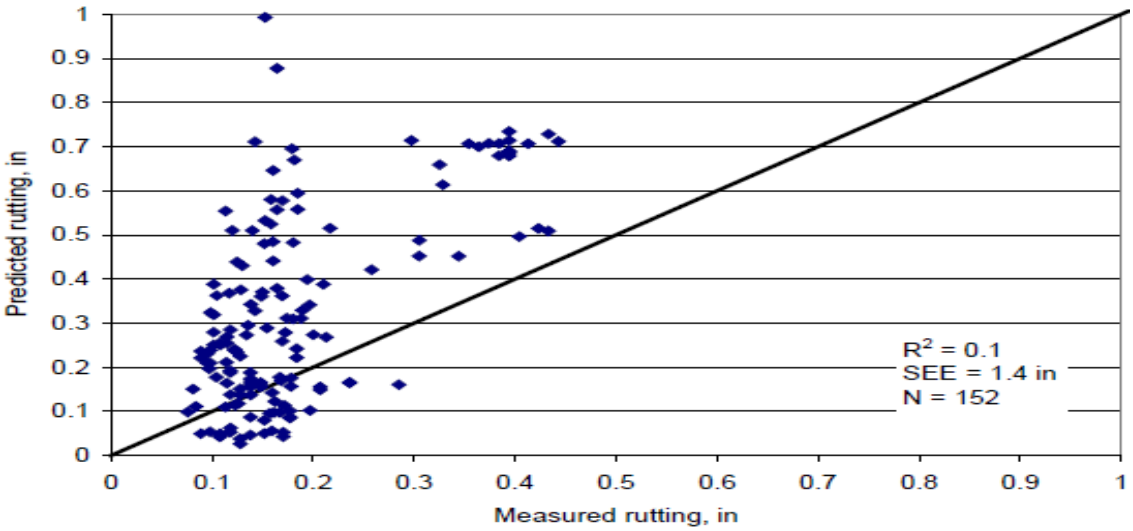

Figure 2.14: Measured v/s predicted total rutting

A statistical comparison of measured and predicted distresses was performed to determine the accuracy and precision of the model, results shown in Table 2-11.

Table 2.11: Statistical comparison of measured v/s predicted rutting

N = 152							
R^2 = 0.101							
SEE = 1.4 in.							
Hypothesis Testing							
Hypothesis	DF	Parameter Estimate	Std. Error	t value	p-value (Pr>|t|)	95 percent confidence limits	
Ho: Intercept = 0	1	-0.463	0.246	-1.88	0.0625	-0.951	0.245
Ho:Slope = 1.0	1	2.922	0.548	5.33	0.0006	1.839	4.004
Ho: Measured rutting - MEPDG predicted rutting =0	152			2.22	0.0281		

After investigating the poor goodness of fit and bias in the predicted rutting it was concluded that:

- Nationally calibrated rutting model predicted rutting adequately for older pavements constructed using viscosity binder grade (AC-10 and AC-20).
- The new HMA built using the SuperPave binders, the nationally calibrated models predicted rutting poorly.
- The nationally calibrated model was calibrated using older pavement constructed using viscosity binder grade and not SuperPave binder.

The nationally calibrated model predicts rutting adequately for older UDOT HMA pavements. There was a need to calibrate the models locally suitable for newer HMA pavement design in Utah.

Determination of Bias

Bias gives the amount of over or under prediction of the distresses/IRI. The bias is determined by performing a simple linear regression using the measured and predicted values

of the distresses/IRI and performing a statistical hypothesis with a 5% significance level to validate the results. The two hypotheses performed are: one for the determination of the intercept of the model and one for the determination of the slope. Also a paired t-test is performed to check for the similarity of the population.

Local Calibration of Rutting Submodels

The local calibration was performed using the UDOT PMS projects. Statistical Analysis Software (SAS) was used for the optimization of the model coefficients. The locally calibrated model along with the new model coefficients is shown in Equation 2-33.

$$\Delta_{p(total)} = \beta_{1r} k_z \varepsilon_{r(HMA)} 10^{k_{1r}} n^{k_{2r}\beta_{2r}} T^{k_{3r}\beta_{3r}} + \beta_{B1} k_{B1} \varepsilon_{vbase} h_{base} \left(\frac{\varepsilon_o}{\varepsilon_r}\right) e^{-\left(\frac{\rho}{n}\right)^{\beta}} + \beta_{s1} k_{s1} \varepsilon_{vsubgrade} h_{subgrade} \left(\frac{\varepsilon_o}{\varepsilon_r}\right) e^{-\left(\frac{\rho}{n}\right)^{\beta}} \quad (2\text{-}33)$$

All the parameters in Equation 2-33 are defined earlier in chapter 2 of this report.

The locally calibrated coefficients are listed in the Table 2-12.

Table 2.12: Locally calibrated coefficients

HMA	Base	Subgrade
$\beta_{1r} = 0.560$	$\beta_{B1} = 0.604$	$\beta_{S1} = 0.400$

The new locally calibrated model removes the bias present in the nationally calibrated MEPDG rutting model.

2.4.5 North Carolina MEPDG Calibration Study

Local calibration of MEPDG for North Carolina Department of Transportation (NCDOT) involves three major steps: 1) Data extraction and evaluation, 2) verification, 3) calibration, and 4) validation. [*3*]

1. Data extraction and evaluation: Data was extracted from the LTPP database and NCDOT pavement management unit (PMU).

2. Verification: Verification runs were performed on the pavement sections using the nationally calibrated coefficients to check the goodness of fit between the measured and the predicted distresses. The important point about the selection of section is that none of the sections selected for verification process were a part of the national calibration process that took place under the NCHRP 1-37A project. The sections selected for the verification runs showed the best availability of data. A null hypothesis is performed to check for the presence of bias. Bias is defined as the residual errors between the measured and the predicted distresses. From Table 2-13 it can be seen that null hypothesis is rejected for permanent deformation model for the verification runs and therefore the bias needs to be eliminated by recalibrating the model to local conditions.
3. Calibration: As the null hypothesis is rejected for the verification runs, the bias needs to be eliminated. The bias is reduced or eliminated by varying the respective model coefficients suggested in the NCHRP 1-40B report. For HMA rutting model, k_1 factor is varied by applying a fitting process using Microsoft Solver to eliminate the bias between the measured and predicted rutting values. Similarly for unbound base and subgrade rutting models, β_{GB} and β_{SG} are varied to eliminate the bias between the measured and the predicted rutting values.

Table 2.13: Calibration results summary (statistics) of permanent deformation prediction

	AC		GB		SG		Total	
	Before	After	Before	After	Before	After	Before	After
Average (in)	0.1178	0.103	0.0442	0.0344	0.1551	0.1026	0.3171	0.2399
Se (in)	0.054	0.047	0.027	0.021	0.084	0.056	0.154	0.109
Bias (in)	-0.0149	0	-0.0098	0	-0.0525	0	-0.0771	0
p-value	0.00662 <0.05	0.499 >0.05	0.0002 <0.05	0.5 >0.05	1.6E-9 <0.05	0.5 >0.05	2.9E-7 <0.05	0.499 >0.05
N[b]	111	111	111	111	111	111	111	111

Se (in) = Standard Error

N^b = Number of data points

Validation: In this step the locally calibrated models are checked for their reasonableness in the performance prediction of the distresses. The observed standard error is higher than the local calibrated standard error as shown in Table 2-14. Chi-square test is used to determine the difference between the standard error and the local calibration. Table 2-15 shows the Chi-square results and it can be deduced that the validation check is successful and the calibrated model can be used until more rigorous calibration is done. The validation results are presented in Table 2.14:

Table 2.14: Validation results statistics summary

	AC	GB	SG	Total
Average (in)	0.0656	0.033	0.0899	0.1885
Se (in)	0.0298	0.0077	0.0661	0.1445
Bias (in)	0.012	-0.014	0.035	0.033
N^c	26	26	26	26

N^c = Number of data points

Table 2.15: Validation Result

Statistical Results	Permanent Deformation
Chi-Square Statistics	36.82374
Degrees of Freedom	25
p-value	0.0599>0.05 (alpha)

The final set of calibration factors are given in the Table 2-16:

Table 2.16: Final set of calibration factors (Rutting Model)

Distress Model	Calibration Factors	Local Calibration
AC	k1	-3.41273
	k2	1.5606
	k3	0.479244
GB	βGB	1.5803
SG	βSG	1.10491

SUMMARY OF EFFORTS FOR MEPDG CALIBRATION:

Table 2.17: Summary of local calibration factors

	HMA	Unbound base	Subgrade	AC Fatigue	Longitudinal Cracking	Alligator Cracking
OHIO	β_{r1} = 0.51	β_{B1} =0.32	β_{s1} =0.33	-	-	-
WASHINGTON STATE	β_{r1} = 1.05	-	-	β_{f1} = 0.96	C_1 = 6.42	C_1 = 1.071
	β_{r2} = 1.109			β_{f2} = 0.97	C_2 = 3.596	C_2 = 1
	β_{r3} = 1.1			β_{f3} = 1.03	-	-
UTAH	β_{1r} = 0.560	β_{B1} = 0.604	β_{S1} = 0.400	-	-	-
NORTH CAROLINA	k1 = -3.41273	β_{GB} = 1.5803	β_{SG} = 1.10491	-	-	-
	k2 = 1.4606			-	-	-
	k3 = 0.479244			-	-	-

The calibration summary for the MEPDG calibration efforts for local conditions is documented in chapter 4 of this report.

CHAPTER 3

DATA ASSEMBLY

The data collection process was an important step in this research, time and effort was employed in obtaining the data from the LTPP database. The LTPP database contains data on 29 flexible pavement sections located in the North Eastern states of the country that can potentially be used for the local calibration process. This data was extracted and evaluated for completeness. The extracted data from the database that was used for the calibration process is appended in the APPENDIX A.

3.1 Selection of LTPP sections

The selection of the LTPP sections was based on the proximity of the states that closely represents the New York conditions because this study involved local calibration of MEPDG for New York State. The list of LTPP sections selected for the local calibration process is given in Table 3-1. In this study the main emphasis was on GPS-1 and 2 experiments. Out of 29 LTPP sections, 21 sections were GPS-1 sections and eight were GPS-2 sections. Eighteen sections were selected for the calibration process and the remaining eleven sections were removed due to unavailability of performance and/or traffic data. After the first simulation run of the MEPDG, seventeen sections were finalized (Table 3-1) and one section was discarded from the analysis due to erroneous result in the prediction of rutting and cracking; the predicted distresses were more than the order of magnitude higher than the measured values.

Construction Date and Number of Lanes: Using the MS Access database, the date of construction of the pavement section and the number of lanes in the test section are extracted for the retained LTPP sections into MS Excel file format. The construction date of the test section is extracted from the administration database of the primary data set module

of the LTPP (SECTION_LAYER_STRUCTURE). The total number of lanes in the pavement is extracted from the traffic database of the traffic module (TRF_BASIC_INFO) of the LTPP.

Table 3.1: List of Total LTPP sections for the study-All GPS Sections

#	State Code	State	SHRP ID	Total Lanes	Structural Type	Construction Date	
						1	2
1	9*	Connecticut	1803	2	Flexible	01-Jul-88	17-Jan-95
2	23*	Maine	1001	4	Flexible	01-Jul-88	06-Jun-95
3	23*	Maine	1009	2	Flexible	01-Jul-88	22-Aug-93
4	23*	Maine	1028	2	Flexible	01-Jul-88	12-May-92
5	25*	Massachusetts	1003	2	Flexible	01-Jun-88	07-Jun-88
6	34*	New Jersey	1003	4	Flexible	01-Aug-88	08-Apr-94
7	34*	New Jersey	1011	4	Flexible	01-Jul-88	28-Apr-98
8	34*	New Jersey	1030	4	Flexible	01-Dec-88	24-Feb-91
9	34*	New Jersey	1031	4	Flexible	01-Jul-88	04-Apr-96
10	34*	New Jersey	1033	4	Flexible	01-Jul-88	11-Sep-97
11	34*	New Jersey	1034	4	Flexible	01-Dec-88	-
12	34*	New Jersey	1638	4	Flexible	01-Dec-88	-
13	42*	Pennsylvania	1597	2	Flexible	01-Aug-88	12-Jun-90
14	42*	Pennsylvania	1599	2	Flexible	01-Aug-88	01-Jun-99
15	50*	Vermont	1002	2	Flexible	01-Aug-88	-
16	50*	Vermont	1004	2	Flexible	01-Aug-88	06-Oct-98
17	50*	Vermont	1681	2	Flexible	01-Jun-89	08-Sep-91
18	50*	Vermont	1683	2	Flexible	01-Jun-89	23-Sep-91
SECTIONS WITH MISSING TRAFFIC DATA							
19	23	Maine	1012	4	Flexible	01-Jul-88	-
20	23	Maine	1026	2	Flexible	01-Jul-88	26-Sep-96
21	25	Massachusetts	1002	6	Flexible	01-Jun-88	05-Jun-88
22	25	Massachusetts	1004	4	Flexible	01-Aug-88	01-Jun-01
23	33	New Hampshire	1001	4	Flexible	01-Aug-88	01-Aug-01
24	36	New York	1008	4	Flexible	01-May-89	25-Aug-89
25	36	New York	1011	4	Flexible	01-Jun-88	14-Sep-93
26	36	New York	1643	2	Flexible	01-May-89	12-Oct-89
27	36	New York	1644	2	FLexible	01-May-89	19-Jun-96
28	42	Pennsylvania	1605	2	Flexible	01-Aug-88	14-Jun-95
29	42	Pennsylvania	1618	2	Flexible	01-Dec-88	27-Aug-89
*Sections with traffic data							

3.2 Extraction of Traffic Data

Traffic data is the paramount input data required by the MEPDG for the structural design and analysis of the pavement structures since it is needed to predict the vehicle loads

applied to the pavement structure during its entire design life. The traffic data requirements are the same for the design of flexible and rigid pavements as well as for new and rehabilitated pavement structures. The three traffic data types required by the MEPDG are: traffic volume, vehicle classification count, and axle load spectra (weight data). Traffic volume is usually determined using the Automatic Traffic Recorder (ATR) which provides an estimate of Average Annual Daily Traffic (AADT). The vehicle classification (VC) data is provided by Automatic Vehicle Classifiers (AVC) and is based on the Federal Highway Administration's (FHWA) vehicle classification system given in Table 3-2. The FHWA classification system has 13 different vehicle classes, the same as those used in the MEPDG [*21*]. The traffic data extracted from the LTPP database for use in calibration process is appended in APPENDIX A.

Table 3.2: FHWA Vehicle Classification System

Vehicle Class	Description
1	Motorcycles
2	Passenger Cars
3	Other 2-axle,4-tire single unit vehicles
4	Buses
5	2-axle, 6-tire single-unit trucks
6	3-axle single-unit trucks
7	4+ axle single-unit trucks
8	4-axle or fewer single trailer trucks
9	5-axle single trailer trucks
10	6+axle single trailer trucks
11	5-axle or fewer multi-trailer trucks
12	6-axle multi-trailer trucks
13	7+ axle multi-trailer trucks

Data for 18 pavement sections was extracted from the LTPP database for the traffic input and consist of data on Average Annual Daily Truck Traffic, Traffic Adjustment Factors, and the Vehicle Classification data. The traffic data extracted from the MS Access database using the state code and SHRP IDs was converted into MS Excel file format for further use in the design of the pavements. The relevant traffic data extracted consist of Axle Load Distribution Factor (ALDF), Axles per Truck, Vehicle Class Distribution (VCD), Monthly Adjustment Factors

(MAF), and Average Annual Daily Truck Traffic (AADTT). Examples of traffic data input extracted from the LTPP databases for selected sections are shown in the tables of APPENDIX A as follows:

- Table A-1: Average Annual Daily Truck Traffic (AADTT)
- Table A-2: Vehicle Class Distribution (VCD)
- Table A-3: Monthly Adjustment Factor (MAF)
- Table A-4: Number of Axles per Truck
- Axle Load Spectra: A major enhancement of the MEPDG method compared to other design methods for pavement structures is that it does not convert axle loads into an equivalent axle loads; it computes the damage induced to the pavement by each axle group at a spectra of load magnitudes. In this way, the concept of equivalent axle or wheel is not used; the equivalency method has always been empirical. The MEPDG software provides the user with a default set of load spectra values. Axle and weight data are produced by weigh-in-motion (WIM) device. It is the most important traffic input which describes the ranges of axle weights and its application on the pavement structure. The Axle Load Spectra (ALS) represents the distribution of axle weights with respect to axle types (single, tandem, tridem, and quad) and vehicle class. The axle load adjustment distribution factors input for MEPDG require each month (January to December) and vehicle class (4–13) of distribution data. The ALDF represents the percentage of the total load applications within each interval of load range for each axle type (single, tandem, tridem and quad) and vehicle class (4-13).

  Single Axle: 3000lbs – 41,000lbs

  Tandem Axle: 6000lbs – 82,000lbs

  Tridem and Quad Axle: 12,000lbs – 102,000lbs

To account for the are monthly variations in the truck traffic volumes and weights, the data collected by WIM stations will be used to estimate the changes in axles load patterns during different months of the year. In this way, the design of the pavement structure becomes more effective. It is important to note that data on the Hourly Adjustment Factor (HAF) was not extracted because it is not considered in the design of new flexible pavements.

In addition to the data directly extracted from the LTPP database, the growth factor for the exponential growth of the traffic volume was estimated form the Average Annual Daily Truck Traffic (AADTT) data. MEPDG assumes that the axle load distribution factors remains constant over the entire design period.

The growth rate is calculated using the Annual Average Daily Truck Traffic (AADTT) obtained from the LTPP MS Access database. The AADTT data was extracted from the LTPP database (TRF_MEDPG_AADTT_LTPP_LN) into an MS Excel file format for the retained 18 sections. The growth formula used to predict future traffic based on the traffic volume in the base year and the growth rate and is given by: [*22*]

$$AADTT_X = AADT_{BY} * (GR)^{AGE} \quad (3\text{-}1)$$

Where,

$AADTT_X$ = Annual Average Daily Truck Traffic at age x

$AADT_{BY}$ = Annual Average Daily Truck Traffic for base year

GR= Growth Rate

The AADTT after the opening date of the facility was used as initial AADTT of the base year. Microsoft Excel Solver was used to minimize the sum of square of errors between the LTPP measured AADTT (Table 3-3) and the predicted AADTT using equation (3-1). The growth factor was calculated between the years when the traffic was opened and when the first repair work was started. Table 3-3 shows the calculated growth factor and the predicted AADTT (in Bold and Italics) of the retained LTPP sections.

Table 3.3: Exponential Growth Rate for LTPP selected sections [*22*]

SHRP ID	CN ASSIGN DATE		1988	1989	1990	1991	1992	1993	1994	1995	1996	1997	1998	1999	2000	2001	2002	2003	2004	2005	2006	2007	GF
	1	2																					
91803	01-Jul-88	17-Jan-95	110	117	125	204	100	110	170	190	***210***	***210***	***210***	***184***	-	-	-	-	***170***	***170***	***160***	-	6.57
231001	01-Jul-88	06-Jun-95	547	554	560	550	570	570	590	600	**614**	**627**	**639**	**574**	-	**660**	**640**	**630**	-	-	-	-	1.15
231009	01-Jul-88	22-Aug-93	361	363	365	360	365	375	***390***	***400***	***407***	***417***	***427***	***486***	***290***	-	***290***	***280***	-	-	***300***	-	0.49
231028	01-Jul-88	12-May-92	192	203	215	230	240	***250***	***265***	***280***	***290***	***304***	***317***	***449***	***250***	***270***	***310***	***290***	***320***	***300***	***360***	***400***	5.90
251003	01-Jun-88	07-Jun-88	204	***202***	***200***	***69***	***100***	***90***	***120***	***228***	***283***	***200***	***200***	-	-	-	-	-	-	-	-	-	-1.09
341003	01-Aug-88	08-Apr-94	1239	1056	900	940	980	-	670	***750***	***940***	***1520***	***1020***	***640***	***820***	***830***	***750***	***790***	***870***	-	-	-	-14.79
341011	01-Jul-88	28-Apr-98	1481	1385	1295	1265	1530	1100	950	1000	1050	1220	-	***1330***	***1340***	***1460***	***1510***	***190***	***1600***	***1420***	-	***1230***	-6.50
341030	01-Dec-88	24-Feb-91	420	420	420	420	***465***	***360***	***360***	***350***	***320***	***330***	-	***390***	-	***360***	-	-	-	-	***390***	***330***	0.00
341031	01-Jul-88	04-Apr-96	512	561	615	879	1208	-	1050	1120	1040	-	***1310***	***1340***	-	-	-	-	-	-	-	-	9.59
341033	01-Jul-88	11-Sep-97	598	467	365	300	230	-	260	270	-	-	-	***320***	***320***	-	***300***	***250***	***290***	-	-	-	-21.86
341034	01-Dec-88	-	1271	***1260***	***1250***	***1430***	***1615***	***1190***	***1180***	***1223***	***1300***	***1290***	***1340***	***1310***	***1370***	***1450***	***1560***	***1570***	***1640***	-	-	***1330***	-0.83
341638	01-Dec-88	-	1273	***1262***	***1250***	***1430***	***1615***	-	***1150***	***1170***	***1300***	***1250***	***1270***	***1180***	-	-	***1610***	***1910***	***1960***	***1700***	-	***1350***	-0.92
421597	01-Aug-88	12-Jun-90	62	65	68	***70***	-	-	-	-	***78***	-	***90***	***90***	-	-	-	-	***150***	***130***	***160***	***130***	4.68
421599	01-Aug-88	01-Jun-99	228	225	222	-	228	-	-	-	180	-	450	470	***510***	***490***	-	***490***	***490***	***490***	***500***	***530***	-1.39
501002	01-Aug-88	-	206	***213***	***220***	***225***	***240***	***220***	***220***	***220***	***250***	***260***	***260***	***380***	***370***	***320***	***290***	***300***	***280***	***310***	***490***	***380***	3.33
501004	01-Aug-88	06-Oct-98	146	149	152	156	170	160	170	-	210	210	210	***180***	***200***	***200***	***190***	***180***	***190***	***200***	-	-	1.91
501681	01-Jun-89	08-Sep-91	261	306	360	423	***452***	***390***	***400***	***400***	***434***	***440***	***490***	***530***	***540***	***560***	***520***	***570***	***660***	***710***	***710***	-	17.50
501683	01-Jun-89	23-Sep-91	261	306	360	423	***452***	***380***	***400***	***400***	***430***	***430***	***470***	***510***	***520***	***550***	***630***	***490***	***510***	***570***	***480***	-	17.50
Number in Bold and Italics: Predicted AADTT																							
Not Bold and Italics: Measured																							

3.3 Structural Data

The data defines the pavement layer structural properties and the materials used in each layer. The structural input required depends upon the type of pavement and the type of design (new, rehabilitation, and overlay). The primary input required for the characterization of the Hot Mix Asphalt Concrete (HMAC) is the dynamic modulus (E*) of the asphalt concrete. For level1 analysis, MEPDG recommends the E* value from the lab testing of asphalt concrete samples following the test protocol given in AASHTO TP 62 or ASTM D3497 and the complex shear modulus, G*, and phase angle, δ, of the asphalt binder (AASHTO T 315). These values are required to develop the master curve for the asphalt concrete. For level 2 and 3 analyses, Witczak's dynamic modulus prediction model can be used; it requires HMA gradation, air voids, volumetric binder content, and asphalt binder grade or rheological data as an input to estimate the E* [*23*].

For chemically stabilized (Lean concrete, cement stabilized, soil cement, lime, and fly ash treated) layers, the elastic modulus is required as an input. For Level 1 analysis, the characterization of the unbound materials in the MEPDG is done by using the resilient modulus of the soil at the optimum moisture content measured using AASHTO T-239. For Levels 2 and 3, the inputs required are optimum moisture content, maximum dry density, specific gravity, California Bearing Ratio, R-value, and soil classification, and gradation.

The list of extracted structural data from the LTPP database for the retained sections is appended in APPENDIX B as follows:

- Table B-1: General Information on the selected LTPP sections
- Table B-2: Gradation Data of HMA Aggregates
- Table B-3: Binder Content
- Table B-4: Binder Grade Data
- Table B-5: Subgrade Soil Type

- Table B-6: Base Layer Information
- Table B-7: Layer Thickness Data

3.4 Climatic File Generation

Climatic conditions play a major role in the performance of the pavement and have a significant effect on the pavement materials. Climatic factors, such as moisture, precipitation, freeze-thaw cycles, frost penetration and ground water table, play a key role in affecting the pavement materials and the performance of the pavement. The susceptibility of the pavement materials to freeze-thaw cycles, quality of drainage in the pavement layers and the capillarity of the soils define the extent to which the pavement will be affected by climatic conditions.

The MEPDG models the effects of moisture and temperature profiles in the pavement structure and the subgrade with the Enhanced Integrated Climatic Model (EICM). The model computes the moisture, temperature, and other parameters of the pavement under a given climatic condition. The MEPDG software incorporates a climatic database from which the designer can create a climatic file for any location of a pavement project in the United States.

The MEPDG has two options for creating the climatic file for a given design project: 1) by selecting the closest weather station that are already included in the MEPDG software database (latitude and longitude) near the pavement test section, or 2) by creating a virtual weather station thru interpolation of the data collected by up to five weather stations nearby the location of the pavement section to be designed. The inputs required for creating the climatic file are latitude, longitude, elevation and depth of water table.

For all eighteen LTPP pavement sections selected for local calibration in this study, the MEPDG software contains climatic data only from the year 1996 (partial) to 2006 (partial), the climatic data required for the period 1985 to 1996 when the eighteen LTPP pavement sections were monitored is not available. On the other hand, the LTPP database contains climatic data for the 1985 to 996 period, but only in daily and monthly average values and not hourly data as

required by MEPDG. Therefore, the assembly of climatic data for the local calibration was done in the following steps:

Step 1: The annual average precipitation values for the years 1985 to 1996 were extracted from the LTPP database for each of the 18 projects listed in Table 3-1.

Step 2: From MEPDG climatic files for the years 1996 to 2006 for the weather stations corresponding to the 18 LTPP project locations; the annual average precipitation values for each year were calculated.

Step 3: The annual average precipitation from the MEPDG software database climatic files (covering the period from 1996 to 2006) and from the LTPP database (from 1985 to 1996) were compared for similarity.

Step 4: Where such a pair of years from the two periods were found, the hourly data from the MEPDG climatic file (1996-2006) was copied to the corresponding year in the 1985 to 1996 period. The wind speed and percent sunshine data were also copied

Step 5: The hourly temperature data for the period 1985 to 1996 was also taken from the corresponding MEPDG climatic file, but adjustments were made by subtracting the difference between the average daily temperatures recorded for that day in the MEPDG climatic file and in the LTPP climatic file. For example, if for a given pavement section, the average annual precipitation values recorded in LTPP in 1992 and in MEPDG database in 2001 were similar, 1992 and 2001 became paired years and the temperature on July 3 at 2:00PM in 1992 was computed as:

$$T_{1992\ [July3,\ 2;\ 00PM]} = \{T_{2001\ [July3,\ 2;\ 00PM]} + T_{1992\ [Avg.\ July\ 3]} - T2001_{\ [Avg.\ July\ 3]}\} \quad (3\text{-}2)$$

Where,

$T_{2001\ [July3,\ 2;\ 00PM]}$ - generated temperature data for July 3, 1992 at 2:00PM

$T_{1992\ [Avg.\ July\ 3]}$ - average daily temperature for July 3, 1992 in the LTPP database

$T_{2001\ [Avg.\ July\ 3]}$ - average daily temperature for July 3, 2001 in the MEPDG climatic database

Step 6: The hourly climatic database file was incorporated in the MEPDG parent folder and a new weather station for each SHRP IDs was created.

3.5 LTPP Pavement Performance Data

The pavement performance data required for the calibration process was extracted from the LTPP database for the retained sections.

List of LTPP tables for the distresses data are:

- Total Rutting – MON_RUT_DEPTH (Monitoring Database)
- Alligator Cracking – MONITOR_DIS_PADIAS42_AC (Monitoring Database)
- Longitudinal Cracking - MONITOR_DIS_PADIAS42_AC (Monitoring Database)
- Transverse Cracking - MONITOR_DIS_PADIAS42_AC (Monitoring Database)
- IRI – MON_PROFILE_MASTER (Monitoring Database)

The distresses data for the selected sections are reported in Appendix C.

- Table C1 - Total Rutting
- Table C2 - Alligator Cracking
- Table C2 - Longitudinal Cracking
- Table C2 - Transverse Cracking
- Table C2 - IRI

CHAPTER 4

DEVELOPMENT OF CALIBRATION FACTORS

4.1 Introduction

The term model calibration refers to the minimization of the error or difference between the measured and predicted performance data through changes to the parameters or coefficients of a model; the new coefficients are typically found through a mathematical process. The data required for the national calibration process was obtained from the Long Term Pavement Performance (LTPP) database as described in Chapter 3 of this report. The calibration factors for the Northeastern region of the United States were obtained by comparing the measured distresses data with the distresses data predicted by MEPDG. The prediction was done initially with the national calibrated coefficients (where all β=1) and successively with adjusted calibration coefficients.

4.2 Permanent Deformation Model

The Design Guide uses the concept of incremental damage to estimate rutting or damage in each sub-layer of the pavement structure [*14*]. Permanent deformation models for each layer compute the accumulated plastic strain at the mid-depth of each sub-layer at the end of each sub-season. The total permanent deformation is calculated as the sum of permanent deformation of all sub-layers and is mathematically expressed by Equation 2-20.

Total Rutting = AC Rutting + Base Rutting + Subgrade Rutting (4-1)

The calibration of the permanent deformation models for all three layers was done simultaneously. First, the MEPDG software run was made with the nationally calibrated model (β_{r1}=1.0, β_{GB}=1.0, β_{SG}=1.0). Then the ratio of the predicted rutting in each layer to the total predicted rutting was calculated. The measured total rut depth obtained from the LTPP

database was then multiplied with these ratios to obtain the measured rutting in each pavement layer; the same procedure was used when the national calibration was performed [*14*].

Once the measured and predicted values of permanent deformation in each layer were obtained, the local calibration was done by performing a simple linear regression with no intercept, with the measured permanent deformation as the independent variable. Then the local calibration coefficients were calculated as the inverse of the slope in the linear regression with no intercept. The linear regression with no intercept is performed to account for the proportionality of the coefficients. The calibration coefficients are a direct multiplier of the model and therefore it has to be modified proportionally. The same process was conducted to calculate the calibration coefficients (β_{r1}, β_{GB}, and β_{SG}) for the asphalt concrete, base, and subgrade layers respectively. The obtained calibration coefficients are given in Table 4-1.

Table 4.1: Local Calibration Coefficients for the Permanent Deformation Models

Layers	Model	Flexible Pavements
HMA Surface Layer	$\frac{\varepsilon_p}{\varepsilon_r} = k_z * \beta_{r1} * (10^{-3.35412} T^{1.5606} N^{0.4791})$	β_{r1} = 1.308
Base Layer	$\partial_a(N) = k_1 * \beta_{GB} \left(\frac{\varepsilon_o}{\varepsilon_r}\right) e^{-\left(\frac{\rho}{N}\right)^{\beta}} \varepsilon_v h$	β_{GB} = 2.0654
Subgrade Layer	$\partial_a(N) = k_1 * \beta_{SG} \left(\frac{\varepsilon_o}{\varepsilon_r}\right) e^{-\left(\frac{\rho}{N}\right)^{\beta}} \varepsilon_v h$	β_{SG} = 1.481

Figures 4-1 to 4-6 show the measured vs. predicted rutting in each pavement layer before and after local calibration. The plot suggest that the local calibration coefficients give a better fit between measured and predicted permanent deformation in all layers. Figure 4-7 and 4-8 show the measured versus predicted total permanent deformation. As for the permanent deformation in individual layers, the total predicted permanent deformation fits better than the measured total deformation when the local calibration coefficients are used. The fanning effect in the measured versus predicted plot is due to low measured values of rutting in the initial years which increases with the pavement age. The rutting (distresses) increases with time and progresses to

higher values as the pavement gets distressed with time and traffic loadings. Therefore a large spread of the points is observed at the end which gives the plot a fanning effect.

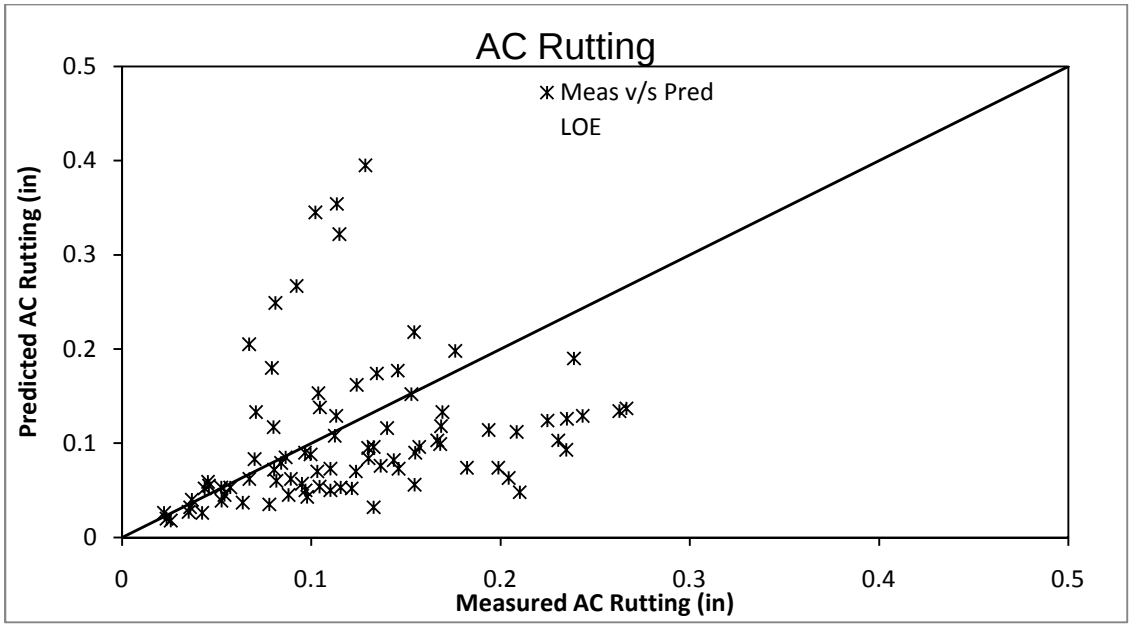

Figure 4.1: Measured v/s predicted AC rutting (National Calibration)

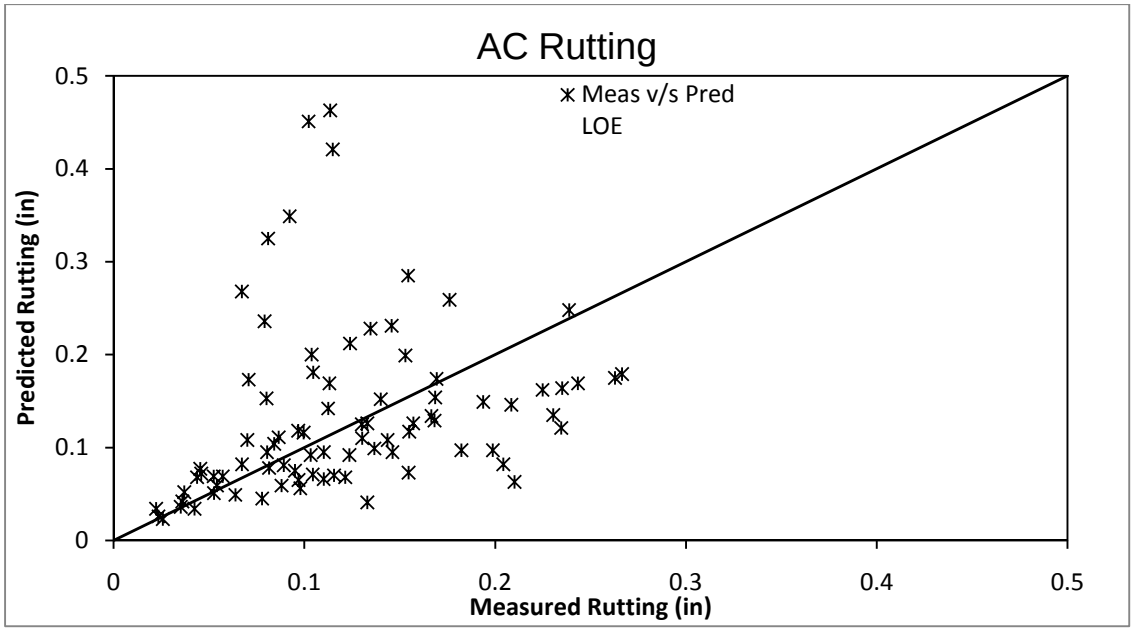

Figure 4.2: Measured v/s predicted AC rutting (Local Calibration)

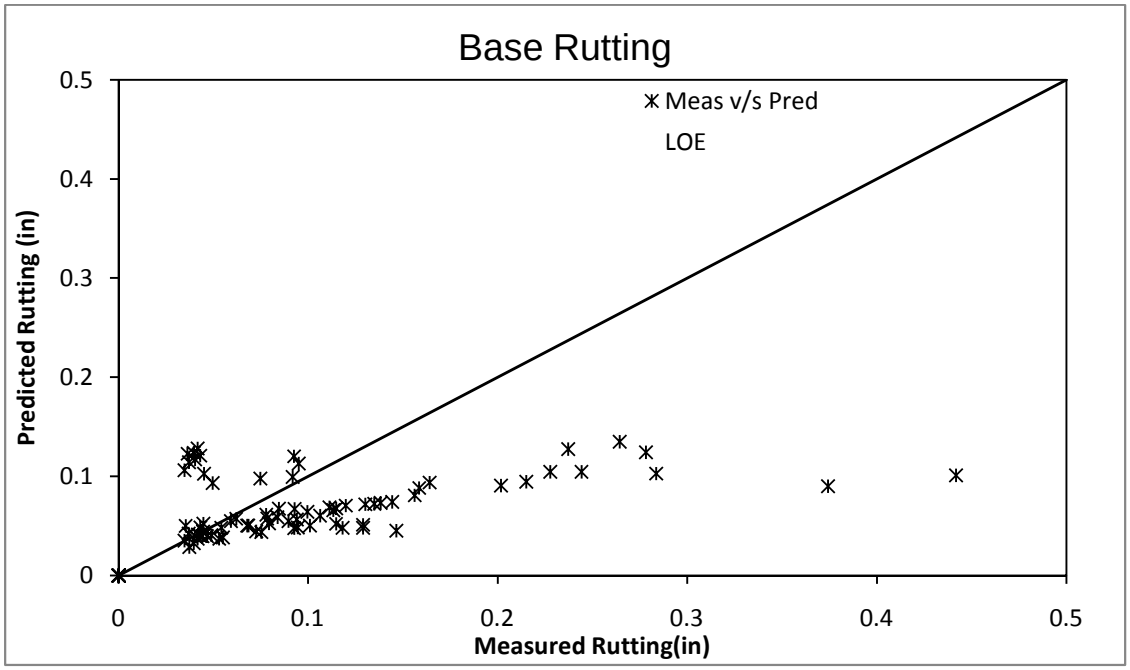

Figure 4.3: Measured v/s predicted base rutting (National Calibration)

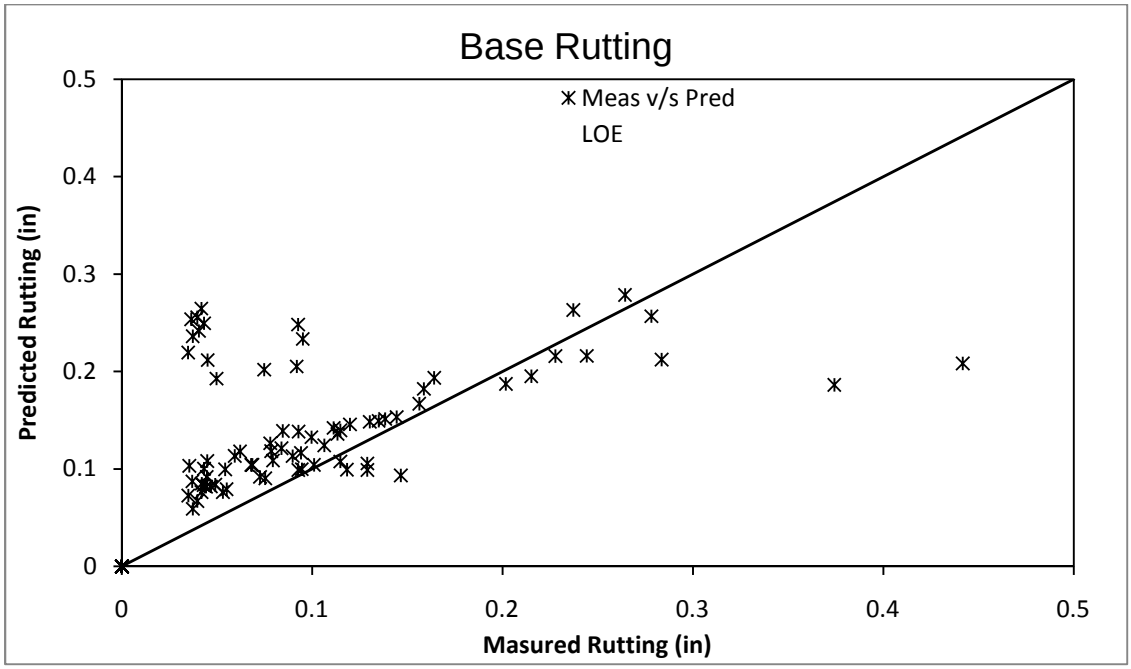

Figure 4.4: Measured v/s predicted base rutting (Local Calibration)

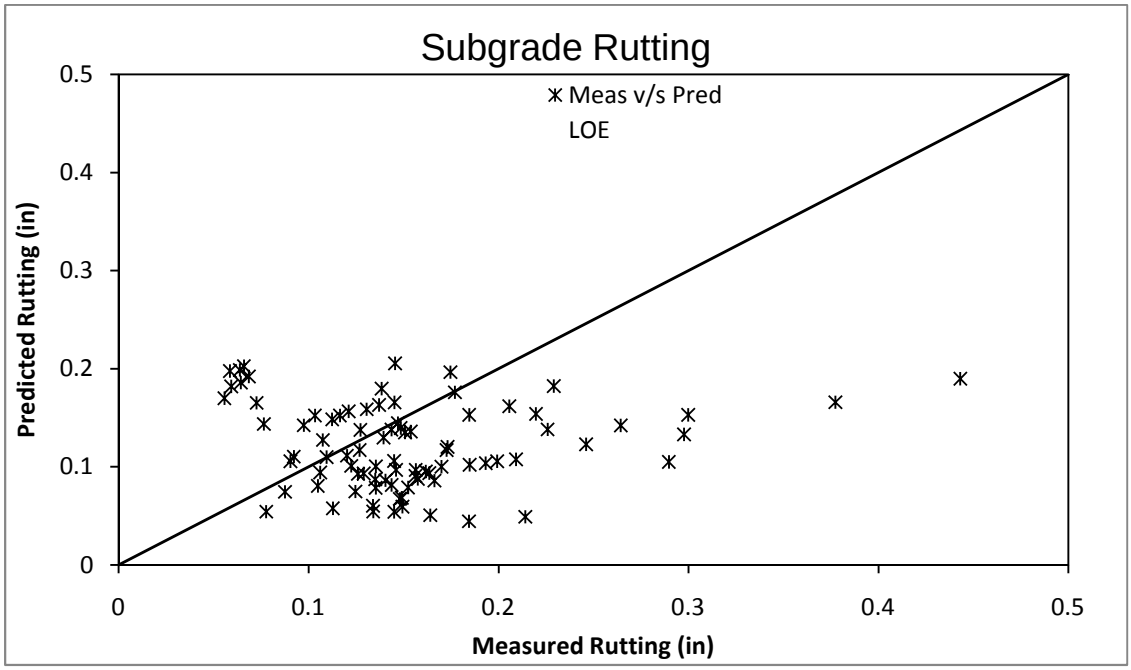

Figure 4.5: Measured v/s predicted subgrade rutting (National Calibration)

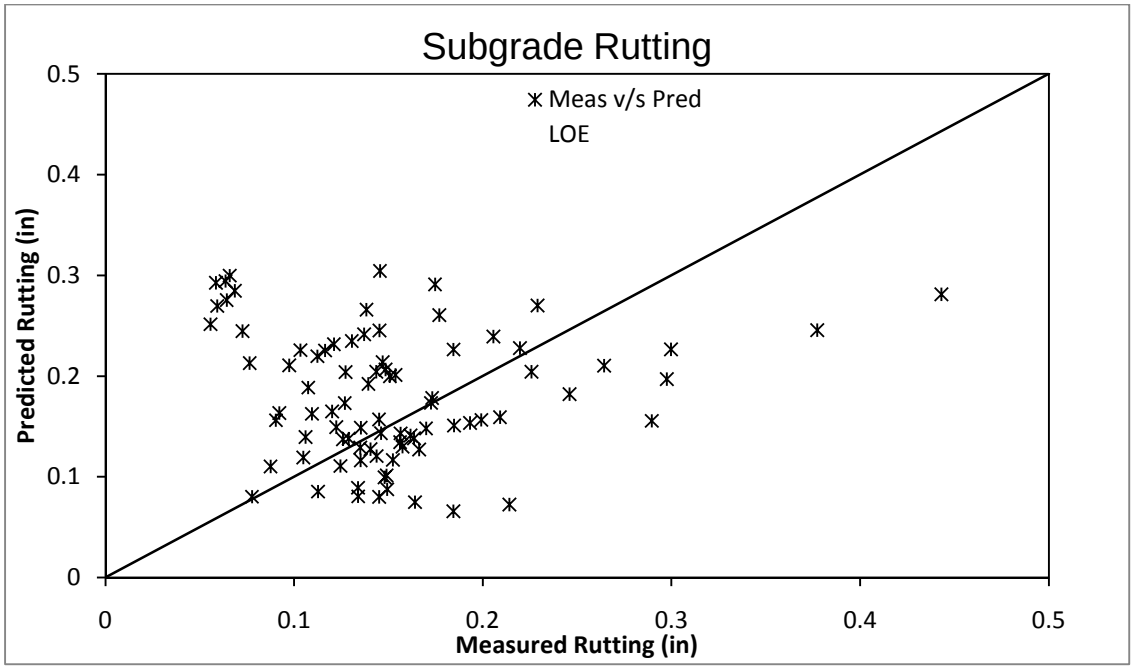

Figure 4.6: Measured v/s predicted subgrade rutting (Local Calibration)

After looking at each layer predictions and the charts with calibrated coefficients, total rutting was observed. The total rutting after recalibration seems to be improved. The sum of square of the error between the measured and predicted values decreased after local calibration.

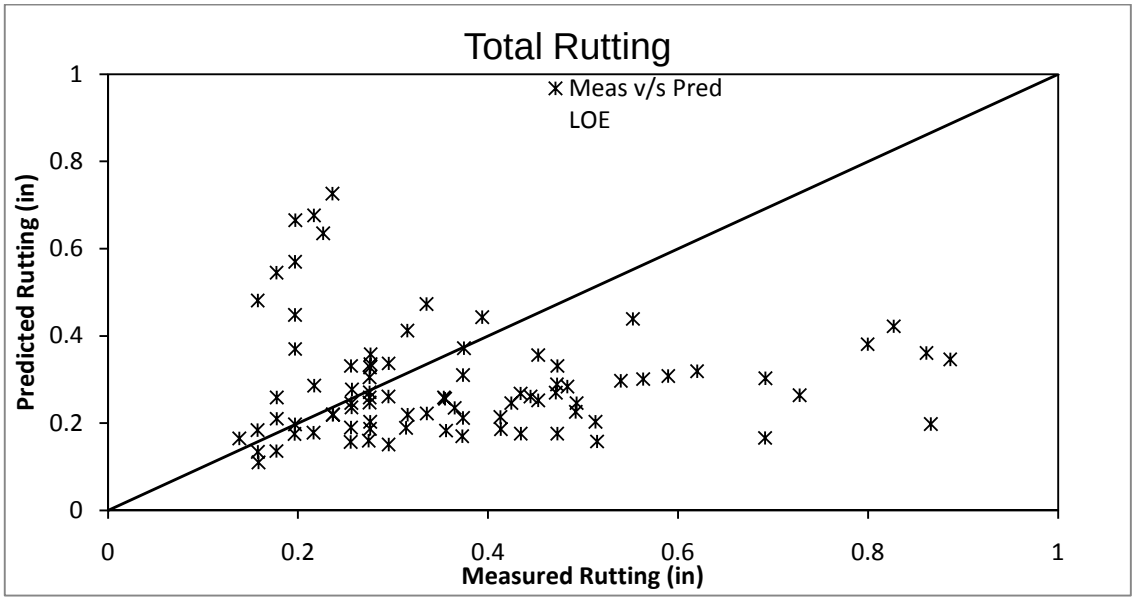

Figure 4.7: Measured v/s predicted total rutting (National Calibration)

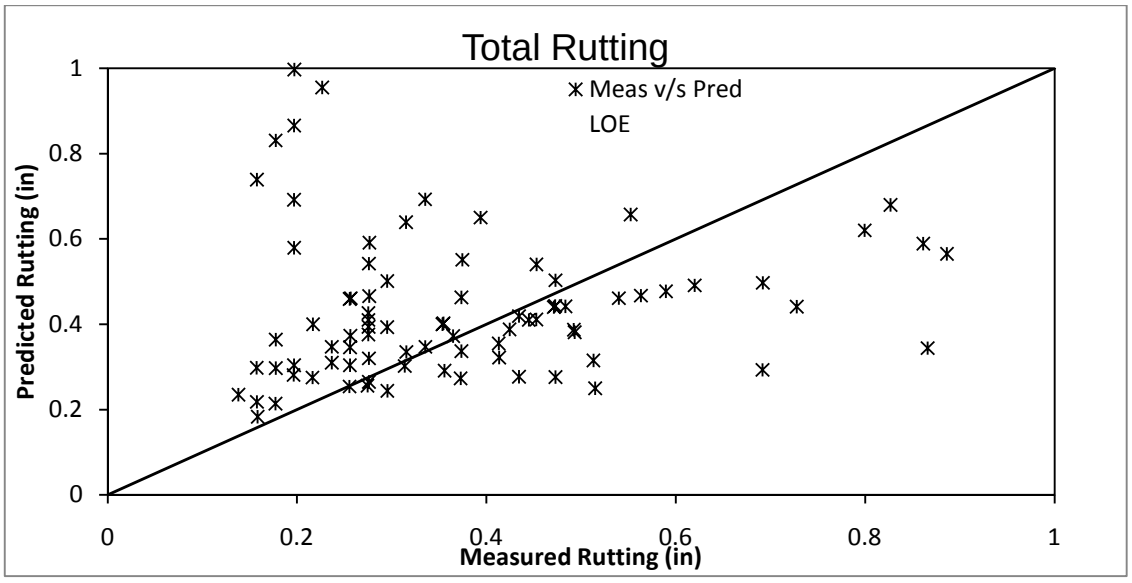

Figure 4.8: Measured v/s predicted total rutting (Local Calibration)

4.3 Bottom-Up Fatigue Cracking Model

The alligator cracking in the LTPP database is measured in metric units (square meters) and therefore was converted to US customary (square feet) and then to percentage of the surface area. The alligator cracking is recorded in the LTPP database for a 500 ft. long surveyed portion of the LTPP section. Also, values are recorded separately for three severity levels: high, medium and low. However, for the calibration of the MEPDG, the values for the three severity levels are summed up to calculate the total area with alligator cracking. Then, the obtained value was converted into percent cracked area considering the total area of the surveyed portion (12*500 = 6000 ft^2) [7].

Since the MEPDG software output gives the fatigue damage, D, calculated for each month of the design life, the calibration consisted of the determination, using Microsoft Excel Solver, of the set of coefficients C_1,C_2,and C_4 in the model (Equation 2-5) that lead to the smallest sum of square difference between the predicted and measured alligator cracking. The sum of square of the error for national calibration was 63.48 and for local calibration it was 43.48. The values obtained for the three coefficients were: C_1 = -0.06883, C_2 =1.27706, and C_4 =6000 for flexible pavements. Figures 4-9 show the correspondence between the measured longitudinal cracking and the predicted cracking with the nationally calibrated coefficients, while Figures 4-10 show the same correspondence but with the alligator cracking predicted with the model calibrated in this study. Figures 4-9 and 4-10 show that the regional calibrated model gives a better prediction of the alligator cracking for flexible pavement structures; the national calibrated model severely under-predicts the extent of alligator cracking (Figure 4-9).

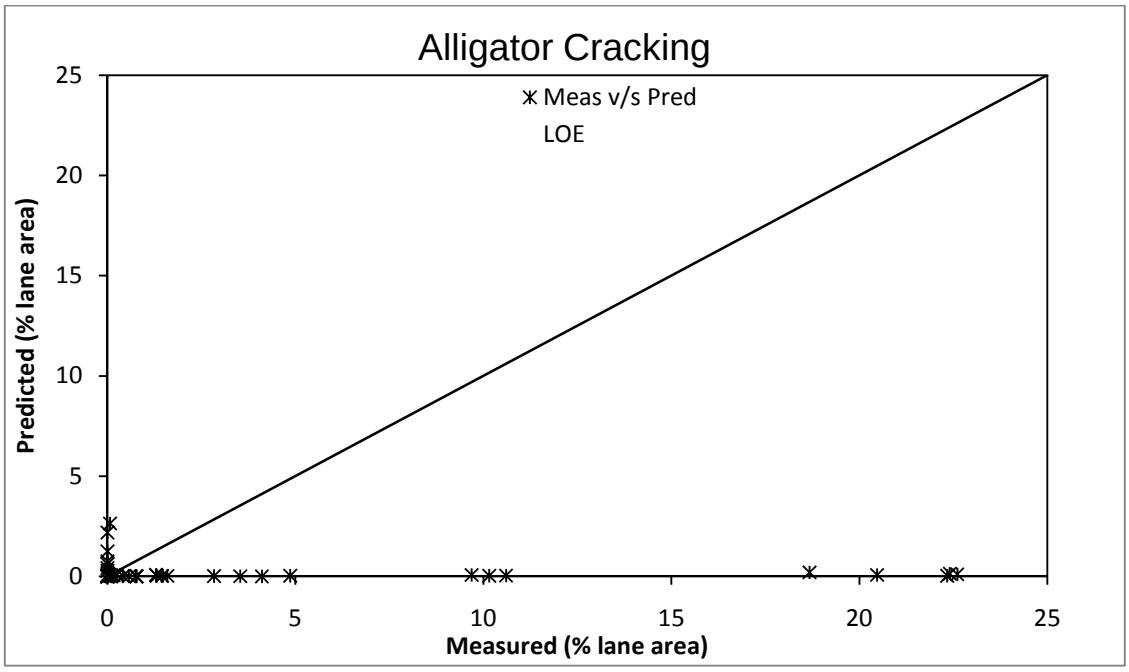

Figure 4.9: Measured v/s predicted alligator cracking (National Calibration)

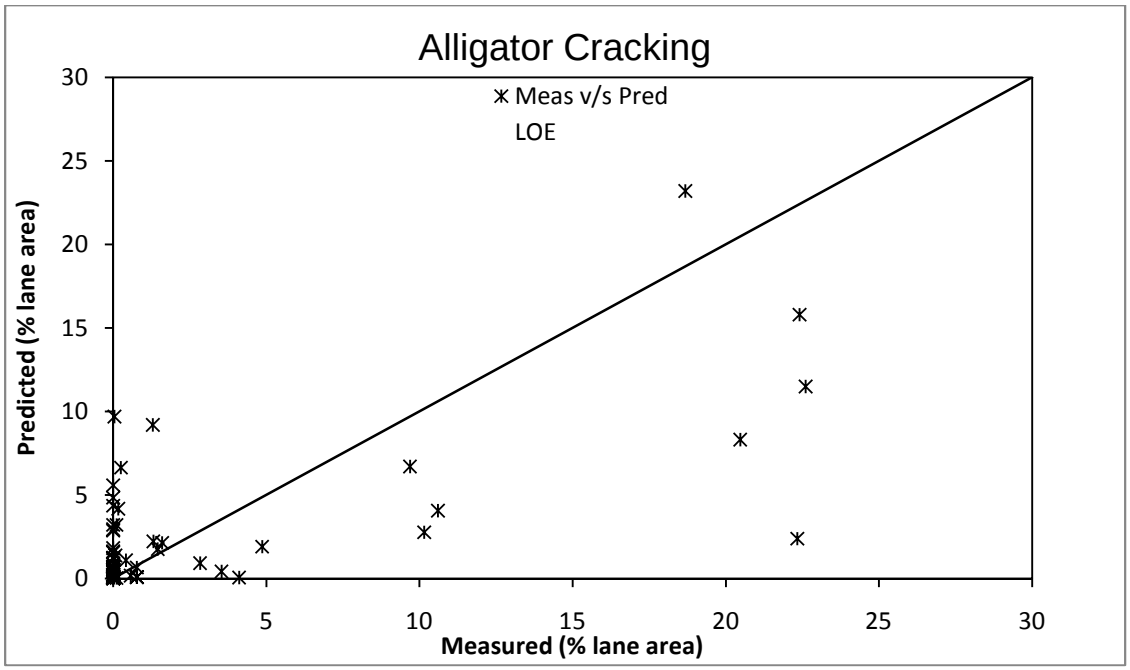

Figure 4.10: Measured v/s predicted alligator cracking (Local Calibration)

4.4 Top – Down Fatigue Cracking Model

The damage transfer function used in the MEPDG for longitudinal cracking (Top-Down) is given in Equation 2-1. For each LTPP section, the longitudinal cracking values recorded in the LTPP database are in meters and were recorded on a 152.4 meter (500ft.) long portion of the LTPP test section. The longitudinal cracking length is recorded in the LTPP database separately for three severity levels: high, medium and low. However, for the national calibration of the MEPDG, the values for the three severity levels are summed up to calculate the total longitudinal cracking length. Then, the obtained value was multiplied by 10.56 to convert it from longitudinal meters for the 500 feet long portion into crack length in feet per mile [7].

In this study, the calibration of longitudinal fatigue cracking model was carried out in a similar manner to that of alligator cracking model. Since the MEPDG software output gives the fatigue damage, D, calculated for each month of the design life, the calibration consisted of the determination, using Microsoft Excel Solver, of the set of coefficients C_1 ,C_2, and C_4 in the model (Equation 2-4) that lead to the smallest sum of square difference between the predicted and measured longitudinal cracking. The sum of square of the error for national calibration was 58.18 and for local calibration it was 25.67. The values obtained for the coefficients were: C_1 =-1, C_2 =2, and C_4 =1856 for flexible pavements. Figure 4-11 show the correspondence between the measured longitudinal cracking and the predicted cracking with the nationally calibrated coefficients, while Figure 4-12 show the same correspondence but with the longitudinal cracking predicted with the model calibrated in this study. Figures 4-11 to 4-12 show that the regional calibrated model gives a better prediction of the longitudinal cracking for flexible pavement structures with minimized sum of square of the error; the national calibrated model severely under-predicts the extent of longitudinal cracking (Figure 4-11).

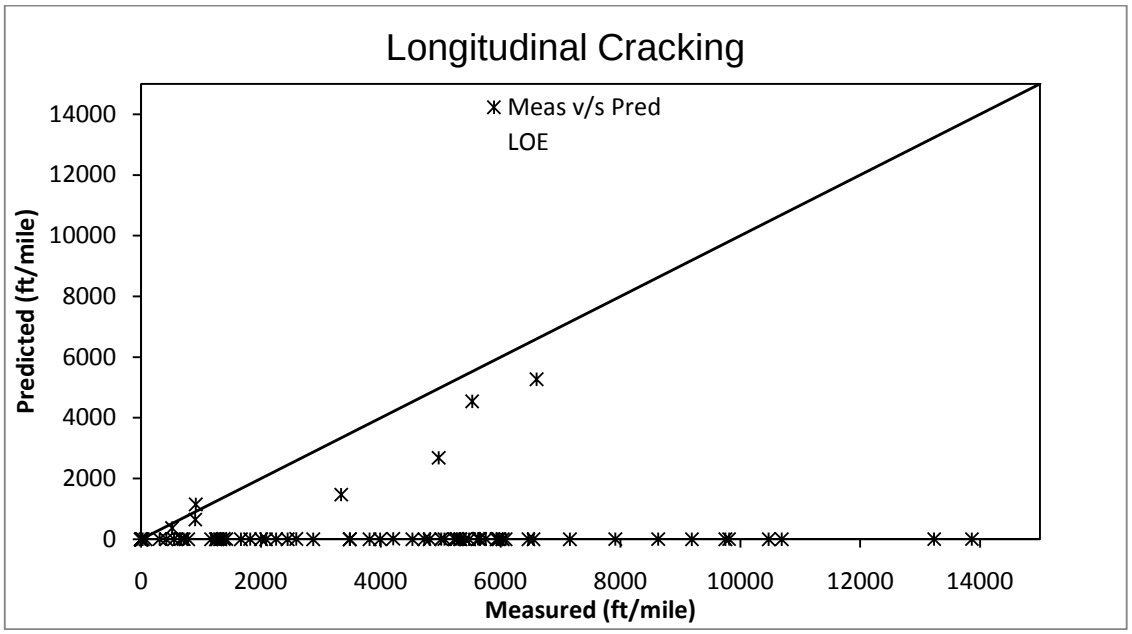

Figure 4.11: Measured v/s predicted longitudinal cracking (National Calibration)

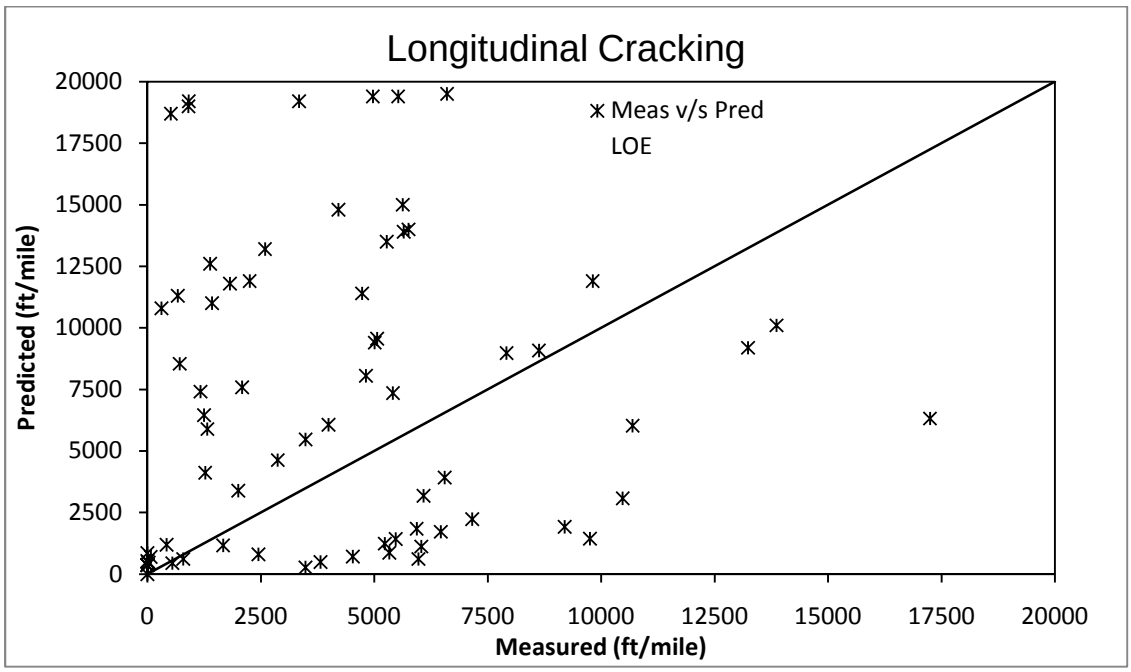

Figure 4.12: Measured v/s predicted longitudinal cracking (Local Calibration)

4.5 Transverse Cracking Calibration

The first step in the calibration of the transverse cracking was to run the MEPDG and obtain the predicted transverse cracking with the national calibrated coefficients. Figure 4-13, shows the predicted versus measured transverse cracking values. The figure shows that, for many sections, the measured values in the LTPP database do not increase in time, as the predicted values do. This is a clear indication that, for several sections retained for this study, the transverse cracking data was erroneously recorded. Due to unreliability of the measured data, it was decided to exclude transverse cracking model from the calibration process, and to keep the nationally calibrated coefficient of 1.0 for this model.

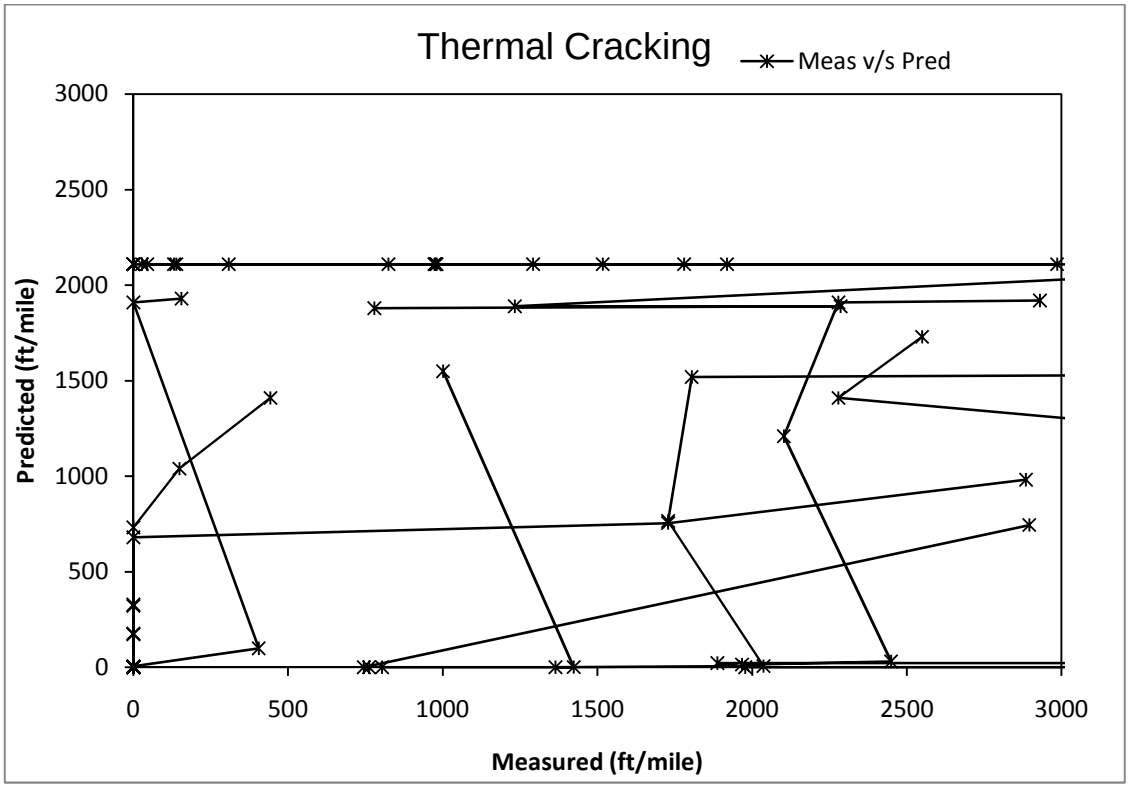

Figure 4.13: Measured v/s predicted thermal cracking (National Calibration)

After the MEPDG default run, several other values of coefficients of thermal cracking were tried to look at the distribution of the measured and predicted thermal cracking values. The measured versus predicted graph showed that the measured values are unrealistic and therefore a very poor fit between the measured and predicted values can be seen in Figure 4-14.

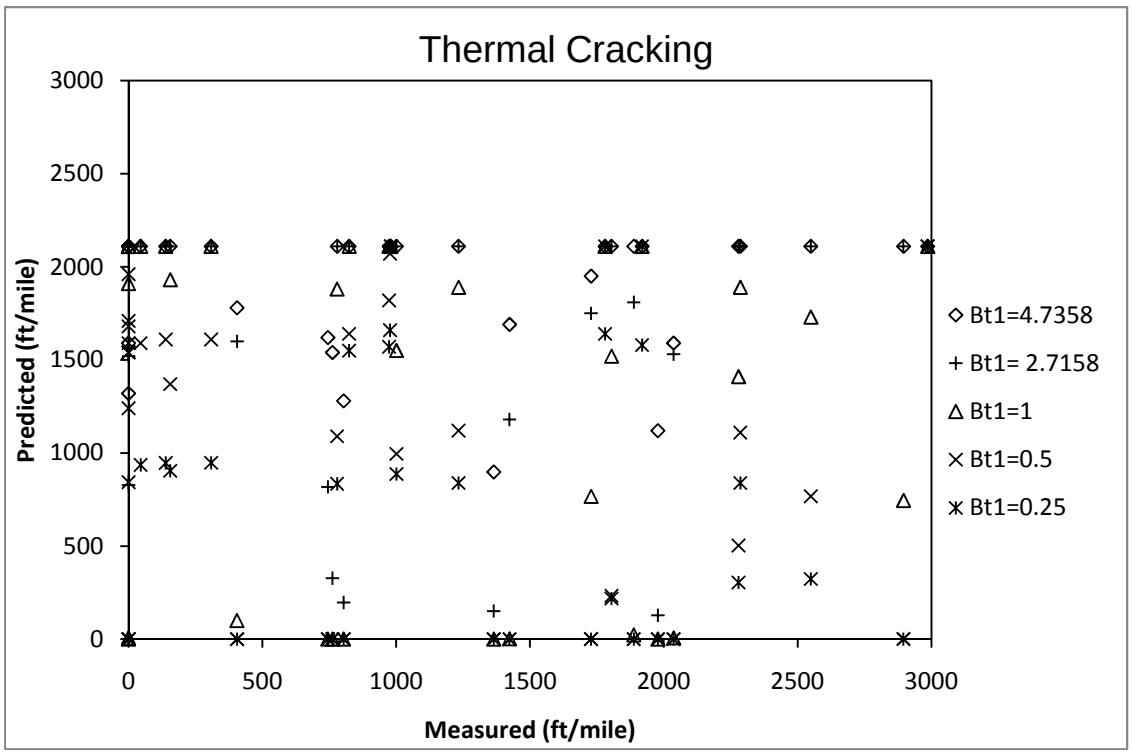

Figure 4.14: Measured v/s Predicted thermal cracking

4.6 Smoothness Prediction Model (International Roughness Index)

Road users' perception of pavement condition has been found to be highly related to the smoothness of the longitudinal profile. Therefore, smoothness is a critical distress and must be predicted as accurate as possible by any pavement design model. Many methods have been developed for the past three decades to measure pavement smoothness and to identify the best measuring units. The most popular way to express pavement smoothness nowadays the

International Roughness Index (IRI), which was developed by The World Bank in 1980's. The unit of measurement of IRI is in/mile (m/km) [*24*].

In MEPDG the IRI is predicted for flexible pavements from the values of other distresses and subgrade properties with the following model:

$$IRI = IRI_o + C_1*(RD) + C_2*(FC_{Total}) + C_3*(TC)\ C_4*(SF) \quad (4\text{-}4)$$

Where,

IRI_o = initial IRI

SF = site factor, dependent on pavement age, plasticity index, average annual precipitation, and freezing index

$$SF = Age\ *0.02003*(PI+1) + 0.007947*(Precip+1) + 0.000636*(FI+1) \quad (4\text{-}5)$$

Age = pavement age

PI = plasticity index of the soil

Precipitation = average annual rainfall (inches)

Freezing Index (FI) = average annual freezing index

FC_{Total} = area of fatigue cracking (combined alligator, longitudinal, and reflection cracking under the wheel path), in percent of total lane area.

TC = length of transverse cracking in ft/mile

RD = average rut depth in inches.

The first step in the IRI model calibration was to run the MEPDG and obtain predicted IRI values with nationally calibrated coefficients. Two sections (341030 and 341033) were removed from the IRI model calibration due to very high measured initial values. The measured IRI values were compared with the predicted values to find the standard error between the two IRI values. The coefficients for IRI model (C_1, C_2, C_3, and C_4) were estimated by performing a regression analysis between the IRI (Difference between measured IRI and initial IRI) and values of other

measured distresses (SF, TC, RD, and FC_{Total}). The estimated calibration coefficients for flexible pavements are C_1 =51.6469, C_2 =0.000218, C_3 = 0.00810, and C_4 =-0.9351.

The IRI model with the local calibration coefficients is:

$$IRI = IRI_o + 51.6469*RD + 0.000218*FC_{Total}\ 0.0081\ *TC\ -0.9351*SF \quad (4\text{-}6)$$

Figure 4-15 shows the measured versus the predicted IRI with the national calibrated model and it suggests a very poor correlation between the values, especially for the high measured IRI values. The SSE for national calibration was 1.557.

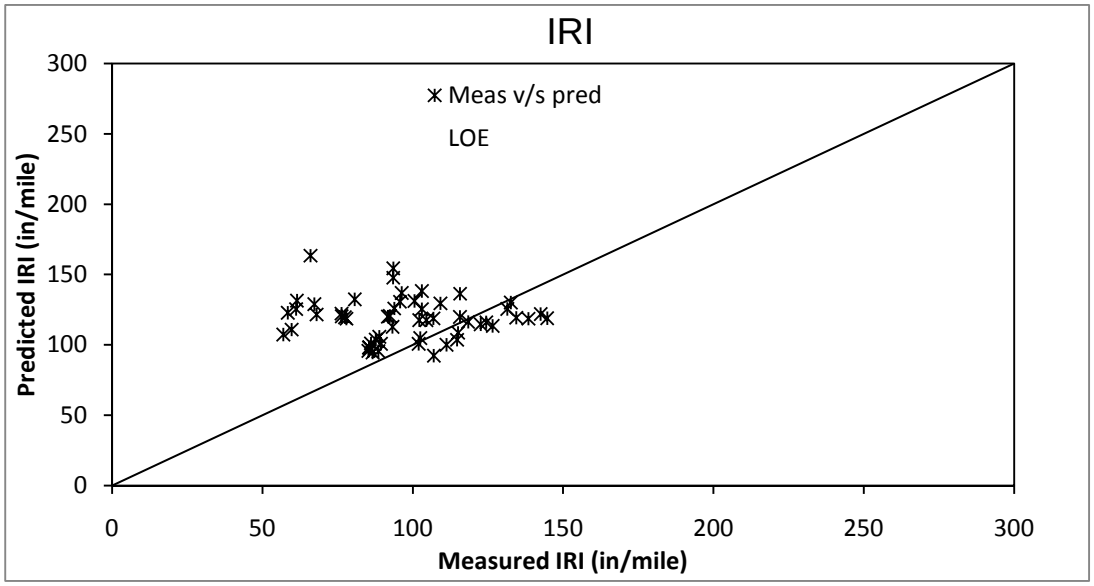

Figure 4.15: Measured v/s predicted IRI (National Calibration)

Figure 4-16 shows the measured versus the predicted IRI with the local calibrated model. The figure suggests that the local calibration did improve the IRI prediction compared to national calibration. After recalibrating the IRI model, the SSE was improved and the value of SSE was 0.799.

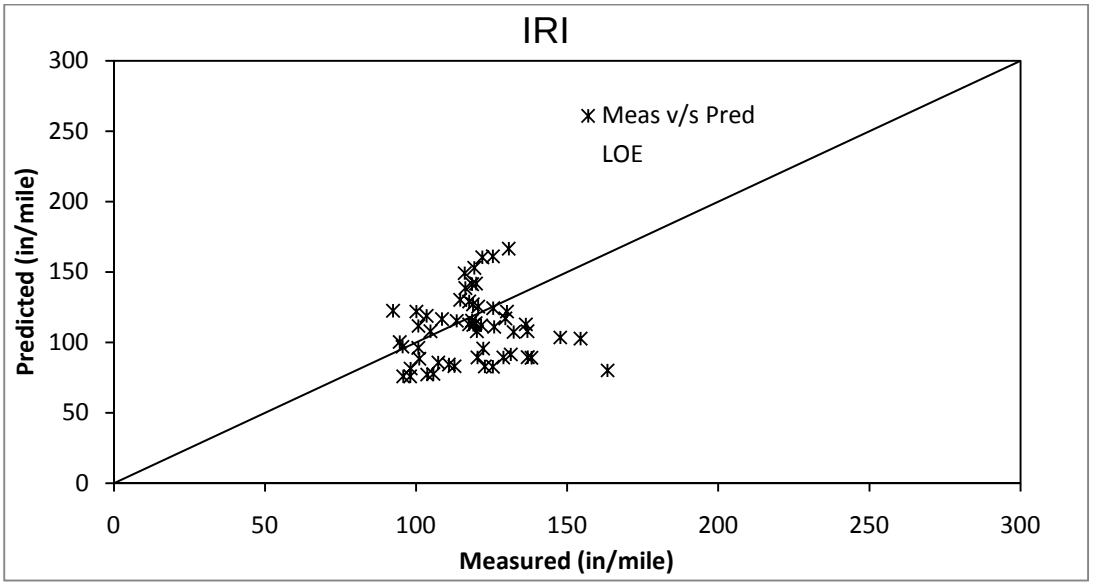

Figure 4.16: Measured v/s predicted IRI (Local Calibration)

4.7 Calibration Summary

Table 4-2 lists the local calibration coefficients obtained in this study along with the national calibration coefficients and the calibration coefficients obtained in several other studies conducted in the Unites States. The table indicates the following:

1. In this study only LTPP (GPS-1 and -2) pavement sections were considered for the calibration process.
2. Utah considered LTPP sections as well as UDOT PMS data for the validation and local calibration process. A total of 30 sections were selected in which 26 sections were new pavement sections and 04 sections were overlay type (HMA over HMA). Since most of the UDOT PMS sections were constructed using SuperPave binders, the rutting measurements were adjusted to make it compatible with LTPP rutting measurements. This affects the local calibration coefficients in comparison to national calibration coefficients because the national calibration was carried out with LTPP pavement sections which are constructed using viscosity graded binders and not SuperPave. For

pavement sections constructed using SuperPave binders, the rutting predictions were very low and therefore the local calibration coefficients vary from the national calibration coefficients.

3. Ohio considered only the LTPP sections SPS-1 and -9 for the local calibration process. The SPS-1 and -9 sections consisted of asphalt treated base and permeable asphalt treated base in the pavement layers. The recalibration of the MEPDG models consisted of SPS projects which were relatively young, with approximately 10 years of distress data. Also for Ohio HMA mixtures, MEPDG over-predicts rutting for lower magnitudes of measured rutting and under-predicts for higher magnitudes of measured rutting. This required adjustment to the β_{2r} and β_{3r} of the HMA rutting submodel. The adjustment to these coefficients should be based on laboratory test on permanent deformation with repeated loadings. Since the laboratory test was not performed, the HMA rutting submodel coefficients β_{2r} and β_{3r} were not adjusted. The recalibration was limited to modifying the HMA, base and subgrade coefficients for local calibration which resulted in poor rutting prediction. The local calibration coefficient is almost 40 percent less than the national calibration because of very small dataset, very young pavement section, and also due to Ohio mixtures strange rutting predictions. The recalibrated model was still deficient in predicting rutting and it was concluded to perform a more comprehensive evaluation of ODOT mixture and also to conduct repeated load permanent deformation test.
4. Washington State calibrated the permanent deformation model using Washington State Pavement Management System data. The local calibration coefficients obtained are very close to national calibration coefficients. It should be noted that Washington State used only the WSPMS sections with very thick base layers (12-14.4 inches) with subgrade rutting set to zero; as Washington State flexible pavements does not typically

experience rutting in base and subgrade layers. The data available for the calibration process consisted of more than thirty years of distress data from the Washington PMS archives. Therefore a wide range of distress data was available for the calibration process which led to a very close local calibration coefficients to national calibration coefficients.

5. The North Carolina local calibration of MEPDG included thirty LTPP sections and 23 NCDOT monitored sections. The LTPP sections consisted of 16 new flexible pavement and 14 rehabilitated sections. For NCDOT sections, the rutting reported in NCDOT PMU is based on the amount of rutting as severe, moderate, light and none. These ratings were converted to numerical values to perform the calibration process. The sections selected for the study consisted of granular base, asphalt treated and cement treated base. But, for the calibration of rutting model only the granular base sections were considered and NCDOT sections were discarded. The local calibration process involved a large data set of 111 data points which provided a better correlation between the measured and predicted rutting and a very close local calibration coefficient to national calibration coefficients.

Table 4.2: Local Calibration Coefficients for Flexible Pavement Performance Models

	Layer	Equation	Coeff.	This study	National	Ohio	Utah	Washington State	North Carolina
Permanent Deformation	HMA	2-22	β_{r1}	1.308	1	0.51	0.560	β_{r1} =1.05	1.017
			β_{r2}	-	-	-	-	β_{r2} =1.109	-
			β_{r3}	-	-	-	-	β_{r3} =1.1	-
	Base	2-29	β_{GB}	2.0654	1	0.32	0.604	-	1.5803
	Subgrade	2-29	β_{SG}	1.481	1	0.33	0.4	-	1.10491
Alligator Cracking	HMA	2-4	C_1	-0.06883	1	-	-	1.071	-
			C_2	1.27706	1	-	-	1	-
Longitudinal Cracking	HMA	2-3	C_1	-1	7	-	-	6.42	-
			C_2	2	3.5	-	-	3.596	-
			C_4	1856	1000	-	-	-	-
IRI	HMA	4-4	C_1	51.6469	40	-	-	-	-
			C_2	0.000218	0.4	-	-	-	-
			C_3	0.00810	0.008	-	-	-	-
			C_4	-0.9351	0.015	-	-	-	-

CHAPTER 5

CONCLUSION AND RECOMMENDATIONS

The Mechanistic-Empirical Pavement Design Guide (MEPDG) developed under the National Cooperative Highway Research Program (NCHRP) 1-37A project is based on mechanistic-empirical analysis of the pavement structure to predict the performance of the pavement under different set of conditions (traffic, structure, and environment). MEPDG takes into account the advanced modeling concepts and pavement performance models in performing the analysis and design of pavement. The mechanistic part of the design concept relies on the application of engineering mechanics to calculate stresses, strains, and deformations in the pavement structure induced by the vehicle loads. The empirical part of the concept is based on laboratory developed performance models that are calibrated with the observed distresses in the in-service pavements with known structural properties, traffic loadings, and performances. These models in the MEPDG were calibrated using a national database of pavement performance data (Long Term Pavement Performance, LTPP) and will provide design solution for pavements with a national average performance. In order to improve the performance prediction of the models and the efficiency of the design for a given state, it is necessary to calibrate it to local conditions by taking into consideration local materials, traffic information and the environmental conditions.

The objective of this study was to calibrate the MEPDG flexible pavement performance models to local conditions of Northeastern region of United States. To achieve this, seventeen pavement sections were selected for the calibration process and the relevant data (structural, traffic, climatic, and pavement performance) was obtained from the LTPP database. MEPDG

software (*Version 1.1*) simulation runs were made using the nationally calibrated coefficients and the predicted distresses were compared with the measured distresses. The predicted distresses showed fair agreement with the measured distresses but still significant differences were found.

The difference between the measured and the predicted distresses were minimized thru recalibration of the MEPDG distress models. For the permanent deformation models in each layer, a simple linear regression with no intercept was performed and a new set of model coefficients (β_{r1}, β_{GB}, *and* β_{SG}) for asphalt concrete, granular base and subgrade layer models were calculated. The calibration of alligator and longitudinal cracking was done by deriving the appropriate model coefficients (C_1, C_2, and C_4) since the fatigue damage is given in MEDPG software output; the coefficients were found using the Microsoft Excel Solver. The calibration of IRI model was done by computing the model coefficients (C_1, C_2, C_3, and C_4) based on other distresses (rutting, total fatigue cracking, and transverse cracking) by performing a simple linear regression.

The following conclusions were made from this study:

- As expected, the local calibration reduces the standard error between the measured and predicted distresses values.
- The permanent deformation calibration coefficients for HMA surface and subgrade layer is almost more than forty percent of the national calibration factors. This may be due to small data set of only 17 sections. The base layer calibration coefficient is almost double the national calibration factor because several sections contain zero values of measured rutting from the LTPP database which gives a very low slope value of the measured versus predicted value.
- In permanent deformation measured versus predicted plot, it is observed that rutting values are very low during the initial period or early age of pavement and then increases

with time. This phenomenon of lower rutting at early age and higher values at the end of design life gives the plot a fanning effect.

- The longitudinal cracking calibration factors C_1 is very low and C_4 is very high as compared to national calibration factors. It is due to high measured and low predicted longitudinal cracking values. The MEPDG predictions are too low when compared with the measured longitudinal cracking.
- The alligator cracking calibration factor C_1 is very low as compared to national calibration factor. It is because the MEPDG predicts very high values of alligator cracking as compared to measured. While in many sections the measured cracking is zero, the corresponding predictions are too high. Use of low calibration factor somewhat minimizes the standard error between the measured and predicted cracking values.
- The thermal cracking values reported in the LTPP database do not increase with time and it was deemed unreliable to be used in the calibration process.
- The local calibration of IRI model was not performed because of very high IRI values recorded in the LTPP database for the selected LTPP sections. Since the local calibration did not significantly improve the difference between the measured and predicted IRI values, it was decided to keep the IRI model with the nationally calibrated coefficients.

The following recommendations are resulting from this study:

- The number of sections for the calibration process should be increased by adding PMS monitored sections to the ones retrieved from the LTPP database.
- If such sections are available, more detailed material characterization data, as those required in Level 1 design, should be assembled. This would lead to a more robust calibration of the models.
- It is also recommended to take cores and forensic investigation of the layers to determine the permanent deformation accumulated in each sub-layers of the pavement structure.

- For longitudinal and alligator cracking measured values, the upper limit of the corresponding distresses should be fixed and distresses data above the limit should be excluded from the calibration process.
- For thermal cracking, a more rigorous and thorough data collection should be done to ensure that the recorded values increase with time. This would allow the calibration of the thermal cracking model in MEPDG.

APPENDIX A

LONG TERM PAVEMENT PERFORMANCE (LTPP) TRAFFIC DATA

Table A-1: Annual Average Daily Truck Traffic

SHRP ID	YEAR	AADTT	SHRP ID	YEAR	AADTT
091803	1992	100	341003	2003	790
091803	1993	110	341003	2004	870
091803	1994	170	341011	1993	1100
091803	1995	190	341011	1994	950
091803	2004	170	341011	1995	1000
091803	2005	170	341011	1996	1050
091803	2006	160	341011	1997	1220
231001	2001	660	341011	1999	1330
231001	2002	640	341011	2000	1340
231001	2003	630	341011	2001	1460
231009	2000	290	341011	2002	1510
231009	2002	290	341011	2003	1590
231009	2003	280	341011	2004	1600
231009	2006	300	341011	2005	1420
231028	2000	250	341011	2007	1230
231028	2001	270	341030	1993	360
231028	2002	310	341030	1994	360
231028	2003	290	341030	1995	350
231028	2004	320	341030	1996	320
231028	2005	300	341030	1997	330
231028	2006	360	341030	1999	390
231028	2007	400	341030	2001	360
251003	1992	100	341030	2006	390
251003	1993	90	341030	2007	330
251003	1994	120	341031	1994	1050
251003	1995	170	341031	1995	1120
251003	1996	230	341031	1996	1040
251003	1997	200	341031	1998	1310
251003	1994	120	341031	1994	1050
251003	1995	170	341031	1995	1120
251003	1994	120	341031	1994	1050

Table A-1: Continued

SHRP ID	YEAR	AADTT	SHRP ID	YEAR	AADTT
251003	1995	170	341031	1995	1120
251003	1996	230	341031	1996	1040
251003	1997	200	341031	1998	1310
251003	1998	200	341031	1999	1340
341003	1994	670	341033	1994	260
341003	1995	750	341033	1995	270
341003	1996	940	341033	2000	320
341003	1997	1520	341033	2002	300
341003	1998	1020	341033	2003	250
341003	1999	640	341033	2004	290
341003	2000	820	341034	1994	1190
341003	2001	830	341034	1995	1180
341003	2002	750	341034	1996	1230
341034	2004	1640	341034	1997	1290
341034	2007	1330	341034	1998	1340
341638	1994	1150	341034	1999	1310
341638	1995	1170	341034	2000	1370
341638	1996	1190	341034	2001	1450
341638	1997	1250	341034	2002	1560
341638	1998	1270	341034	2003	1570
341638	1999	1180	501002	2005	310
341638	2002	1610	501002	2006	490
341638	2003	1910	501002	2007	380
341638	2004	1960	501004	1992	170
341638	2005	1700	501004	1993	160
341638	2007	1350	501004	1994	170
361643	1995	770	501004	1996	210
421597	1998	90	501004	1997	210
421597	1999	90	501004	1998	210
421597	2004	150	501004	1999	180
421597	2005	130	501004	2000	200

Table A-1: Continued

SHRP ID	YEAR	AADTT	SHRP ID	YEAR	AADTT
421597	2006	160	501004	2001	200
421597	2007	130	501004	2002	190
421599	1998	450	501004	2003	180
421599	1999	470	501004	2004	190
421599	2000	510	501004	2005	200
421599	2001	490	501681	1992	400
421599	2003	490	501681	1993	390
421599	2004	490	501681	1994	400
421599	2005	490	501681	1995	400
421599	2006	500	501681	1996	410
421599	2007	530	501681	1997	440
501002	1992	240	501681	1998	490
501002	1993	220	501681	1999	530
501002	1994	220	501683	1992	390
501002	1995	220	501683	1993	380
501002	1996	250	501683	1994	400
501002	1997	260	501683	1995	400
501002	1998	260	501681	2006	710
501002	1999	380	501683	1996	410
501002	2000	370	501683	1997	430
501002	2001	320	501683	1998	470
501002	2002	290	501683	1999	510
501002	2003	300	501683	2000	520
501002	2004	280	501683	2001	550
501681	2000	540	501683	2002	630
501681	2001	560	501683	2003	490
501681	2002	520	501683	2004	510
501681	2003	570	501683	2005	570
501681	2004	660	501683	2006	480
501681	2005	710			

Table A-2: Vehicle Class Distribution

SHRP ID	Year	Vehicle Class										Total
091803	1992	0.87	50.95	17.49	12.75	2.75	14.52	0.51	0.14	0.01	0.01	100
231001	2002	3.45	20.82	2.32	0.05	3.47	57.85	11.03	0.87	0.13	0.01	100
231009	2000	9.49	35.83	10.71	2.05	8.17	23.71	9.89	0.15	0	0	100
231028	2000	6.71	18.51	7.85	2.29	2.5	24.48	37.61	0	0	0.05	100
251003	1993	1.75	56.96	24.43	0.31	7.37	8.88	0.26	0.04	0	0	100
341003	1994	1.05	61.56	9.98	0.24	4.95	21.62	0.5	0.1	0	0	100
341011	1993	1.6	31.16	17.69	1.64	8.9	36.53	1.13	1.19	0.06	0.1	100
341030	1999	1.82	62.91	12.14	4.9	3.95	13.82	0.46	0	0	0	100
341031	1998	1.74	28.45	5.25	9.68	7.25	44.94	1.96	0.7	0.02	0.01	100
341033	2002	2.54	48.96	14.17	1.23	6.12	25.95	0.7	0.26	0.05	0.02	100
341034	1997	2.23	41.07	9.47	3.58	7.68	34.19	1.19	0.55	0.02	0.02	100
341638	1996	1.59	37.31	6.4	3.38	9.68	39.95	1.05	0.61	0.02	0.01	100
421597	2004	4.69	42.94	14.61	3.43	8.21	23.62	0.35	2.11	0.01	0.03	100
421599	2001	1.02	15.98	9.49	9.13	4.55	58.67	0.45	0.54	0.03	0.14	100
501002	1992	3.45	32.84	18.81	1.26	8.21	33.28	0.77	0.74	0.63	0.01	100
501004	1994	1.91	53.98	10.32	0.19	10.21	22.59	0.51	0.1	0.19	0	100
501681	1992	2.52	26.82	8.2	0.39	8.81	50.24	2.24	0.76	0.02	0	100
501683	1992	2.52	26.56	8.62	0.52	9.7	49.86	1.72	0.45	0.04	0.01	100

Table A-3: Monthly Adjustment Factors

Site: 231001-2002

Month	Class 4	Class 5	Class 6	Class 7	Class 8	Class 9	Class 10	Class 11	Class 12	Class 13
January	1.2	0.84	1.56	0	1.08	1.2	1.08	1.32	1.344	0
February	1.2	0.96	1.44	0	1.2	1.272	1.08	1.08	1.332	0
March	1.2	0.84	1.92	0	0.96	1.296	1.08	1.32	1.332	0
April	1.32	1.08	1.92	0	1.08	1.296	1.2	1.32	1.332	0
May	1.44	1.32	1.68	6	1.32	1.296	1.32	1.32	1.332	0
June	1.56	1.68	1.44	0	1.5	1.08	0.96	1.44	1.332	0
July	1.32	1.68	2.04	0	1.5	1.08	1.08	1.44	1.332	0
August	0	0	0	0	0	0	0	0	0	0
September	0	0	0	0	0	0	0	0	0	0
October	1.08	1.44	0	6	1.2	1.2	1.44	1.08	1.332	0
November	0.84	1.2	0	0	1.08	1.2	1.44	0.84	1.332	0
December	0.84	0.96	0	0	1.08	1.08	1.32	0.84	0	0

Site: 231009-2000

Month	Class 4	Class 5	Class 6	Class 7	Class 8	Class 9	Class 10	Class 11	Class 12	Class 13
January	0	0	0	0	0	0	0	0	0	0
February	0.924	0.792	0.792	1.188	1.056	1.056	0.66	0	0	0
March	1.056	0.792	0.792	1.056	1.32	1.056	0.924	0	0	0
April	1.056	0.66	1.056	1.548	1.188	0.924	1.188	0	0	0
May	1.32	0.924	1.188	1.056	1.32	1.188	1.32	2.64	0	0
June	1.452	1.32	1.452	1.452	1.32	1.452	1.32	2.64	0	0
July	1.452	1.452	1.584	1.188	1.056	1.188	1.452	2.64	0	0
August	1.452	1.848	1.452	1.188	1.32	1.452	1.512	0	0	0
September	1.056	2.112	1.188	0.792	1.056	1.188	0.924	0	0	0
October	1.188	1.452	1.452	1.536	1.32	1.452	1.524	2.64	0	0
November	1.188	1.056	1.452	1.536	1.188	1.188	1.452	2.64	0	0
December	1.056	0.792	0.792	0.66	1.056	1.056	0.924	0	0	0

Table A-3: - Continued
Site: 231028-2000

Month	Class 4	Class 5	Class 6	Class 7	Class 8	Class 9	Class 10	Class 11	Class 12	Class 13
January	1.98	1.056	0.528	1.056	1.188	1.056	1.188	0	0	0
February	2.244	1.056	0.66	1.188	1.188	1.056	1.32	0	0	0
March	1.32	0.924	0.66	1.188	1.188	1.188	1.32	0	0	0
April	1.188	0.792	0.792	0.792	1.188	1.056	1.056	0	0	0
May	0.924	0.924	1.32	0.792	1.188	1.32	1.056	0	0	0
June	0.924	1.188	1.716	1.716	1.32	1.32	1.32	0	0	0
July	0.792	1.452	1.452	0.792	1.188	1.188	1.188	0	0	0
August	0.792	1.716	1.716	2.112	1.452	1.32	1.32	0	0	0
September	1.056	1.716	1.452	1.056	1.188	1.188	1.056	0	0	0
October	1.056	1.584	1.584	1.848	1.188	1.32	1.32	0	0	0
November	0.924	0.792	1.32	0.66	0.924	1.188	1.056	0	0	0
December	0	0	0	0	0	0	0	0	0	0

Site: 251003-1993

Month	Class 4	Class 5	Class 6	Class 7	Class 8	Class 9	Class 10	Class 11	Class 12	Class 13
January	1.308	1.188	1.836	0	2.592	1.404	0	0	0	0
February	1.356	1.296	2.16	0	1.728	1.728	0	0	0	0
March	1.356	1.404	1.836	0	2.052	1.404	0	0	0	0
April	1.356	0.972	2.376	0	1.728	2.916	0	0	0	0
May	1.356	1.188	0.864	0	1.08	1.404	0	0	0	0
June	0	1.296	0.432	0	0.324	0.54	0	0	0	0
July	1.356	1.08	0.54	0	0.324	0.54	0	0	0	0
August	1.356	1.08	0.108	0	0.324	0.324	0	0	0	0
September	1.356	1.296	0.648	0	0.648	0.54	0	0	0	0
October	0	0	0	0	0	0	0	0	0	0
November	0	0	0	0	0	0	0	0	0	0
December	0	0	0	0	0	0	0	0	0	0

Table A-3: - Continued
Site: 341003-1994

Month	Class 4	Class 5	Class 6	Class 7	Class 8	Class 9	Class 10	Class 11	Class 12	Class 13
January	4.2	1.2	0.6	0	0.84	1.44	0.72	0	0	0
February	4.56	1.32	0.6	0	1.08	1.2	0.72	0	0	0
March	0.72	1.2	0.24	0	0.36	0.24	0	0	0	0
April	1.08	1.2	0.6	0	0.6	0.6	0	0	0	0
May	1.44	0.96	0.6	0	0.72	0.6	0.72	0	0	0
June	0	1.2	1.92	1.68	1.8	1.8	1.56	6	0	0
July	0	1.2	2.04	3.48	1.8	1.68	2.28	6	0	0
August	0	1.56	2.28	3.48	2.16	2.04	3	0	0	0
September	0	1.2	2.04	1.68	1.8	1.68	2.28	0	0	0
October	0	0.96	1.08	1.68	0.84	0.72	0.72	0	0	0
November	0	0	0	0	0	0	0	0	0	0
December	0	0	0	0	0	0	0	0	0	0

Site: 341011-1993

Month	Class 4	Class 5	Class 6	Class 7	Class 8	Class 9	Class 10	Class 11	Class 12	Class 13
January	0	0	0	0	0	0	0	0	0	0
February	0	0	0	0	0	0	0	0	0	0
March	0	0	0	0	0	0	0	0	0	0
April	0	0	0	0	0	0	0	0	0	0
May	4.032	1.44	1.44	2.4	1.248	1.296	1.464	1.344	0	1.2
June	0	1.248	1.92	1.248	1.248	1.296	1.476	1.152	1.62	1.2
July	0	1.152	1.44	0.96	1.248	1.152	1.476	1.248	0	1.2
August	1.44	1.248	1.44	1.152	1.248	1.248	1.344	1.248	1.596	1.2
September	1.344	1.152	1.056	1.056	1.248	1.152	1.056	1.152	1.596	1.2
October	1.152	1.152	0.768	1.152	1.152	1.152	0.96	1.248	1.596	1.2
November	0.96	1.152	0.864	0.864	1.152	1.152	0.96	1.248	1.596	1.2
December	0.672	1.056	0.672	0.768	1.056	1.152	0.864	0.96	1.596	1.2

Table A-3: - Continued
Site: 341030-1999

Month	Class 4	Class 5	Class 6	Class 7	Class 8	Class 9	Class 10	Class 11	Class 12	Class 13
January	1.452	1.716	0.792	0.264	1.056	0.792	0	0	0	0
February	1.32	0.924	0.924	0.396	0.792	1.056	0.792	0	0	0
March	0	0	0	0	0	0	0	0	0	0
April	1.32	1.32	1.452	1.056	1.32	1.32	2.112	0	0	0
May	0.66	1.056	0.924	1.056	0.924	1.188	1.452	0	0	0
June	1.452	1.188	1.452	1.584	1.584	1.584	1.452	0	0	0
July	1.776	1.188	1.512	1.716	1.584	1.32	1.452	0	0	0
August	1.788	1.32	1.32	2.376	1.98	1.32	1.452	0	0	0
September	1.32	1.188	1.056	0.66	1.452	1.188	0.792	0	0	0
October	1.056	1.056	1.056	0.792	1.056	1.188	1.452	0	0	0
November	0.528	1.056	1.188	1.452	0.66	1.056	0.792	0	0	0
December	0.528	1.188	1.524	1.848	0.792	1.188	1.452	0	0	0

Site: 341031-1998

Month	Class 4	Class 5	Class 6	Class 7	Class 8	Class 9	Class 10	Class 11	Class 12	Class 13
January	0	0	0	0	0	0	0	0	0	0
February	0	0	0	0	0	0	0	0	0	0
March	1.32	1.32	1.56	1.32	1.68	1.44	1.56	1.2	12	0
April	0.84	1.08	1.08	0.96	1.44	1.2	1.2	0.72	0	0
May	0.96	1.2	1.08	0.96	1.08	1.08	1.08	0.84	0	0
June	1.56	1.2	1.2	1.32	1.2	1.2	1.32	1.2	0	0
July	1.32	1.32	1.2	1.2	1.2	1.2	0.96	1.08	0	0
August	1.2	1.2	1.08	1.32	1.08	1.2	1.2	1.2	0	0
September	1.32	1.2	1.2	1.32	1.08	1.2	1.2	1.32	0	0
October	1.2	1.2	1.2	1.32	1.08	1.2	1.32	1.32	0	0
November	1.2	1.2	1.2	1.2	1.08	1.2	1.2	1.2	0	0
December	1.08	1.08	1.2	1.08	1.08	1.08	0.96	1.92	0	0

Table A-3: - Continued
Site: 341033-2002

Month	Class 4	Class 5	Class 6	Class 7	Class 8	Class 9	Class 10	Class 11	Class 12	Class 13
January	1.2	0.84	0.96	0.96	1.08	1.2	1.632	1.5	0	0
February	1.2	0.72	0.6	0.36	0.96	0.96	1.08	1.5	0	0
March	0	0	0	0	0	0	0	0	0	0
April	0	0	0	0	0	0	0	0	0	0
May	1.56	1.8	1.32	0.96	1.2	1.32	1.08	1.5	0	0
June	1.2	2.16	1.488	1.32	1.2	1.296	1.08	1.5	0	0
July	1.08	1.56	1.476	1.56	1.38	1.296	1.08	1.5	0	0
August	1.2	1.2	1.2	1.32	1.38	1.296	1.644	1.5	0	0
September	1.2	0.96	1.32	1.68	1.38	1.296	1.08	1.5	0	0
October	1.2	0.96	1.476	1.32	1.38	1.296	1.644	1.5	0	0
November	1.08	0.96	1.2	1.56	1.08	1.2	1.08	0	0	0
December	1.08	0.84	0.96	0.96	0.96	0.84	0.6	0	0	0

Site: 341034-1997

Month	Class 4	Class 5	Class 6	Class 7	Class 8	Class 9	Class 10	Class 11	Class 12	Class 13
January	1.08	1.08	1.08	1.08	1.188	1.296	0.864	1.188	0	0
February	1.188	1.188	1.08	0.864	1.188	1.188	0.864	1.296	0	0
March	1.296	1.08	1.08	0.972	1.08	1.08	1.08	1.296	0	0
April	1.296	1.296	1.296	1.188	1.404	1.404	1.728	1.56	10.8	0
May	1.296	1.296	1.296	1.08	1.404	1.404	1.728	1.572	0	0
June	1.296	1.296	1.296	1.512	1.296	1.296	1.62	1.296	0	0
July	0	0	0	0	0	0	0	0	0	0
August	0	0	0	0	0	0	0	0	0	0
September	0	0	0	0	0	0	0	0	0	0
October	1.296	1.296	1.62	1.944	1.404	1.296	1.188	1.296	0	0
November	1.08	1.08	1.188	1.188	0.972	0.972	0.972	0.756	0	0
December	0.972	1.188	0.864	0.972	0.864	0.864	0.756	0.54	0	0

Table A-3: - Continued
Site: 341638-1996

Month	Class 4	Class 5	Class 6	Class 7	Class 8	Class 9	Class 10	Class 11	Class 12	Class 13
January	0	1.056	1.188	0.528	1.056	1.188	0.792	1.188	0	0
February	0	1.188	1.188	0.66	1.188	1.344	1.056	1.188	0	0
March	0.264	1.188	1.32	1.452	1.188	1.356	1.32	1.188	0	0
April	1.584	1.248	1.38	2.376	1.356	1.356	1.716	1.32	0	0
May	1.908	1.272	1.392	1.98	1.368	1.356	1.32	1.32	0	0
June	1.92	1.272	1.188	1.584	1.188	1.188	1.32	1.188	0	0
July	1.716	1.272	1.188	1.452	1.188	1.188	1.584	1.188	0	0
August	1.716	1.272	1.32	1.188	1.368	1.188	1.584	1.452	0	0
September	0	0	0	0	0	0	0	0	0	0
October	1.452	1.188	0.924	0.66	1.188	1.056	0.66	1.188	0	0
November	1.452	1.188	1.056	0.792	1.056	1.056	1.056	1.188	0	0
December	1.188	1.056	1.056	0.528	1.056	0.924	0.792	0.792	0	0

Site: 421597-2004

Month	Class 4	Class 5	Class 6	Class 7	Class 8	Class 9	Class 10	Class 11	Class 12	Class 13
January	1.188	1.056	0.528	0.792	0.924	0.924	0	0.792	0	0
February	1.188	1.188	0.528	1.056	1.188	1.056	0	1.32	0	0
March	1.584	1.188	0.528	1.056	1.188	1.056	0	1.32	0	0
April	1.584	1.452	0.924	1.056	1.32	1.188	0	1.584	0	0
May	1.32	1.056	1.32	0.792	1.056	1.188	3.3	1.32	0	0
June	0.792	0.924	1.452	1.584	1.32	1.452	0	1.32	0	0
July	0.528	1.056	1.188	1.056	1.188	1.188	0	1.32	0	0
August	0.792	1.188	2.64	2.112	1.188	1.452	3.3	1.32	0	0
September	1.848	1.188	1.056	1.32	1.32	1.32	0	0.792	0	0
October	1.98	1.584	1.452	1.584	1.32	1.32	3.3	1.32	0	0
November	0.396	1.32	1.584	0.792	1.188	1.056	3.3	0.792	0	0
December	0	0	0	0	0	0	0	0	0	0

Table A-3: - Continued
Site: 421599-2001

Month	Class 4	Class 5	Class 6	Class 7	Class 8	Class 9	Class 10	Class 11	Class 12	Class 13
January	0.72	1.2	0.84	0.96	1.2	1.08	0.6	0.96	0	0
February	0	0	0	0	0	0	0	0	0	0
March	0	0	0	0	0	0	0	0	0	0
April	1.08	1.2	1.2	1.08	1.2	1.2	1.2	1.38	0	1.5
May	1.32	1.272	1.56	1.512	1.2	1.2	1.2	1.356	0	1.5
June	1.32	1.2	1.44	1.524	1.32	1.2	1.8	1.356	0	1.5
July	0.72	1.08	1.32	1.32	1.2	1.2	1.8	1.356	0	0
August	1.08	1.284	1.2	1.524	1.2	1.32	1.2	1.356	0	1.5
September	1.32	1.2	1.2	1.2	1.08	1.2	1.2	1.356	0	1.5
October	1.56	1.284	1.32	1.2	1.32	1.32	1.8	0.96	0	1.5
November	1.32	1.2	0.96	0.84	1.2	1.2	0.6	0.96	0	1.5
December	1.56	1.08	0.96	0.84	1.08	1.08	0.6	0.96	0	1.5

Site: 501002-1992

Month	Class 4	Class 5	Class 6	Class 7	Class 8	Class 9	Class 10	Class 11	Class 12	Class 13
January	1.152	0.72	0.864	1.44	1.008	1.296	1.584	0.864	1.776	0
February	1.44	0.576	0.864	1.44	1.008	1.152	0.72	1.536	1.008	0
March	0.864	0.432	1.008	0.864	1.008	1.152	0.72	0.864	1.008	0
April	1.008	1.152	0.864	1.44	1.296	1.296	1.584	1.536	1.008	0
May	1.152	1.296	1.008	0.864	1.152	1.296	0.72	1.536	1.008	0
June	1.44	1.584	1.296	1.44	1.728	1.368	1.584	0.864	1.008	0
July	1.152	1.584	2.16	1.44	1.728	1.296	2.16	1.536	1.008	0
August	1.44	1.44	2.016	0.864	1.44	1.296	1.584	1.536	1.776	0
September	1.44	1.584	1.872	2.88	1.152	1.368	1.584	1.536	1.776	0
October	1.44	1.44	1.008	0.432	1.152	1.008	0.72	0.864	1.008	0
November	0.864	1.296	0.72	0.432	0.864	0.864	0.72	0.864	1.008	0
December	1.008	1.296	0.72	0.864	0.864	1.008	0.72	0.864	1.008	0

Table A-3: - Continued

Site: 501683-1992

Month	Class 4	Class 5	Class 6	Class 7	Class 8	Class 9	Class 10	Class 11	Class 12	Class 13
January	1.296	0.576	0.864	1.152	1.008	1.008	1.152	0.72	0	0
February	1.296	0.576	0.864	1.152	1.008	1.008	1.152	0.72	0	0
March	1.296	0.576	0.864	1.152	1.008	1.152	1.152	0.72	0	0
April	1.296	0.576	0.864	1.152	1.152	1.152	1.152	0.72	0	0
May	0.864	1.296	1.152	1.152	1.152	1.152	1.152	0.72	0	0
June	1.152	1.44	1.296	1.152	1.152	1.152	1.44	1.44	0	0
July	1.296	1.44	1.44	2.016	1.344	1.44	1.872	1.44	0	0
August	1.152	1.512	1.44	1.152	1.356	1.296	1.152	1.44	0	0
September	1.008	1.512	1.296	1.152	1.356	1.296	1.008	1.44	0	0
October	1.584	1.44	1.152	2.016	1.356	1.296	1.152	1.44	0	0
November	1.44	1.44	1.728	1.152	1.356	1.152	1.008	1.44	0	0
December	1.008	1.296	1.296	0.576	1.008	1.152	1.008	1.44	0	0

Site: 501681-1992

Month	Class 4	Class 5	Class 6	Class 7	Class 8	Class 9	Class 10	Class 11	Class 12	Class 13
January	1.152	0.576	1.008	0.864	1.008	1.152	1.152	0.864	0	0
February	2.016	0.576	0.864	0.864	1.152	1.152	1.152	0.864	0	0
March	1.008	0.576	1.008	1.536	1.152	1.152	1.152	0.864	0	0
April	0.864	1.152	1.152	1.536	1.296	1.152	1.008	1.296	0	0
May	0.864	1.44	1.296	1.536	1.152	1.152	1.008	0.864	0	0
June	1.152	1.632	1.44	0.864	1.296	1.296	2.016	1.296	0	0
July	1.296	1.632	1.296	1.536	1.296	1.296	1.296	1.296	0	0
August	1.152	1.632	1.44	1.536	1.44	1.296	1.008	1.872	0	0
September	1.44	1.44	1.296	0.864	1.296	1.296	1.296	1.296	0	0
October	1.44	1.44	1.44	1.536	1.152	1.152	1.296	1.296	0	0
November	1.008	1.152	1.152	0.864	1.008	1.152	1.008	1.296	0	0
December	1.008	1.152	1.008	0.864	1.152	1.152	1.008	1.296	0	0

Table A-3: - Continued

Site: 501004-1994

Month	Class 4	Class 5	Class 6	Class 7	Class 8	Class 9	Class 10	Class 11	Class 12	Class 13
January	0	0	0	0	0	0	0	0	0	0
February	0	0	0	0	0	0	0	0	0	0
March	0	0	0	0	0	0	0	0	0	0
April	0	0	0	0	0	0	0	0	0	0
May	1.44	1.056	0.96	0	1.056	1.152	1.92	0	4.8	0
June	1.44	1.152	1.248	0	1.44	1.32	1.92	0	4.8	0
July	1.152	1.272	1.248	0	1.248	1.152	0	0	0	0
August	0.768	1.272	1.248	0	1.248	1.308	1.92	0	0	0
September	1.44	1.272	1.248	0	1.248	1.308	0	0	0	0
October	1.44	1.272	1.248	0	1.248	1.248	1.92	0	0	0
November	1.152	1.152	1.152	0	1.056	1.152	1.92	0	0	0
December	0.768	1.152	1.248	9.6	1.056	0.96	0	0	0	0

Table A-4: Axles Per Truck

Site	Axles	Vehicle Class									
		4	5	6	7	8	9	10	11	12	13
091803	Single	1.84	2	1	1	2.36	1.05	1.01	2	4	1
	Tandem	0.67	0	1	0.11	0.72	1.96	0.99	0	1	0
	Tridem	0	0	0	1	0.82	0.08	0.99	1	0	2
	Quad	0	0	0	0	0	0	0.26	0	0	0
231001	Single	1.83	2.14	1	1.01	2.34	1.47	1.01	5	4	1.71
	Tandem	0.17	0.04	1	0.02	0.66	1.76	1.09	0	1	1.82
	Tridem	0	0	0	0.85	0	0	0.91	0	0	0.65
	Quad	0	0	0	0.13	0	0	0	0	0	0
231009	Single	1.76	2.11	1	1	2.19	1.21	1.03	5	4	0
	Tandem	0.24	0.03	1	0	0.81	1.89	1.22	0	1	0
	Tridem	0	0	0	1	0	0	0.78	0	0	0
	Quad	0	0	0	0	0	0	0	0	0	0
231028	Single	1.57	2.17	1	1	2.35	1.45	1.01	5	4	1.16
	Tandem	0.43	0.03	1	0	0.64	1.77	1.11	0	1	0.32
	Tridem	0	0	0	0.99	0	0	0.89	0	0	1.81
	Quad	0	0	0	0.01	0	0	0	0	0	0
251003	Single	1.87	2	1	1	2.18	1.04	1	2.75	0	0
	Tandem	0.64	0.04	1	0	0.83	1.96	1.47	1	0	0
	Tridem	0	0	0	1	0.11	0.17	0.97	0.25	0	0
	Quad	0	0	0	0	0	0	0	0	0	0
341003	Single	1.37	2	1	0.91	2.34	1.07	1.02	2.04	2.5	1
	Tandem	0.66	0.01	1	1.13	0.66	1.95	1.01	0.55	1	0.4
	Tridem	0	0	0	0.91	0	0.02	0.99	1	0.5	2
	Quad	0	0	0	0	0	0	0.31	0	0	0.4
341011	Single	1.33	2	1	0.99	2.11	1.08	1.04	4.12	3.86	1.02
	Tandem	0.67	0	1	0.14	0.89	1.95	1	0.11	1.05	0.9
	Tridem	0	0	0	0.99	0	0.01	0.96	0.37	0.51	1.35
	Quad	0	0	0	0	0	0	0.15	0	0	0.86
341030	Single	1.53	2	1	0.98	2.41	1.1	1.02	0	0	0
	Tandem	0.47	0	1	0.04	0.59	1.95	1.11	0	0	0
	Tridem	0	0	0	0.97	0	0	0.86	0	0	0
	Quad	0	0	0	0.01	0	0	0	0	0	0
341031	Single	1.4	1.99	1	1	2.17	1.09	1.01	4.86	2.53	1.24
	Tandem	0.6	0.01	1	0.02	0.83	1.95	1	0.09	1.16	1.12
	Tridem	0	0	0.01	1	0	0	0.99	0.12	1.09	1.9
	Quad	0	0	0	0	0	0	0.03	0	0	0.84

Table A-4: Continued

Site	Axles	Vehicle Class									
		4	5	6	7	8	9	10	11	12	13
41033	Single	1.61	2.04	1	0.91	2.27	1.16	1.01	4.34	1.33	1
	Tandem	0.39	0.01	1	0.45	0.67	1.91	1.47	0.27	1.08	0.79
	Tridem	0	0	0	0.63	0.02	0	0.52	0	0.72	1
	Quad	0	0	0	0	0	0	0	0	0	0.29
341034	Single	1.48	2	1	0.99	2.19	1.09	1.01	4.64	3.21	1.13
	Tandem	0.52	0	1	0.06	0.81	1.95	1	0.11	0.95	1.15
	Tridem	0	0	0	0.99	0	0.01	0.99	0.23	1.02	1.06
	Quad	0	0	0	0	0	0	0.07	0	0	1.04
341638	Single	1.51	2	1	1	2.19	1.08	1.01	4.69	3.18	1.24
	Tandem	0.49	0	1	0.05	0.81	1.95	1	0.1	1.31	1.86
	Tridem	0	0	0	1	0.01	0.01	0.99	0.19	0.72	1.81
	Quad	0	0	0	0	0	0	0.08	0	0	0.92
421597	Single	1.91	2	1	1	2.26	1.26	1.06	5	4	1.13
	Tandem	0.09	0	1	0	0.74	1.87	1.12	0	1	0.5
	Tridem	0	0	0	1	0	0	0.86	0	0	0.88
	Quad	0	0	0	0	0	0	0	0	0	0.63
421599	Single	1.94	2	1	1	2.33	1.23	1.02	5	4	2.65
	Tandem	0.06	0	1	0	0.67	1.89	1.16	0	1	1.65
	Tridem	0	0	0	1	0	0	0.83	0	0	0.38
	Quad	0	0	0	0	0	0	0	0	0	0.09
501002	Single	1.24	2	1	0.96	2.14	1.02	1.06	2.99	2	1.25
	Tandem	0.76	0.01	1	0.66	0.86	1.98	1.03	1.01	2	2.5
	Tridem	0	0	0	0.96	0	0.02	0.97	0	0.14	1
	Quad	0	0	0	0	0	0	0.39	0	0	0
501004	Single	1.71	2	1	0.89	2.24	1.12	1.07	2	1.54	1
	Tandem	0.42	0	1	1.67	0.77	1.93	1.07	1.08	1.49	1
	Tridem	0	0	0	0.89	0	0.03	0.94	1	0.72	0
	Quad	0	0	0	0	0	0	0	0	0	1
501681	Single	1.3	1.99	1	0.93	2.16	1.03	1.03	3.02	2.28	1
	Tandem	0.7	0.01	1	1.03	0.84	1.97	1.02	0.99	1.86	2.5
	Tridem	0	0	0	0.93	0.01	0.01	0.98	0	0	1.17
	Quad	0	0	0	0	0	0	0.12	0	0	0
501683	Single	1.36	2	1	0.97	2.14	1.02	1.1	3	2.02	2.08
	Tandem	0.64	0.01	1	0.78	0.85	1.98	1.08	1	1.89	1.33
	Tridem	0	0	0	0.97	0	0.01	0.94	0	0.82	1.08
	Quad	0	0	0	0	0	0	0.13	0	0	0

APPENDIX B

LONG TERM PAVEMENT PERFORMANCE (LTPP) STRUCTURAL DATA

Table B-1: General Information on the Selected LTPP Sections

STATE CODE	SHRP ID	CONSTRUCTION DATE		NO. Of LTPP LANES	TOTAL LANES	Functional Class	Direction
		1	2				
9	1803	01-Jul-88	17-Jan-95	1	2	Rural Major Collector	N
23	1001	01-Jul-88	06-Jun-95	2	4	Rural Principal Arterial - Interstate	N
23	1009	01-Jul-88	22-Aug-93	1	2	Rural Principal Arterial - Other	N
23	1028	01-Jul-88	12-May-92	1	2	Rural Principal Arterial - Other	E
25	1003	01-Jun-88	07-Jun-88	1	2	Urban Other Principal Arterial	N
34	1003	01-Aug-88	08-Apr-94	2	4	Rural Minor Arterial	N
34	1011	01-Jul-88	28-Apr-98	2	4	Rural Principal Arterial - Interstate	E
34	1030	01-Dec-88	24-Feb-91	2	4	Rural Principal Arterial - Other	S
34	1031	01-Jul-88	04-Apr-96	2	4	Urban Principal Arterial - Other Freeways	N
34	1033	01-Jul-88	11-Sep-97	2	4	Rural Principal Arterial - Other	S
34	1034	01-Dec-88	-	2	4	Urban Principal Arterial - Other Freeways	S
34	1638	01-Dec-88	-	2	4	Urban Principal Arterial - Other Freeways	N
36	1008	01-May-89	25-Aug-89	2	4	Urban Other Principal Arterial	E
36	1011	01-Jun-88	14-Sep-93	2	4	Urban Principal Arterial - Interstate	S
36	1643	01-May-89	12-Oct-89	1	2	Rural Principal Arterial - Other	N
36	1644	01-May-89	19-Jun-96	1	2	Rural Minor Arterial	W
42	1597	01-Aug-88	12-Jun-90	1	2	Rural Minor Arterial	E
42	1599	01-Aug-88	01-Jun-99	1	2	Urban Other Principal Arterial	W
50	1002	01-Aug-88	-	1	2	Rural Principal Arterial - Other	N
50	1004	01-Aug-88	06-Oct-98	1	2	Rural Principal Arterial - Other	E
50	1681	01-Jun-89	08-Sep-91	1	2	Rural Principal Arterial - Other	N
50	1683	01-Jun-89	23-Sep-91	1	2	Rural Principal Arterial - Other	S

Table B-2: Gradation Data of HMA Aggregates

STATE CODE	SHRP ID	LAYER NO	1	7/8	3/4	5/8	1/2	3/8	#4	#8	#10	#16	#30	#40	#50	#80	#100	#200
			Percent Passing															
23	1001	1												63				45
23	1001	2							63					17				3
23	1001	3					51							8				3
23	1001	4						87	74	64					10			2
23	1001	5	88		62		49	44	36	31		27			11		3	2
23	1001	6	100		99		70		39	33		27			13		7	3
23	1001	7	100	100	100	100	100	98	41	18			9					4
50	1002	2	75				51		24									4
50	1002	3	75		60		52		31	23								1
50	1002	4	100		99		81	71	52	38		29	20		10			2
50	1002	5	100	100	100		99	82	64	48		34	23		12			3
25	1003	1												70				20.3
25	1003	2	83		77		71	66	56		47	31		16		6		3
25	1003	3	100	100	93		65		35		25			12				2
25	1003	4	100	100	100	100	100	88	60		39	26		18		10		4

Table B-2: Continued

STATE CODE	SHRP ID	LAYER NO	1	7/8	3/4	5/8	1/2	3/8	#4	#8	#10	#16	#30	#40	#50	#80	#100	#200
			Percent Passing															
34	1003	2			86				56						9			5
34	1003	3	98				70		50	40					16			
34	1003	4	100	100	100	100	100	98	69	50					19			7
50	1004	1												77				19.5
50	1004	2	69				46		30									5
50	1004	3	79		60		48		28	23								2
50	1004	4	100	100	100		83	72	55	40		29	20		13			3
50	1004	5	100	100	100	100	100	84	61	47		35	25		16			3
23	1009	2												16				2
23	1009	3					61							12				3
23	1009	4			64			47	42	34		25			10		8	3
23	1009	5	100	100	100	100	100	99	71	51		38	25		15		8	4
34	1011	2			91				73						18			4
34	1011	3			87				49	37					15			6
34	1011	4	100	100	100	100	100	98	72	46					18			6

Table B-2: Continued

STATE CODE	SHRP ID	LAYER NO	1	7/8	3/4	5/8	1/2	3/8	#4	#8	#10	#16	#30	#40	#50	#80	#100	#200
			Percent Passing															
23	1028	1												13				1.2
23	1028	2												16				5
23	1028	3					61							16				3
23	1028	4	100		96		77	59	40	32		26	18		12		6	2
23	1028	5	94		73		55	44	35	29		23	16		11		8	3
34	1030	2	100	100	100	100	100		95									6
34	1030	3			67				52					25				6
34	1030	4	7			3												
34	1030	5			83				48	42					17			6
34	1030	6	100	100	100	100	100	97	62	51					19			6
34	1031	2			94				69						12			6
34	1031	3	99				69		36	30					13			3

Table B-2: Continued

STATE CODE	SHRP ID	LAYER NO	1	7/8	3/4	5/8	1/2	3/8	#4	#8	#10	#16	#30	#40	#50	#80	#100	#200
				Percent Passing														
34	1031	4	100	100	100	100	100	93	60	48					18			6
34	1033	2			81				47						11			4
34	1033	3	100				77		49	40					15			7
34	1033	4	100				75		45	32					12			5
34	1033	5	100	100	100	100	100	98	70	51					18			7
34	1034	2	100				74		45	38					16			6
34	1034	3	100		98		82	71	46	40					16			5
42	1597	2	100		76			53	37	27		20						5
42	1597	3																
42	1597	4	100	100	100	100	100	90	63	45		33	23		15		9	7
42	1599	2			76			51	24			6						3
42	1599	3			90		69	57	36	25		16	11		8		6	4.5
42	1599	4	98				69	57	36	25		16	11		8		6	4.5
42	1599	5	100	100	100	100	100	95	60	42		26	17		11		8	5.5
34	1638	3	100				74		45	38					16			6

Table B-2: Continued

STATE CODE	SHRP ID	LAYER NO	1	7/8	3/4	5/8	1/2	3/8	#4	#8	#10	#16	#30	#40	#50	#80	#100	#200
			Percent Passing															
34	1638	4	100		98		82	71	46	40					16			5
50	1681	1												17.6				10.2
50	1681	3	69		66		61	57	47	36		26	18		10		5	3
50	1681	5	100	100	100		93	76	53	37		29	24		20			5
50	1683	1												51.7				41.5
50	1683	3	86		83		78	73	60	51		40	31		20		10	6
50	1683	5	100	100	100		92	79	54			29	23		19			6
9	1803	2						47			34			17			5	2
9	1803	3	100		72				35	30					14			4
9	1803	4	100	100	100		99	78	52	42					17			5

Table B-3: Binder Content

STATE CODE	SHRP ID	LAYER NO	MAX SP.GRAVITY	BULK SP.GRAVITY MEAN	ASPHALT CONTENT MEAN	PERCENT AIR VOIDS MEAN	VOIDS MINERAL AGGREGATE	EFFECTIVE ASPHALT CONTENT	MARSHALL STABILITY	MARSHALL FLOW	HVEEM STABILITY
23	1001	4		2.24	4						28
23	1001	5	2.49	2.38	5.1	4.3	15				50
23	1001	6	2.47	2.33	5.4	5.7	14.7				39
23	1001	7	2.512	2.455	6.2	10.8	22.3				22
33	1001	5	2.521	2.41	4.5	6.7	15.3				
33	1001	6	2.457	2.34	6.3	4.9	17.7		1350	12	
25	1002	4	2.67	2.53	4.4	4.8					
25	1002	5	2.58	2.33	6.3	8.8					
50	1002	4	2.488	2.382	5.5	4.2	15.6	4.9	1616	11	
25	1003	3	2.45	2.27	5	6.5					
25	1003	4	2.39	2.26	6.4	5.3					
25	1004	4	2.63	2.54	4.5	3.6					
25	1004	5	2.63	2.54	4.5	3.6					
50	1004	3	2.502	2.389	5	4.5	14	4.1			
50	1004	4	2.471	2.38	5.5	3.7	14.2	4.5	2341	9	
50	1004	5	2.439	2.359	6.2	3.1	15.4	5.3	2160	18	
23	1009	4	2.49	2.41	5.1		15.5				44
23	1009	5	2.415	2.405	7.1	7.2	16.8				13

Table B-3: Continued

STATE CODE	SHRP ID	LAYER NO	MAX SP.GRAVITY	BULK SP.GRAVITY MEAN	ASPHALT CONTENT MEAN	PERCENT AIR VOIDS MEAN	VOIDS MINERAL AGGREGATE	EFFECTIVE ASPHALT CONTENT	MARSHALL STABILITY	MARSHALL FLOW	HVEEM STABILITY
23	1012	4	2.448	2.405	5.2	1.7	13.5	5			35
23	1012	5	2.397	2.39	6.5	0.2	15.3	6.4			25
23	1026	4	2.545	2.48	5	2.7	14.9				47
23	1026	5	2.515	2.455	5	5	16.6				45
23	1028	4	2.52	2.36	5.1	6.5	18				21
23	1028	5	2.5	2.34	5.1	6.5	17.7				18
42	1599	3	2.637		3.4				2033	11	
42	1599	4	2.571	2.486	4.6	3.3	14	4.3	2533	12	
42	1599	5	2.522	2.425	6	3.9	16.3	5.3	2686	11	
9	1803	3	2.546		4.3	7.6					
9	1803	4	2.526	2.449	5.2	3.1	15.7		2447	12	
34	1003	3			4.4				2580	12	
34	1003	4			5.8				2480	12	
34	1011	3			5						
34	1011	4			5.8						
34	1030	5			4.2						
34	1030	6			5.4						
34	1031	3			4.6				1555	9	
34	1031	4			5.6				1295	12	

Table B-3: Continued

STATE CODE	SHRP ID	LAYER NO	MAX SP.GRAVITY	BULK SP.GRAVITY MEAN	ASPHALT CONTENT MEAN	PERCENT AIR VOIDS MEAN	VOIDS MINERAL AGGREGATE	EFFECTIVE ASPHALT CONTENT	MARSHALL STABILITY	MARSHALL FLOW	HVEEM STABILITY
34	1033	3			4.7		16.4		3400	10	
34	1033	4			4.7		16.6		3000	13	
34	1033	5			5.9		19.5		3328	12	
34	1034	2			4.9				1520	10	
34	1034	3			4.4		13.9		1950	14	
34	1638	3			4.4				1950	12	
34	1638	4			4.9				1522	10	

Table B-4: Binder Gradation

STATE CODE	SHRP ID	LAYER NO	ASPHALT GRADE	ASPHALT SP.GRAVITY	ORIG ASPHALT VISCOSITY 140 F	ORIG ASPHALT VISCOSITY 275 F	ORIG PENETRATION 77 F	LAB VISCOSITY 140 F	LAB VISCOSITY 275 F	LAB DUCTILITY 77 F	LAB PENETRATION 77 F
23	1001	4	AC-10	1.031	1058	350	114	1120	323.8	150	56
23	1001	5	AC-10	1.031	1058	350	114	1120	323.8	150	56
23	1001	6	AC-10	1.031	1058	350	114	1120	323.8	150	56
23	1001	7	AC-20	1.04	1810	418.33	83	1800	425	150	48
50	1002	3	85-100 pen	1.022	1144	308	92				
50	1002	4	85-100 pen	1.022	1144	308	92				
50	1002	5	85-100 pen	1.022	1144	308	92				
25	1003	3	AC-20	1.026	2064	401	73	4042			
25	1003	4	AC-20	1.026	1772	377	82	3976			
34	1003	3	AC-20	1.025	2021		72				
34	1003	4	AC-20	1.025	2021		72				
50	1004	3	85-100 pen	1.022	1159	311	90				58
50	1004	4	85-100 pen	1.023	1159	311	90				60
50	1004	5	85-100 pen	1.023	1159	311	59				60
23	1009	4	85-100 pen	1.023	1778	400	89			150	58
23	1009	5	85-100 pen	1.023	1765	390.5	90			150	60
34	1011	3	85-100 pen	1.025			91				
34	1011	4	85-100 pen	1.029			91				

Table B-4: Continued

STATE CODE	SHRP ID	LAYER NO	ASPHALT GRADE	ASPHALT SP.GRAVITY	ORIG ASPHALT VISCOSITY 140 F	ORIG ASPHALT VISCOSITY 275 F	ORIG PENETRATION 77 F	LAB VISCOSITY 140 F	LAB VISCOSITY 275 F	LAB DUCTILITY 77 F	LAB PENETRATION 77 F
36	1011	4	AC-20	1.024							
23	1028	4	AC-10	1.014	1125	311	120	2420		150	74
23	1028	5	AC-10	1.014	1125	311	120	2420		150	74
34	1030	5	AC-20	1.025							
34	1030	6	AC-20	1.025							
34	1031	3	AC-20	1.025	1793	465	74				
34	1031	4	AC-20	1.025	1968	412	70				
34	1033	3	AC-20	1.025	2124	446	67				
34	1033	4	AC-20	1.025	2124	446	67				
34	1033	5	AC-20	1.025	2124	446	67				
34	1034	2	AC-20	1.02	2108	406	77				
34	1034	3	AC-20	1.02	2108	406	77				
42	1597	3	AC-20		2000						
42	1597	4	AC-20	1.01	2000						
1599	42	3	AC-20	1.024	2037	452	79				
1599	42	4	AC-20	1.024	2037	452	79				
1599	42	5	AC-20	1.024	2037	452	79				

Table B-4: Continued

STATE CODE	SHRP ID	LAYER NO	ASPHALT GRADE	ASPHALT SP.GRAVITY	ORIG ASPHALT VISCOSITY 140 F	ORIG ASPHALT VISCOSITY 275 F	ORIG PENETRATION 77 F	LAB VISCOSITY 140 F	LAB VISCOSITY 275 F	LAB DUCTILITY 77 F	LAB PENETRATION 77 F
34	1638	3	AC-20	1.02	2108	406	77				
34	1638	4	AC-20	1.02	2108	406	77				
50	1681	5	85-100 pen	1.01							
50	1683	5	85-100 pen	1.01							
9	1803	3	AC-20	1.01	2052		69	4462			54
9	1803	4	AC-20	1.01	2052		69	4462			54

Table B-5: Subgrade Soil Data

STATE CODE	SHRP ID	CONSTRUCTION NO	LAYER NO	AASHTO SOIL CLASS	CBR	PLASTICITY INDEX	LIQUID LIMIT	MAXIMUM LAB DRY DENSITY	OPTIMUM LAB MOISTURE CONTENT	IN SITU DRY DENSITY MEAN	IN SITU MOISTURE OPTIMUM MEAN
23	1001	1	1	A-4				135	6.7		
50	1002	1	1	A-7-6							
25	1003	1	1	A-2-4	10			114	12	106	
50	1004	1	1	A-6		0	0	112	12.6	102	82.1
23	1009	1	1	A-4							
23	1028	1	1	A-1a		0	0	128	8.5		
50	1681	1	1	A-1a		3	18				
50	1683	1	1	A-1a		11	26				
9	1803	1	1					122	12.4		118.2
34	1003	1	1	A-7-6							
34	1011	1	1	A-7-6							
34	1030	1	1	A-4							
34	1031	1	1	A-7-6							
34	1033	1	1	A-2-4							
34	1034	1	1	A-1-a							
34	1638	1	1	A-1-b							
42	1597	1	1	A-7-5							
42	1599	1	1	A-7-5							

Table B-6: Base Layer Data

STATE CODE	SHRP ID	CONSTRUCTION NO	LAYER NO	AASHTO SOIL CLASS	PLASTICITY INDEX	MAX LAB DRY DENSITY	OPTIMUM LAB MOISTURE	IN SITU DRY DENSITY MEAN	IN SITU MOISTURE MEAN
23	1001	1	2	A-1-b	1	131	6.5	129	7
23	1001	1	3	A-1-a		139	6.1		
25	1003	1	2	A-1-a		125	8.4		
23	1009	1	2	A-1-b	1	133	10	126	3
23	1009	1	3	A-1-a		139	7.9	139	3
23	1028	1	2	A-1-a		142	6.2	141	4
23	1028	1	3	A-1-a		143	7.4	137	3
34	1031	1	2	A-1-a					7
34	1033	1	2	A-1-a					5
9	1803	1	2	A-1-a		137	7.6	138	5

Table B-7: Layer Thickness

STATE CODE	SHRP ID	LAYER NO	DESCRIPTION	MATERIAL TYPE	MEAN THICKNESS
23	1001	1	Subgrade	Poorly Graded Sand	
23	1001	2	Subbase Layer	Sand	42
23	1001	3	Base Layer	Crushed Stone, Gravel or Slag	4
23	1001	4	AC Layer Below Surface (Binder Course)	Asphalt Bound, Dense Graded, Hot Laid, Central Plant Mix	3
23	1001	5	AC Layer Below Surface (Binder Course)	Asphalt Bound, Dense Graded, Hot Laid, Central Plant Mix	3
23	1001	6	Original Surface Layer	Hot Mixed, Hot Laid Asphalt Concrete, Dense Graded	2.2
23	1001	7	Friction Course	Hot Mixed, Hot Laid Asphalt Concrete, Open Graded (Porous Friction Course)	0.8
50	1002	1	Subgrade	Gravel	
50	1002	2	Base Layer	Crushed Stone, Gravel or Slag	24
50	1002	3	AC Layer Below Surface (Binder Course)	Asphalt Bound, Dense Graded, Hot Laid, Central Plant Mix	5
50	1002	4	AC Layer Below Surface (Binder Course)	Asphalt Bound, Dense Graded, Hot Laid, Central Plant Mix	1.8
50	1002	5	Original Surface Layer	Hot Mixed, Hot Laid Asphalt Concrete, Dense Graded	1.3
25	1003	1	Subgrade	Poorly Graded Sand	
25	1003	2	Base Layer	Gravel (Uncrushed)	12
25	1003	3	AC Layer Below Surface (Binder Course)	Asphalt Bound, Dense Graded, Hot Laid, Central Plant Mix	4.7
25	1003	4	Original Surface Layer	Hot Mixed, Hot Laid Asphalt Concrete, Dense Graded	1.2
34	1003	1	Subgrade	Sandy Silt	
34	1003	2	Subbase Layer	Soil-Aggregate Mixture (Predominantly Coarse-Grained Soil)	24
34	1003	3	AC Layer Below Surface (Binder Course)	Asphalt Bound, Dense Graded, Hot Laid, Central Plant Mix	5.5
34	1003	4	Original Surface Layer	Hot Mixed, Hot Laid Asphalt Concrete, Dense Graded	1.5
50	1004	1	Subgrade	Silt	
50	1004	2	Base Layer	Crushed Stone, Gravel or Slag	24

Table B-7: Continued

STATE CODE	SHRP ID	LAYER NO	DESCRIPTION	MATERIAL TYPE	MEAN THICKNESS
50	1004	3	AC Layer Below Surface (Binder Course)	Asphalt Bound, Dense Graded, Hot Laid, Central Plant Mix	5
50	1004	4	AC Layer Below Surface (Binder Course)	Asphalt Bound, Dense Graded, Hot Laid, Central Plant Mix	1.8
50	1004	5	Original Surface Layer	Hot Mixed, Hot Laid Asphalt Concrete, Dense Graded	1.3
23	1009	1	Subgrade	Poorly Graded Sand	
23	1009	2	Subbase Layer	Soil-Aggregate Mixture (Predominantly Coarse-Grained Soil)	20
23	1009	3	Base Layer	Crushed Stone, Gravel or Slag	4
23	1009	4	AC Layer Below Surface (Binder Course)	Asphalt Bound, Dense Graded, Hot Laid, Central Plant Mix	3
23	1009	5	Original Surface Layer	Hot Mixed, Hot Laid Asphalt Concrete, Dense Graded	3
34	1011	1	Subgrade	Silty Sand	
34	1011	2	Subbase Layer	Soil-Aggregate Mixture (Predominantly Coarse-Grained Soil)	10
34	1011	3	AC Layer Below Surface (Binder Course)	Asphalt Bound, Dense Graded, Hot Laid, Central Plant Mix	7.5
34	1011	4	Original Surface Layer	Hot Mixed, Hot Laid Asphalt Concrete, Dense Graded	1.5
23	1028	1	Subgrade	Poorly Graded Sand	
23	1028	2	Subbase Layer	Soil-Aggregate Mixture (Predominantly Coarse-Grained Soil)	22
23	1028	3	Base Layer	Crushed Stone, Gravel or Slag	2
23	1028	4	AC Layer Below Surface (Binder Course)	Asphalt Bound, Dense Graded, Hot Laid, Central Plant Mix	3
23	1028	5	Original Surface Layer	Hot Mixed, Hot Laid Asphalt Concrete, Dense Graded	3
34	1030	1	Subgrade	Poorly Graded Sand	
34	1030	2	Subbase Layer	Sand	6
34	1030	3	Subbase Layer	Soil-Aggregate Mixture (Predominantly Coarse-Grained Soil)	12
34	1030	4	Base Layer	Crushed Stone, Gravel or Slag	6
34	1030	5	AC Layer Below Surface (Binder Course)	Asphalt Bound, Dense Graded, Hot Laid, Central Plant Mix	4
34	1030	6	Original Surface Layer	Hot Mixed, Hot Laid Asphalt Concrete, Dense Graded	2

Table B-7: Continued

STATE CODE	SHRP ID	LAYER NO	DESCRIPTION	MATERIAL TYPE	MEAN THICKNESS
34	1031	1	Subgrade	Silty Sand	
34	1031	2	Base Layer	Crushed Stone, Gravel or Slag	16
34	1031	3	AC Layer Below Surface (Binder Course)	Asphalt Bound, Dense Graded, Hot Laid, Central Plant Mix	6.5
34	1031	4	Original Surface Layer	Hot Mixed, Hot Laid Asphalt Concrete, Dense Graded	1.5
34	1033	1	Subgrade	Clayey Gravel	
34	1033	2	Subbase Layer	Crushed Stone, Gravel or Slag	14
34	1033	3	Base Layer	Asphalt Bound, Dense Graded, Hot Laid, Central Plant Mix	4
34	1033	4	AC Layer Below Surface (Binder Course)	Asphalt Bound, Dense Graded, Hot Laid, Central Plant Mix	1.5
34	1033	5	Original Surface Layer	Hot Mixed, Hot Laid Asphalt Concrete, Dense Graded	1.5
34	1034	1	Subgrade	Poorly Graded Sand	
34	1034	2	Base Layer	Asphalt Bound, Dense Graded, Hot Laid, Central Plant Mix	10
34	1034	3	Original Surface Layer	Hot Mixed, Hot Laid Asphalt Concrete, Dense Graded	2
42	1597	1	Subgrade	Silty Clay	
42	1597	2	Base Layer	Gravel (Uncrushed)	17
42	1597	3	AC Layer Below Surface (Binder Course)	Asphalt Bound, Dense Graded, Hot Laid, Central Plant Mix	5
42	1597	4	Original Surface Layer	Hot Mixed, Hot Laid Asphalt Concrete, Dense Graded	1.5
42	1599	1	Subgrade	Silty Clay	
42	1599	2	Base Layer	Gravel (Uncrushed)	12
42	1599	3	AC Layer Below Surface (Binder Course)	Asphalt Bound, Dense Graded, Hot Laid, Central Plant Mix	5
42	1599	4	AC Layer Below Surface (Binder Course)	Asphalt Bound, Dense Graded, Hot Laid, Central Plant Mix	4
42	1599	5	Original Surface Layer	Hot Mixed, Hot Laid Asphalt Concrete, Dense Graded	1.5
34	1638	1	Subgrade	Sand	
34	1638	2	Base Layer	Pozzolanic-Aggregate Mixture	8
34	1031	3	AC Layer Below Surface (Binder Course)	Asphalt Bound, Dense Graded, Hot Laid, Central Plant Mix	5

Table B-7: Continued

STATE CODE	SHRP ID	LAYER NO	DESCRIPTION	MATERIAL TYPE	MEAN THICKNESS
34	1031	4	Original Surface Layer	Hot Mixed, Hot Laid Asphalt Concrete, Dense Graded	2
50	1681	1	Subgrade	Gravel	
50	1681	2	Subbase Layer	Sand	12
50	1681	3	Subbase Layer	Gravel (Uncrushed)	20
50	1681	4	Base Layer	Asphalt Bound, Dense Graded, Hot Laid, Central Plant Mix	3
50	1681	5	Original Surface Layer	Hot Mixed, Hot Laid Asphalt Concrete, Dense Graded	3
50	1683	1	Subgrade	Silty Sand	
50	1683	2	Subbase Layer	Sand	12
50	1683	3	Subbase Layer	Gravel (Uncrushed)	20
50	1683	4	Base Layer	Asphalt Bound, Dense Graded, Hot Laid, Central Plant Mix	3
50	1683	5	Original Surface Layer	Hot Mixed, Hot Laid Asphalt Concrete, Dense Graded	3
9	1803	1	Subgrade	Silty Sand	
9	1803	2	Base Layer	Gravel (Uncrushed)	10
9	1803	3	AC Layer Below Surface (Binder Course)	Asphalt Bound, Dense Graded, Hot Laid, Central Plant Mix	4
9	1803	4	Original Surface Layer	Hot Mixed, Hot Laid Asphalt Concrete, Dense Graded	3

APPENDIX C

LONG TERM PAVEMENT PERFORMANCE DISTRESS SUMMARY

Table C-1: Rutting

Site	Year	Month	AC Rutting (in)	Base Rutting (in)	Subgrade Rutting (in)	Total Rutting (in)
231001	1989	August	0.204	0.147	0.164	0.515
	1990	August	0.199	0.129	0.145	0.473
	1991	August	0.182	0.118	0.134	0.434
	1992	April	-	-	-	-
	1993	April	0.235	0.129	0.149	0.513
	1994	August	-	-	-	-
231009	1989	August	0.037	0.092	0.127	0.257
	1990	August	0.044	0.095	0.137	0.276
	1991	August	0.045	0.093	0.138	0.276
	1992	April	-	-	-	-
231028	1989	August	0.104	0.156	0.152	0.413
	1990	August	0.137	0.159	0.158	0.453
	1991	August	0.144	0.164	0.164	0.471
251003	1989	August	0.022	0.045	0.090	0.157
341003	1989	July	0.155	0.284	0.290	0.728
	1990	September	0.230	0.278	0.298	0.861
	1991	August	0.208	0.237	0.264	0.799
	1992	September	0.263	0.264	0.300	0.827
	1993	June	-	-	-	-
341011	1989	October	0.100	0.042	0.154	0.295
	1990	September	0.140	0.049	0.184	0.374
	1991	September	-	-	-	-
	1992	April	0.113	0.037	0.145	0.295
	1993	February	0.153	0.045	0.177	0.375
	1994	June	-	-	-	-
	1995	November	0.176	0.043	0.175	0.394
	1997	July	0.154	0.035	0.146	0.335
341030	1989	July	0.098	0.215	0.377	0.692
	1990	September	0.121	0.244	0.443	0.886
341031	1989	October	0.146	0.101	0.246	0.493
	1990	September	0.157	0.090	0.226	0.472
	1991	September	-	-	-	-
	1992	April	0.169	0.084	0.220	0.473
	1993	February	0.169	0.078	0.206	0.453
	1994	June	-	-	-	-
	1995	November	0.239	0.085	0.229	0.552
341033	1989	October	0.064	0.075	0.135	0.274

Table C-1: Continued

Site	Year	Month	AC Rutting (in)	Base Rutting (in)	Subgrade Rutting (in)	Total Rutting (in)
	1990	September	0.097	0.093	0.166	0.356
	1991	September	-	-	-	-
	1992	April	0.082	0.068	0.126	0.276
	1993	February	0.110	0.079	0.146	0.336
	1994	June	-	-	-	-
341033	1995	November	0.130	0.078	0.145	0.354
	1989	October	0.046	0.000	0.092	0.138
	1990	September	0.103	0.000	0.173	0.276
	1991	September	-	-	-	-
	1992	April	0.070	0.000	0.107	0.178
	1993	February	0.097	0.000	0.139	0.237
	1994	June	-	-	-	-
	1995	November	0.112	0.000	0.144	0.256
	1997	July	0.080	0.000	0.097	0.178
	1998	August	-	-	-	-
	1999	September	-	-	-	-
	2000	July	0.105	0.000	0.112	0.217
	2001	December	-	-	-	-
	2002	June	0.104	0.000	0.103	0.275
	2004	May	-	-	-	-
	2005	November	0.135	0.000	0.121	0.256
341034	2007	June	0.146	0.000	0.131	0.276
	1989	October	0.071	0.050	0.076	0.197
	1990	September	0.124	0.075	0.116	0.315
	1991	August	0.079	0.045	0.073	0.197
	1992	April	-	-	-	-
	1993	February	0.067	0.035	0.056	0.158
	1994	June	-	-	-	-
	1995	November	0.081	0.037	0.059	0.177
	1997	July	0.092	0.040	0.064	0.197
	1998	August	-	-	-	-
	1999	September	-	-	-	-
	2000	July	0.115	0.043	0.069	0.227
	2001	December	-	-	-	-
	2002	June	0.102	0.036	0.059	0.197
	2003	May	0.113	0.040	0.064	0.217
341638	2004	May	-	-	-	-

Table C-1: Continued

Site	Year	Month	AC Rutting (in)	Base Rutting (in)	Subgrade Rutting (in)	Total Rutting (in)
341638	2005	November	0.129	0.042	0.066	0.236
421597	1989	August	0.026	0.055	0.078	0.158
	1989	August	0.035	0.037	0.105	0.177
	1990	September	0.054	0.040	0.122	0.216
	1991	August	0.052	0.035	0.109	0.197
	1992	October	-	-	-	-
	1993	March	0.089	0.053	0.173	0.315
	1995	June	0.080	0.044	0.151	0.275
	1996	July	0.084	0.043	0.148	0.275
	1997	November	-	-	-	-
421599	1998	March	0.087	0.042	0.147	0.275
	1989	August	0.088	0.095	0.113	0.295
	1990	August	0.110	0.115	0.148	0.373
	1991	September	0.095	0.094	0.125	0.314
	1992	July	-	-	-	-
	1993	April	0.124	0.106	0.144	0.374
	1994	August	0.130	0.100	0.135	0.365
	1995	October	0.155	0.113	0.156	0.424
	1996	October	0.133	0.093	0.129	0.355
	1997	October	0.168	0.115	0.162	0.445
	1998	June	0.167	0.111	0.156	0.434
	1999	November	0.194	0.120	0.170	0.483
	2000	June	0.225	0.130	0.185	0.540
	2001	September	0.235	0.135	0.193	0.563
	2002	May	0.243	0.138	0.199	0.590
	2003	November	0.267	0.144	0.209	0.620
501002	2004	April	-	-	-	-
	1989	August	0.024	0.047	0.088	0.158
	1990	August	0.042	0.073	0.140	0.255
	1991	September	0.036	0.054	0.106	0.196
	1992	July	-	-	-	-
	1993	April	0.053	0.068	0.135	0.256
	1994	July	-	-	-	-
	1995	October	0.057	0.059	0.120	0.237
501004	1997	November	0.067	0.062	0.127	0.256
501681	1989	August	0.078	0.202	0.134	0.413
	1990	August	0.115	0.228	0.149	0.492
501683	1989	August	0.133	0.374	0.184	0.692
	1990	August	0.210	0.442	0.214	0.866

Table C-2: Cracking

Site	Year	Month	Longitudinal Cracking (ft/mi)	Alligator Cracking (%)	Transverse Cracking (ft/mi)	IRI (in/mi)
231001	1989	August	4814.515	0.000	779.328	118.407
	1990	August	5008.481	0.000	2286.029	138.492
	1991	August	5060.436	0.771	1233.070	115.695
	1992	April	-	-	-	109.651
	1993	April	668.490	0.000	4010.941	-
	1994	August	-	-	-	125.275
231009	1989	August	4727.923	1.597	824.356	61.231
	1990	August	5753.172	0.000	973.294	67.238
	1991	August	5625.016	1.292	1780.332	61.485
	1992	April	-	-	-	62.258
231028	1989	August	8628.027	0.000	803.574	85.523
	1990	August	9812.605	0.000	1423.572	86.056
	1991	August	5271.721	0.000	1001.004	91.707
251003	1989	August	17245.663	0.000	3082.675	122.564
341003	1989	July	1246.925	22.335	3262.787	124.471
	1990	September	1818.432	22.604	3245.468	-
	1991	August	1378.545	22.407	2279.101	102.998
	1992	September	5649.262	18.675	2549.268	95.750
	1993	June	-	-	-	103.442
341011	1989	October	5971.384	0.000	1364.690	101.972
	1990	September	6033.731	0.000	2036.644	102.529
	1991	September	-	-	-	108.548
	1992	April	5472.614	0.000	1728.376	102.136
	1993	February	5933.284	0.000	1804.577	109.220
	1994	June	-	-	-	115.645
	1995	November	10474.168	0.036	6383.562	115.746
	1997	July	-	-	-	117.951
341030	1989	July	2590.833	10.602	744.691	225.004
	1990	September	4208.371	20.469	2895.636	252.857
341031	1989	October	9750.259	3.534	3532.954	111.247
	1990	September	7155.963	2.834	1977.761	114.720
	1991	September	-	-	-	121.791
	1992	April	6082.222	4.862	1887.706	115.100
	1993	February	6549.819	10.154	6179.205	126.593
	1994	June	-	-	-	155.409
	1995	November	10692.380	9.688	5898.647	144.702
341033	1989	October	1271.171	0.000	1967.370	201.726

Table C-2: Continued

Site	Year	Month	Longitudinal Cracking (ft/mi)	Alligator Cracking (%)	Transverse Cracking (ft/mi)	IRI (in/mi)
	1990	September	1319.662	0.000	2448.822	173.796
	1991	September	-	-	-	176.610
	1992	April	1167.260	1.310	2102.454	184.010
	1993	February	710.054	0.108	2279.101	181.716
	1994	June	-	-	-	183.845
341033	1995	November	1420.109	0.251	2930.273	199.115
	1989	October	2002.007	0.000	0.000	85.245
	1990	September	2871.391	0.000	0.000	85.447
	1991	September	-	-	-	88.159
	1992	April	3484.462	0.000	0.000	87.678
	1993	February	3990.159	0.000	0.000	88.843
	1994	June	-	-	-	90.820
	1995	November	5410.268	0.000	0.000	93.279
	1997	July	-	-	-	94.153
	1998	August	-	-	-	94.964
	1999	September	-	-	-	93.545
	2000	July	13234.721	0.000	1728.376	-
	2001	December	-	-	-	98.525
	2002	June	13865.111	0.161	2885.245	96.320
	2004	May	-	-	-	96.206
	2005	November	-	-	-	97.612
341034	2007	June	-	-	-	101.655
	1989	October	516.088	0.000	0.000	56.923
	1990	September	904.020	0.000	0.000	59.685
	1991	August	-	-	-	60.762
	1992	April	910.948	0.000	0.000	56.973
	1993	February	3338.988	0.000	0.000	58.469
	1994	June	-	-	-	60.864
	1995	November	4966.917	0.000	0.000	-
	1997	July	-	-	-	65.261
	1998	August	-	-	-	63.297
	1999	September	-	-	-	65.121
	2000	July	5524.570	0.000	148.938	-
	2001	December	-	-	-	67.364
	2002	June	6601.774	0.072	443.351	65.989
	2003	May	-	-	-	64.627
341638	2004	May	-	-	-	65.311

Table C-2: Continued

Site	Year	Month	Longitudinal Cracking (ft/mi)	Alligator Cracking (%)	Transverse Cracking (ft/mi)	IRI (in/mi)
341638	2005	November	-	-	-	66.059
421597	1989	August	547.261	0.000	762.010	107.015
	1989	August	0.000	0.000	0.000	86.651
	1990	September	0.000	0.000	0.000	88.590
	1991	August	72.737	0.000	405.251	89.414
	1992	October	-	-	-	92.151
	1993	March	0.000	0.000	0.000	93.836
	1995	June	-	-	-	100.552
	1996	July	422.569	0.000	155.866	-
	1997	November	-	-	-	102.491
421599	1998	March	-	-	-	103.011
	1989	August	0.000	0.000	0.000	77.958
	1990	August	27.709	0.000	0.000	77.439
	1991	September	786.255	0.000	0.000	68.023
	1992	July	-	-	-	70.697
	1993	April	2445.358	0.000	976.758	-
	1994	August	-	-	-	80.090
	1995	October	1666.030	0.000	980.221	80.727
	1996	October	-	-	-	78.136
	1997	October	-	-	-	82.502
	1998	June	-	-	-	82.143
	1999	November	-	-	-	86.170
	2000	June	6463.227	0.413	4748.705	93.494
	2001	September	-	-	-	91.986
	2002	May	9192.607	0.072	4533.957	93.514
	2003	November	-	-	-	93.332
501002	2004	April	-	-	-	95.116
	1989	August	3480.998	0.000	45.028	104.544
	1990	August	3813.512	0.108	138.547	106.825
	1991	September	4527.030	4.108	308.268	92.379
	1992	July	-	-	-	93.329
	1993	April	5330.604	0.771	1918.879	131.459
	1994	July	-	-	-	131.789
	1995	October	5230.157	0.574	2985.692	132.600
501004	1997	November	-	-	-	129.495
	1989	August	2085.135	0.000	27.709	76.361
501681	1990	August	308.268	0.000	131.620	76.311
	1989	August	7914.509	0.771	1291.953	134.450
501683	1990	August	2251.392	1.453	1517.092	142.560

REFERENCES

1. Jagannath Mallela, Leslie Titus Glover, Michael I. Darter, Harold Von Quintus, Alex Gotlif, Mark Stanley, Suri Sadasivam. *Guidelines for Implementing NCHRP 1-37A M-E Design Procedures in Ohio: Volume 1- Summary of Findings, Implementation Plan, and Next Steps.* Applied Research Associates, Inc. 100 Trade Centre Drive, Suite 200. Champaign, IL 61820. November, 2009
2. Vidya Sagar Bethu. *Contribution to the Implementation of the NCHRP Design Guide for Flexible Pavement Structures.* Manhattan, Kansas, 2005
3. Muthadi, Naresh Reddy. *Local Calibration of the MEPDG for Flexible Pavement Design*. Raleigh, North Carolina. 2007
4. Sunghwan Kim, Halil Ceylan, Kasthurirangan Gopalakrishnan, Omar Smadi, Chris Brakke, Fereidoon (Ben) Behnami. *Verification of Mechanistic-Empirical Pavement Design Guide (MEPDG) Performance Predictions Using Pavement Management Information System (PMIS).* Transportation Research Board 89th Annual Meeting, January, 2010
5. National Cooperative Highway Research Program. *2002 Design Guide:Design of New and Rehabilitated Pavement Structures.* Draft Final Document. NCHRP Study 1-37A. Transportation Research Board, National Research Council, August 2003.
6. Virginia Department of Transportation. *VDOT Preparation Plan for the Implementation of The Mechanistic-Empirical Guide for Design of New and Rehabilitated Pavement Structures.* January 2007
7. National Cooperative Highway Research Program (NCHRP, 2004), Transportation Research Board, National Research Council. *Appendix II-1: Calibration of Fatigue*

Cracking Models for Flexible Pavements. NCHRP 1-37 A Final Document, ARA Inc., ERES Division, Champaign, Illinois. February, 2004.

8. Myungook Kang, Teresa M. Adams. *Local Calibration for Fatigue Cracking Models Used in the Mechanistic-Empirical Pavement Design Guide.* Department of Civil and Environmental Engineering. University of Wisconsin, Madison Proceedings of the 2007 Mid-continent Transportation Research Symposium, Ames, Iowa, August 2007
9. Fujie Zhou, Emmanuel Fernando, and Tom Scullion. *A Review of Performance Models and Test Procedures with Recommendations for Use in the Texas M-E Design Program.* Texas Transportation Institute, The Texas A&M University System. October 2007
10. Priyam Saxena, Derek Tompkins, Lev Khazanovich, Jose Tadeu Balbo. *Evaluation of Characterization and Modeling of Cementitiously Stabilized Layers in the MEPDG.* Transportation Research Board, 89th Annual Meeting. Washington, D.C. January 2010
11. Aleksander Zborowski. *Development of a Modified Superpave Thermal Cracking Model for Asphalt Concrete Mixtures Based on the Fracture Energy Approach.* Arizona State University. December 2007
12. Suresh Immanuel Selvaraj. *Development of Flexible Pavement Rut Prediction Models from the NCAT Test Track Structural Study Sections Data.* Auburn, Alabama. August, 2007.
13. Nusrat Siraj. *Verification of Asphalt Concrete Performance Prediction Using Level 2 and Level 3 Inputs of Mechanistic-Empirical Pavement Design Guide for Flexible Pavements of the State of New Jersey.* August, 2008
14. National Cooperative Highway Research Program (NCHRP, 2004), Transportation Research Board, National Research Council. *Appendix GG-1: Calibration of Permanent Deformation Models for Flexible Pavements*. NCHRP 1-37 A Final Document, ARA Inc., ERES Division, Champaign, Illinois. February, 2004.

15. US Department of Transportation, Federal Highway Administration. *Long-Term Pavement Performance Information Management System: Pavement Performance Database User Reference Guide.* Publication No. FHWA-RD-03-088 (Interim Update)

    Research, Development, and Technology, Turner-Fairbank Highway Research Center, 6300 Georgetown Pike, McLean, VA22101-2296. November, 2008

16. US Department of Transportation, Federal Highway Administration, Turner-Fairbank Highway Research Center. *Long-Term Pavement Performance.*

    http://www.tfhrc.gov/pavement/ltpp/reports/03088/index.htm

17. Leslie Titus Glover, Jagannath Mallela. *Guidelines for Implementing NCHRP 1-37A M-E Design Procedures in Ohio: Volume 4-MEPDG Models Validation and Recalibration.* Applied Research Associated, Inc. Champaign, Illinois-61820. November, 2009

18. Kyle Hoegh, Lev Khazanovich, and Maureen Jensen. *Local Calibration of MEPDG Rutting Model for MNROAD Test Sections.* Transportation Research Board 89th Annual Meeting. January 10-14, 2010

19. Jianhua Li, Linda M. Pierce, and Jeff Uhlmeyer. *Calibration of Flexible Pavement in Mechanistic-Empirical Pavement Design Guide for Washington State.* Transportation Research Record: Journal of the Transportation research Board, No. 2095, Transportation research Board of the national Academies, Washington, D.C., 2009, pp. 73-83

20. Michael I. Darter, Leslie Titus-Glover, and Harold L. Von Quintus. *Implementation of the Mechanistic-Empirical Pavement Design Guide in Utah: Validation, Calibration, and Development of the UDOT MEPDG User's Guide.* Utah Department of Transportation Research Division. October 2009

21. Shane Buchanan. *Traffic Load Spectra Development for the 2002 AASHTO Pavement Design Guide.* Mississippi State University, Department of Civil Engineering, Construction Materials Research Center. December, 2004

22. Pankaj Hyalij. *Data Collection for Local Calibration of MEPDG for Flexible Pavement Design.* The University of Texas at Arlington. June 2010
23. Taamneh Madhar Mohammad. *Long Term Monitoring and Evaluation of Drainable Bases at I-90 Test Road.* August, 2009
24. Jose Pablo Aguiar-Moya. *Improving on Flexible Pavement IRI Predictions by Correlating for Possible Bias.* The University of Texas at Austin, USA
    jpaguiar@mail.utexas.edu
25. Adam Joel Taylor. *Mechanistic Characterization of Resilient Moduli for Unbound Pavement Layer Materials.* Auburn, Alabama. August 9, 2008
26. Sunghwan Kim, Halil Ceylan, Michael Heitzman. *Sensitivity of Design Input Parameters for Two Flexible Pavement Systems Using the Mechanistic-Empirical Pavement Design Guide.* Proceedings of the 2005 Mid-Continent Research Symposium, Ames, Iowa
    Iowa State University. August 2005
27. Nicholas Stires. *A Study of Mechanistic Empirical Pavement Design Guide for South Carolina. University of South Carolina.* Theses and Dissertations. 2009

BIOGRAPHICAL INFORMATION

Shariq A. Momin is originally from Mumbai (Bombay), India. He received his Bachelor of Engineering degree from the University of Mumbai (Bombay), India in June, 2007. After completion of his Bachelors degree, he worked for 3 months with Dr. Prabhat Shrivastav (Professor, Dept. of Civil Engineering, SPCE) as a research assistant and then later joined an infrastructure company and worked there for an year before pursuing his masters degree. In January, 2009, he started his Masters of Science program in Civil Engineering at The University of Texas at Arlington in the area of pavement and transportation engineering. Throughout his masters he was guided by his supervising professor Dr. Stefan Romanoschi and graduated in August, 2011.